



Title	Nicotinic acetylcholine receptors in a songbird brain
Author(s)	Asogwa, Norman Chinweike; Toji, Noriyuki; He, Ziwei; Shao, Chengru; Shibata, Yukino; Tatsumoto, Shoji; Ishikawa, Hiroe; Go, Yasuhiro; Wada, Kazuhiro
Citation	The journal of comparative neurology, 530(11), 1966-1991 <a href="https://doi.org/10.1002/cne.25314">https://doi.org/10.1002/cne.25314</a>
Issue Date	2022-08
Doc URL	<a href="http://hdl.handle.net/2115/90351">http://hdl.handle.net/2115/90351</a>
Rights	This is the peer reviewed version of the following article: Asogwa, N. C., Toji, N., He, Z., Shao, C., Shibata, Y., Tatsumoto, S., Ishikawa, H., Go, Y., & Wada, K. (2022). Nicotinic acetylcholine receptors in a songbird brain. <i>J Comp Neurol</i> , 530, 1966– 1991. , which has been published in final form at <a href="https://doi.org/10.1002/cne.25314">https://doi.org/10.1002/cne.25314</a> . This article may be used for non-commercial purposes in accordance with Wiley Terms and Conditions for Use of Self-Archived Versions. This article may not be enhanced, enriched or otherwise transformed into a derivative work, without express permission from Wiley or by statutory rights under applicable legislation. Copyright notices must not be removed, obscured or modified. The article must be linked to Wiley ' s version of record on Wiley Online Library and any embedding, framing or otherwise making available the article or pages thereof by third parties from platforms, services and websites other than Wiley Online Library must be prohibited.
Type	article (author version)
File Information	J. Comp. Neurol._ 530_1966.pdf



[Instructions for use](#)

1 Title:

2 **Nicotinic acetylcholine receptors in a songbird brain**

3

4 Norman Chinweike Asogwa<sup>1#</sup>, Noriyuki Toji<sup>2#</sup>, Ziwei He<sup>1</sup>, Chengru Shao<sup>1</sup>, Yukino  
5 Shibata<sup>1</sup>, Shoji Tatsumoto<sup>3</sup>, Hiroe Ishikawa<sup>3</sup>, Yasuhiro Go<sup>3,4,5</sup>, and Kazuhiro Wada<sup>1, 2\*</sup>

6

7 <sup>1</sup>Graduate School of Life Science, Hokkaido University, Sapporo, Japan

8 <sup>2</sup> Faculty of Science, Hokkaido University, Sapporo, Japan

9 <sup>3</sup>Cognitive Genomics Research Group, Exploratory Research Center on Life and Living  
10 Systems, National Institutes of Natural Sciences, Okazaki, Japan

11 <sup>4</sup>School of Life Science, SOKENDAI (The Graduate University for Advanced Studies),  
12 Okazaki, Japan

13 <sup>5</sup>Department of Physiological Sciences, National Institute for Physiological Sciences,  
14 Okazaki, Japan

15

16 # These authors contributed equally to this work.

17

18 \*Correspondence

19 Kazuhiro Wada, MD, PhD

20 Faculty of Science, Hokkaido University,

21 Room 910, Building No.5,

22 North 10, West 8, Kita-ku, Sapporo, Hokkaido

23 060-0810, Japan,

24 Email: [wada@sci.hokudai.ac.jp](mailto:wada@sci.hokudai.ac.jp)

25

26 **Abstract**

27 Nicotinic acetylcholine receptors (nAChRs) are ligand-gated ion channels that mediate fast  
28 synaptic transmission and cell signaling, which contribute to learning, memory, and the  
29 execution of motor skills. Birdsong is a complex learned motor skill in songbirds. Although  
30 the existence of 15 nAChR subunits has been predicted in the avian genome, their expression  
31 patterns and potential contributions to song learning and production have not been  
32 comprehensively investigated. Here we cloned all the 15 nAChR subunits (Chrna1–10, B2–  
33 4, D, and G) from the zebra finch brain and investigated the mRNA expression patterns in  
34 the neural pathways responsible for the learning and production of birdsong during a critical  
35 period of song learning. Although there were no detectable hybridization signals for Chrna1,  
36 A6, A9, and A10, the other 11 nAChR subunits were uniquely expressed in one or more  
37 major subdivisions in the song nuclei of the songbird brain. Of these 11 subunits, Chrna3–  
38 5, A7, and B2 were differentially regulated in the song nuclei compared with the surrounding  
39 anatomically related regions. Chrna5 was upregulated during the critical period of song  
40 learning in the lateral magnocellular nucleus of the anterior nidopallium. Furthermore, single-  
41 cell RNA sequencing revealed Chrna7 and B2 to be the major subunits expressed in neurons  
42 of the vocal motor nuclei HVC and robust nucleus of the arcopallium, indicating the potential  
43 existence of Chrna7-homomeric and Chrb2-heteromeric nAChRs in limited cell  
44 populations. These results suggest that relatively limited types of nAChR subunits provide  
45 functional contributions to song learning and production in songbirds.

46

47

48 **Keywords**

49 acetylcholine, nicotinic receptors, sensorimotor learning, zebra finch, vocal learning

50

51 **Abbreviations**

52 **A**, arcopallium; **AA**, anterior arcopallium; **AD**, dorsal arcopallium; **AI**, intermediate  
53 arcopallium; **AId**, dorsal part of AI; **AIV**, ventral part of AI; **AMVi**, intermediate part of the  
54 medial ventral arcopallium; **AP**, posterior arcopallium; **Area X**, striatum song nucleus Area  
55 X; **B**, nucleus basorostralis; **Cb**, cerebellum; **CMM**, caudomedial mesopallium; **DLM**,  
56 dorsolateral nucleus of medial thalamus; **DM**, dorsal medial nucleus of the midbrain; **dn**,  
57 deep nuclei of the cerebellum; **E**, entopallium; **g**, granular layer of the cerebellar cortex; **Gp**,  
58 globus pallidus; **H**, hyperpallium; **Hp**, hippocampus; **HVC**, acronym as proper name used  
59 for the song nucleus; **IPc**, nucleus isthmi pars parvocellularis; **L**, field L subdivision of  
60 nidopallium; **LMAN**, lateral magnocellular nucleus of the anterior nidopallium; **MMAN**,  
61 medial magnocellular nucleus of the anterior nidopallium; **M**, mesopallium; **m**, molecular  
62 layer of the cerebellar cortex; **MLd**, nucleus mesencephalicus lateralis pars dorsalis; **N**,  
63 nidopallium; **NCM**, caudomedial nidopallium; **P**, pallidum; **p**, Purkinje cell layer of the  
64 cerebellar cortex; **Pt**, nucleus pretectalis; **RA**, robust nucleus of the arcopallium; **Rt**, nucleus  
65 rotundus; **SP**, nucleus subpretectalis; **Spl**, nucleus spiriformis lateralis; **Str**, striatum; **TeO**,  
66 tectum opticum; **Tha**, thalamus; **TnA**, nucleus taenia; **w**, white matter layer in the cerebellum  
67

## 68 **Introduction**

69 In the CNS, acetylcholine receptors (AChRs) mediate acetylcholine (ACh) function in the  
70 arousal-related enhancement of sensory processing (Fu et al., 2014; Herrero et al., 2008; Shea,  
71 Koch, Baleckaitis, Ramirez, & Margoliash, 2010), cognition and memory (Anagnostaras et  
72 al., 2003; Hasselmo, 2006; Wallace & Bertrand, 2013), motor skill acquisition (Conner,  
73 Culbertson, Packowski, Chiba, & Tuszynski, 2003; H. Q. Li & Spitzer, 2020; Thouvarecq,  
74 Protais, Jouen, & Caston, 2001), and selective attention (Noudoost & Moore, 2011; Parikh,  
75 Kozak, Martinez, & Sarter, 2007; Sarter, Bruno, & Turchi, 1999). These AChR-mediated  
76 physiological processes are likely shared among vertebrate species because of the high  
77 conservation of AChR protein sequences and their related signaling pathways (Dajas-  
78 Bailador & Wonnacott, 2004; Gotti & Clementi, 2004; Pedersen, Bergqvist, & Larhammar,  
79 2019). However, except for the extensively studied species of mammals, fundamental  
80 knowledge about the expression of AChRs in the CNS is limited in vertebrates, including  
81 avian species.

82

83 AChRs comprise two major classes: muscarinic and nicotinic receptors (Gotti & Clementi,  
84 2004; Kruse et al., 2014). Nicotinic AChRs (nAChRs) are ligand-gated ion channels that are  
85 permeable to  $\text{Na}^+$ ,  $\text{K}^+$ , and  $\text{Ca}^{2+}$  ions. Hence, nAChRs mediate not only fast synaptic  
86 transmission but also intracellular signaling via  $\text{Ca}^{2+}$ -dependent signaling machinery (Dajas-  
87 Bailador & Wonnacott, 2004; Gotti et al., 2009; Wonnacott, 1997; M. Zoli, Pucci, Vilella, &  
88 Gotti, 2018). Functional nAChRs exist in either homo- or hetero-pentameric configurations  
89 formed from  $\alpha$  subunits (ChrnAs) as the ligand binding subunits and  $\beta$  subunits (ChrnBs) as  
90 structural subunits (Couturier et al., 1990; Gotti et al., 2009; N. Le Novere, Corringer, &  
91 Changeux, 2002; M. Zoli, Pistillo, & Gotti, 2015). To date, the existence of 15 nAChR  
92 subunits (ChrnA1–10, B2–4, D, and G) is predicted in the genome of avian species. In  
93 comparison, mammals do not retain ChrnA8 but express two additional subunits, ChrnB1  
94 and ChrnE. Although the number and types of nAChR subunits are not perfectly conserved  
95 between avian and mammalian species, the phylogenetic relationship between homologous  
96 subunit genes is highly conserved (Lovell et al., 2020; Pedersen et al., 2019; Sargent, 1993;  
97 Wada et al., 1988) (**Figure 1(a)**).

98

99 Based on their pharmacological and structural properties, nAChR subunits are divided into  
100 three major functional groups: muscle subunits (ChrnA1, B1, D, E, and G), standard neuronal  
101 subunits that form heteromeric receptors with pairwise  $\alpha$  (ChrnA2–6) and  $\beta$  (ChrnB2–4)

102 subunit combinations, and other neuronal subunits (ChrnA7–10) that can form homomeric  
103 nAChRs (Gotti et al., 2009; M. Zoli et al., 2015). These different combinations are associated  
104 with specific physiological and developmental features (Gotti et al., 2009; Role & Berg,  
105 1996; Michele Zoli, Le Novere, Hill, & Changeux, 1995). Some neuronal nAChR subunits  
106 are selectively expressed in specific subregions of the CNS in vertebrates, including  
107 mammals (Dineley-Miller & Patrick, 1992; Han et al., 2000; Wada et al., 1988; Winzer-  
108 Serhan & Leslie, 1997; Michele Zoli et al., 1995) and birds (Halvorsen & Berg, 1990; Lovell,  
109 Huizinga, Friedrich, Wirthlin, & Mello, 2018; Morris et al., 1990; Whiting et al., 1991).  
110 However, at the single-cell level, the combinations of nAChR subunits that are coexpressed  
111 in the CNS have not yet been fully elucidated.

112

113 Oscine songbirds learn birdsong, a complex vocal skill, during a critical period that  
114 comprises the sensory and sensorimotor learning phases (Brenowitz & Beecher, 2005; Doupe  
115 & Kuhl, 1999; Marler & Slabbekoorn, 2004). During the sensory learning phase, a juvenile  
116 bird listens to and memorizes a copy of the tutor song, while during the sensorimotor learning  
117 phase, the pupil bird practices singing repeatedly and refines its vocal outputs to mimic the  
118 memorized tutor song model through auditory feedback. Song acquisition is shaped by  
119 singing subsong, plastic song, and crystallized song. The learning and production of birdsong  
120 are controlled by specialized neural circuits known as song pathways (**Figure 1(b)**). These  
121 song pathways are organized into two anatomically and functionally distinct neural circuits  
122 called the anterior pathway (AFP) and vocal motor pathway (VMP), with interconnecting  
123 song nuclei. The AFP consists of a pallial–basal ganglia–thalamic connection with three song  
124 nuclei: the lateral magnocellular nucleus of the anterior nidopallium (LMAN), nucleus Area  
125 X in the striatum, and anterior part of the medial nucleus of the dorsolateral thalamus (aDLM,  
126 the part of DLM that receives afferent input from Area X and sends output projection to  
127 LMAN) (Luo, Ding, & Perkel, 2001). The VMP comprises the HVC (acronym as proper  
128 name) and robust nucleus of the arcopallium (RA). Although the VMP participates in song  
129 production, the AFP is not required for singing but is a crucial neural circuit for song learning  
130 and maintenance by generating vocal fluctuations (Andalman & Fee, 2009; Bottjer, Miesner,  
131 & Arnold, 1984; Brainard & Doupe, 2000; Kao, Doupe, & Brainard, 2005; Nottebohm,  
132 Stokes, & Leonard, 1976; Scharff & Nottebohm, 1991).

133

134 In songbirds, ACh and associated enzymes such as acetylcholinesterase (AChE) and  
135 choline acetyltransferase (ChAT) exist in several song nuclei (Ryan & Arnold, 1981;

136 Sakaguchi & Saito, 1989; Zuschratter & Scheich, 1990). Song nucleus HVC receives  
137 cholinergic afferents from the ventral pallidum of the basal forebrain, a brain region  
138 homologous to the nucleus basalis of Meynert in mammals (R. Li & Sakaguchi, 1997; Reiner  
139 et al., 2004). In addition, the concentration of ACh increases in the song nuclei HVC, RA,  
140 and LMAN of male zebra finches during the early critical period of song learning (Sakaguchi  
141 & Saito, 1989). Similarly, AChE is highly enriched in the song nuclei HVC, RA, and LMAN  
142 during this critical period (Ryan & Arnold, 1981; Sadananda, 2004; Sakaguchi & Saito,  
143 1991). These findings suggest the expression of AChRs in the song nuclei that mediates  
144 cholinergic functions during song learning and production. Our previous investigation  
145 revealed developmental regulation and inter- and intra-specific differences in the expression  
146 of muscarinic AChR subunits (mAChRs) in the song pathways (Asogwa, Mori, Sanchez-  
147 Valpuesta, Hayase, & Wada, 2018). In contrast to mAChRs, only a limited number of nAChR  
148 subunits have been reported to be expressed in the songbird brain (Lovell, Clayton, Replogle,  
149 & Mello, 2008; Lovell et al., 2018; Watson, Adkins - Regan, Whiting, Lindstrom, &  
150 Podleski, 1988). ZEBRA, the online public repository of gene expression in the zebra finch  
151 brain (<http://www.zebrafinchatlas.org/>), currently provides *in situ* hybridization information  
152 for nAChR subunits ChrnA3–5, A7, B2, and B3 (Lovell et al., 2020). However, the precise  
153 number of nAChR subunits involved and their expression levels and patterns, particularly in  
154 the song nuclei, during song development have not been fully investigated.

155

156 Here, we cloned 15 nAChR subunits from the zebra finch brain; however, no detectable  
157 signal was obtained in the brain sections by *in situ* hybridization for four subunits. The  
158 remaining 11 subunits were expressed to varying levels in at least one brain subdivision  
159 (pallium, hippocampus, subpallium, midbrain, or cerebellum). Specifically, the expression  
160 of ChrnA3–5, A7, and B2 revealed unique specializations in one or more song nuclei. In  
161 addition, the single-cell transcriptional analysis revealed the potential existence of ChrnA7-  
162 homomeric and ChrnB2-heteromeric nAChRs in the vocal motor nuclei.

163

## 164 **Materials and Methods**

### 165 **Animals**

166 Male zebra finches (*Taeniopygia guttata*) were used for this study at the three stages of song  
167 development: subsong (30–45 post-hatching day [phd], n = 6), plastic song (50–65 phd, n =  
168 6), and the crystallized song (>120 phd, n = 6). Because of the limited number of brain  
169 sections available in one of six brains, only five birds at the subsong stage were utilized for  
170 *in situ* hybridization with ChrnA4, A5, and A10 probes. For that same reason, *in situ*  
171 hybridization for ChrnA4 and A10 probes was performed with five birds at the plastic song  
172 stage. The birds were used from our breeding colonies at Hokkaido University, Sapporo,  
173 Japan. Photoperiod was maintained at 13h light/11 hr dark cycle with free access to food and  
174 water. Song developmental stages were confirmed by the probability density distribution of  
175 syllable duration in songs (Aronov, Veit, Goldberg, & Fee, 2011). All animal-based  
176 procedures complied with the regulations of the Committee on Animal Experiments of  
177 Hokkaido University. These regulations are requirements of the National Regulations for  
178 Animal Welfare in Japan (Law for the Humane Treatment and Management of Animals,  
179 partial amendment number No.105, 2011).

180

### 181 **RT-PCR and cloning of nAChR subunits**

182 Attempts were made to clone, from the zebra finch brain, all 15 nAChR subunits identified  
183 or predicted in birds (Pedersen et al., 2019; Sargent, 1993). The ChrnA7-like subunit in the  
184 National Centre for Biotechnology Information (NCBI, accession # XM\_002187662) was  
185 labeled as ChrnA8. RT-PCR was performed on total RNA collected from adult male zebra  
186 finch brains before light-ON in the morning. Total RNA was extracted by TRIzol Reagent  
187 (Thermo Fisher), treated with DNaseI to digest contamination from genome DNA, and  
188 transcribed to complementary DNA (cDNA) using Superscript Reverse Transcriptase  
189 (Invitrogen) with oligo(dT) primers. In the first attempt to clone the targeted subunits, we  
190 designed PCR oligo-primers to target protein regions that are conserved between mammals,  
191 birds, reptiles, and amphibians (**Table 1**). When the initial cloning failed, we used putative  
192 mRNA sequences predicted by the NCBI for primer design. Partial DNA fragment of each  
193 targeted nAChR subunit was amplified by PCR (Ex Taq polymerase, Takara Bio) using the  
194 synthesized cDNA template and cloned into pGEM-T easy plasmids (Promega) based on a  
195 previous method (Asogwa et al., 2018; Wada, Sakaguchi, Jarvis, & Hagiwara, 2004). The  
196 cloned cDNA fragments were verified by DNA sequencing. The sequence identities of  
197 cloned cDNA fragments and their predicted amino acids were authenticated by comparison



198 with the transcripts of nAChR subunits in the zebra finch, chicken, and human in the NCBI,  
199 using Nucleotide and Protein BLASTs. The cloned partial cDNA sequences of 15 nAChR  
200 subunits were assigned in GenBank with accession numbers OL679454–OL679467 and  
201 OM201170 (Table 1).

202

### 203 **Radioisotope *in situ* hybridization and quantification of mRNA expression**

204 Brain tissues were sampled from birds in dark, silent, and non-singing conditions. To ensure  
205 that mRNA expression was not due to singing or hearing songs, the birds were kept in a  
206 sound-attenuation box under these conditions for at least 10 hr prior to euthanasia and  
207 sacrifice. Brain tissues were put in plastic molds with tissue-compounding medium (Tissue-  
208 Tek, Sakura) and immediately transferred onto crushed dry ice. Subsequently, they were  
209 stored at -80°C until sectioning. The brain tissues were sectioned at 12 µm-thickness on the  
210 sagittal plane and mounted on silane-coated slides. The radioisotope *in situ* hybridization and  
211 quantification of expressed mRNA levels were conducted according to previous studies  
212 (Asogwa et al., 2018). Using specific T7 or SP6 RNA polymerases (Roche) to the inserted  
213 sense-/antisense direction of nAChR subunits, <sup>35</sup>S-labeled riboprobes were synthesized from  
214 the T7 or SP6 promoter sites of pGEM-T. Fresh frozen brain sections were fixed in 3%  
215 paraformaldehyde/1×phosphate-buffered saline (PBS, pH 7.0), washed three times in 1×PBS,  
216 acetylated, washed three times in 2×SSPE, dehydrated in ascending ethanol concentrations  
217 (50, 70, 90, and 100%), and then air-dried. Each Riboprobe (10<sup>6</sup> cpm) was mixed with 150  
218 µl of hybridization buffer (50% formamide; 10% dextran sulfate; 1×Denhart's solution; 12  
219 mM EDTA, pH 8.0; 10 mM Tris–HCl, pH 8.0; 30 mM NaCl; 0.5 µg/µl yeast tRNA; and 10  
220 mM dithiothreitol. Hybridization was performed in an oil bath for 14 hr at 65°C. Slides were  
221 next washed stepwise in two changes of chloroform, in 2×SSPE/0.1% 2β-mercaptoethanol  
222 for 30 min, in 50% formamide/0.1% 2β-mercaptoethanol for 60 min, twice in 2×SSPE/0.1%  
223 2β-mercaptoethanol for 30 min each, and twice in 0.1× SSPE/0.1% 2β-mercaptoethanol for  
224 15 min each. For ChrnA2, because of the high %GC contents (65% GC) of its probe,  
225 hybridization and washing temperatures were set at 68.5°C. The slides were dehydrated in  
226 ascending ethanol concentrations (50, 70, 90, and 100%), air-dried, and exposed to BioMax  
227 MR Films (Kodak) for 4–5 days before development. mRNA signals were quantified from  
228 X-ray films by digitally scanning them under a microscope (Z16 Apo, Leica, Buffalo Grove,  
229 IL) that was connected to a CCD camera (DFC490, Leica), with Leica Application Suite,  
230 version 3.3.0 (Leica). Light and camera settings were maintained constant for all images to  
231 avoid biased comparisons. Images were converted to a 256-gray scale. mRNA expression

232 levels were quantified as mean pixel intensities using Adobe Photoshop (CS2, Adobe  
233 Systems, San Jose, CA, RRID: SCR\_014199). After X-ray film exposure, brain slides were  
234 Nissl-stained with Cresyl violet acetate solution (Sigma, St Louis, MO, USA) to aid visual  
235 evaluation of anatomical subregions. For the figure presenting mRNA expression in the brain,  
236 images of *in situ* hybridization taken in sagittal sections were oriented with the rostral side to  
237 the right and the dorsal side upward, and the black-and-white negatives were inverted, so that  
238 white represents mRNA signal. Based on careful comparison of *in situ* hybridization images  
239 taken from 10 birds, we were able to distinguish real signals from artifacts. Apparent artifacts  
240 from *in situ* hybridization images were identified as shown in Figures 2, 3, and 4, and were  
241 removed in Photoshop using The Spot Healing Brush Tool function.

242

### 243 **Single-cell RNA sequencing**

244 The brain of an adult male zebra finch was used for single-cell RNA sequencing (scRNA-  
245 seq) experiment. The bird was placed in a sound-attenuating box overnight under silent and  
246 dark conditions. The next morning before light onset, the bird under deep anesthesia was  
247 perfused with ice-cold Cutting Buffer (Saunders et al., 2018). Then, the telencephalon was  
248 removed and kept in ice-cold Cutting Buffer until sectioning. Brain sections were cut at 400  
249  $\mu\text{m}$  in the sagittal plane in ice-cold Cutting Buffer with a microslicer (DTK-1000, DOSAKA  
250 EM). HVC and RA tissues were punched out with Miltex Biopsy Punch (1 mm diameter;  
251 Ted-pella Inc.), frozen in sample storage buffer with 0.2 U/mL RNase inhibitor (Takara), and  
252 10% DMSO in 1xPBS and stored at  $-80\text{ }^{\circ}\text{C}$  until nuclei isolation. Punched tissues were  
253 homogenized in 750  $\mu\text{l}$  of ice-cold Nuclei PURE Lysis Buffer using a glass Dounce tissue  
254 grinder (Wheaton) (40 times with tight pestle), centrifuged at 500x g for 10 minutes at  $4\text{ }^{\circ}\text{C}$ ,  
255 washed with 1 mL of Nuclei Wash and Resuspension Buffers. After centrifugation, the  
256 supernatant was removed, while the nuclei were suspended in 120  $\mu\text{L}$  of Nuclei Wash and  
257 Resuspension Buffers with DAPI and filtered with 40  $\mu\text{m}$  cell strainers. Isolated cell nuclei  
258 were purified with a cell sorter (SH800, Sony) using DAPI fluorescence. The 10 $\times$  Chromium  
259 libraries were prepared using Chromium Single Cell Library Kit v3 (PN-1000092, 10x  
260 Genomics) according to the manufacturer's protocol. cDNA along with cell barcode  
261 identifiers were PCR-amplified, while sequencing libraries were prepared. The constructed  
262 library was sequenced on MGI DNBSEQ-G400 (150 bp Paired-end) platform. The Cell  
263 Ranger Software Suite (v4.0.0) was used to perform sample de-multiplexing, barcode  
264 processing, and single-cell 3' unique molecular identifier (UMI) counting. Splicing-aware  
265 aligner STAR was used in FASTQs alignment with a zebra finch reference genome

266 (bTaeGut1\_v1.p, GCF\_003957565.1 based custom reference genome). Cell barcodes were  
267 determined based on the distribution of UMI counts automatically.

268

### 269 **Cell cluster Analysis**

270 The R package Seurat v.3 was used for the following data filtering and analyses (Stuart et al.,  
271 2019). Filtering criteria applied to the data, using ‘CreateSeuratObject,’ included min.cells =  
272 3, and min.features = 200. After filtering, a total of 6,510 and 6,977 cells in HVC and RA,  
273 respectively, were left for further analysis. The filtered gene-barcode matrix was first  
274 normalized using “LogNormalize” methods with default parameters. The top 2,000 variable  
275 genes were then identified using the “vst” method in Seurat FindVariableFeatures function.  
276 Principal component analysis (PCA) was performed using the top 2,000 variable genes.  
277 UMAP was performed on 27 to 31 principal components for visualizing the cells. Meanwhile,  
278 graph-based clustering was performed on the PCA-reduced data for clustering analysis with  
279 Seurat v.3. Clusters were determined using FindNeighbors (with 27 to 31 principal  
280 components) and FindClusters (resolution=1). The expression of established marker genes  
281 was used to assign identities for each cluster: SLC17A6 for glutamatergic neurons; GAD1  
282 and GAD2 for GABAergic neurons; SOX4 and SOX11 for neuronal precursors; SLC15A2,  
283 SLC1A2, and ASPA for astrocytes; PDGFRA and NKX2.2 for oligodendrocyte precursor  
284 cells (OPCs); PLP1 and ST18 for oligodendrocytes; and CSF1R and IKZF1 for microglia  
285 (Saunders et al., 2018; Tasic et al., 2016; Tasic et al., 2018; Zhang et al., 2014). Subclusters  
286 in glutamatergic neurons in HVC were identified based on a previous report (Colquitt,  
287 Merullo, Konopka, Roberts, & Brainard, 2021) and *in situ* hybridization database, ZEBRA  
288 (Lovell et al., 2020): GFRA1 and UTS2B were used as marker genes for HVC<sub>(RA)</sub> neurons  
289 projecting to RA (Bell et al., 2019); NTS and SCUBE1 for HVC<sub>(X)</sub> neurons projecting from  
290 HVC to Area X and RA neurons projecting to the nucleus of cranial nerve XII; GRIA4,  
291 GRM1, and CACNA2D1 for surrounding caudal nidopallium (cN) neurons; and CACNA1H,  
292 MGAT4C, and ADYAP1 for RA surrounding arcopallial neurons. Three unknown clusters  
293 with no specific marker gene and several small clusters (less than 60 cells in each) were  
294 filtered out. Each neural cell-type was isolated and re-clustered based on the expression of  
295 ChrnA3–5, A7, and B2 and two to four other genes specifically expressed in each using PCA  
296 implemented in the RunPCA function of Seurat. Subtype specific genes included KCNH1  
297 and ROBO2 for HVC<sub>(RA)</sub> neurons; SRD5A2 and SLIT3 for HVC<sub>(X)</sub> neurons; SRD5A2 and  
298 SLC4A11 for RA projection neurons; GPC6, FOXP2, MAF, and VSTM2A for interneurons;  
299 and CELF2, DACH2, LOC115498355, and SDCCAG8 for HVC progenitor neurons. Then

300 UMAP was performed on all principal components in each cell type for visualizing cell  
301 clusters formation based on CHRN family gene expression patterns.

302

### 303 **Statistical analyses**

304 Data obtained on the developmental regulation of different AChR subunits were analyzed  
305 with statistical software SPSS (IBM Statistics, Armonk, NY). Differences in mRNA  
306 expression levels of ChrnA3–5, A7, and B2 in the song nuclei were analyzed after a test for  
307 homogeneity of variance, using one-way analyses of variance (ANOVA) followed, when  
308 appropriate, by Scheffe's *F* tests.

## 309 **Results**

### 310 **nAChR subunits expressed in zebra finches**

311 Using cDNAs synthesized from the brain tissues of an adult male zebra finch and oligo-  
312 primers specific to protein-coding regions of nAChR, we cloned partial cDNA fragments of  
313 all 15 nAChR subunits (ChrnA1–10, B2–4, D, and G) predicted in avian species using RT-  
314 PCR (**Table 1**). The partial cDNAs and the corresponding translated amino acid sequences  
315 of the 15 cloned nAChRs were verified by comparing each nAChR subunit transcript  
316 predicted for the zebra finch with those previously identified in chicken and human. We  
317 confirmed that the match between each cloned partial nAChR subunit and the predicted full-  
318 length mRNA of the targeted subunits in the zebra finch was  $\geq 98.6\%$  at nucleotide level and  
319  $\geq 99.3\%$  at protein level (**Tables 1 and 2**). This result was consistent with the NCBI database  
320 prediction of nAChR transcripts from the zebra finch genome and indicated that 15 nAChR  
321 subunits were expressed in the zebra finch brain.

322

323 To evaluate the confounding cross-hybridization potential of *in situ* hybridization probes,  
324 we calculated the fraction (as a percentage) of sequence identities between each cloned  
325 subunit fragment and all non-targeted nAChR subunit protein-coding regions (**Table 2**). This  
326 analysis revealed that while the cloned partial cDNAs had near perfect match ( $\geq 98.6\%$   
327 similarity highlighted in red on the diagonal) with their targeted subunit sequences (as  
328 described above), the match with any non-targeted cross-nAChR subsequence was  $\leq 76.8\%$   
329 (off-diagonal similarity values). Only 21 (10%) of the 210 off-diagonal values were greater  
330 than 50% (entries in various shades of pink). We speculated that this level of mismatch was  
331 sufficient to avoid confounds from cross-hybridization with non-targeted nAChR subunits.

332

333 The cloned partial fragments of ChrnA1–10, B2–4, D, and G was used in *in situ*  
334 hybridization experiments to reveal the distribution of nAChR subunit expression in the brain  
335 tissues of adult male zebra finches. Eleven (ChrnA2–5, A7, A8, B2–4, D, and G) of the 15  
336 cloned subunits were expressed in unique patterns in at least one of the following brain  
337 regions: pallium, thalamus, midbrain, and cerebellum (**Figures 2, 3, 4**). In contrast, the four  
338 remaining receptor subunits, ChrnA1, A6, A9, and A10, exhibited few or no detectable  
339 mRNA signals throughout the whole brain. Therefore, no further investigations into mRNA  
340 expression were conducted for these four subunits.

341

### 342 **Expression of nAChR subunits in telencephalic subregions**

343 The pattern of mRNA expression and amount of each nAChR subunit available were  
344 evaluated in the following five major pallial telencephalic brain subdivisions: hyperpallium,  
345 mesopallium, nidopallium, arcopallium, and hippocampus. ChrnA4 and A7 were highly  
346 expressed in the mesopallium, arcopallium, and hippocampus compared with the other pallial  
347 subdivisions (**Figures 2, 3, 5**). In contrast, ChrnA2, A5, and B2 showed consistent but  
348 relatively low-level expression within all telencephalic subdivisions. As distinct exceptions,  
349 ChrnA3 and B4 showed similar expression patterns, strictly restricted to the mesopallium.  
350 Taken together, the mRNA for ChrnA3, A4, A7, and B4 exhibited a higher level of  
351 expression in the mesopallium than in the other pallial subdivisions (**Figure 5**).

352

353 Consistent with the pattern of nAChR subunit expression in the nidopallium, mRNAs of  
354 ChrnA2, A7, and B2 were uniformly throughout the caudomedial nidopallium (NCM), which  
355 is known as the avian secondary auditory area (**Figure 6**). Conversely, ChrnA5 expression  
356 was more restricted to the rostral portion of NCM, where its expression was higher than in  
357 the anterior nidopallium. ChrnA3, A4, and B4 were expressed at very low or undetectable  
358 levels in NCM as in most of the other nidopallial regions.

359

360 Subunits ChrnA4 and ChrnA7 showed differential expression in the subdomains (Mello,  
361 Kaser, Buckner, Wirthlin, & Lovell, 2019) of the arcopallium (**Figure 7(a)**). ChrnA4 was  
362 intensely expressed in most arcopallial subdomains except in the dorsal part of AI (AId),  
363 where it was almost fully suppressed. ChrnA7 distinctly showed higher expression in the  
364 caudal areas, including AD and the ventral part of AP, than in all other subdomains. ChrnA2,  
365 A5, and B2 were expressed with nearly uniform intensities at low-to-moderate levels  
366 throughout the subdomains of the arcopallium. ChrnA3 and B4 expressions were  
367 undetectable. Quite uniquely, ChrnA8 mRNA expression was well-defined and confined in  
368 the intermediate part of the medial ventral arcopallium (AMVi), so-called nucleus taenia  
369 (TnA) (**Figure 7(b)**).

370

371 The primary sensory input regions located within the nidopallium, including field L  
372 (auditory), entopallium (visual), and nucleus basorostralis (somatosensory/trigeminal), are  
373 anatomically defined in Nissl-stained tissue by a higher cell density relative to the  
374 surrounding nidopallium. While ChrnA2 mRNA was lightly expressed with near uniform  
375 intensity in each surrounding region of the nidopallium, expression of all other nAChR  
376 subunits was apparently absent in the primary sensory input regions (**Figures 2, 3, 4**).

377 Similarly, Chrna3, A5, and B4 expressions were suppressed in the subpallial striatum and  
378 globus pallidus. In contrast, Chrna4 was uniquely expressed in the striatal region, with small  
379 dots, suggesting its selective expression in a specific cell type (**Figure 2**). The cells labeled  
380 for Chrna4 expression, seen as intense isolated small dots, were clearly identified as a sparse  
381 cell population in the striatum by the Zebra Finch Expression Brain (ZEBRA) atlas based on  
382 digoxigenin-based labeling *in-situ* hybridization method. Similarly, Chrnb3 mRNA  
383 expression was observed specifically in the lateral pallium (**Figure 4**). In contrast, Chrna2,  
384 A7, and B2 expressions in the striatum and pallidum were similar to those in pallial regions.  
385

386 In the hippocampus, we observed a unique form of nAChR subunit specialization that was  
387 further portrayed according to the delineation of the hippocampus into dorsal and ventral  
388 subdivisions (**Figure 8**) with Chrna3 expression occurring dorsally and Chrna4 and A7  
389 ventrally, suggesting a potential distinction of ACh function between the proximal and distal  
390 parts. Furthermore, Chrna4 and A7 were even more expressed in the mesopallium,  
391 exhibiting seamless expression from the mesopallium to the ventral hippocampus. Notably,  
392 the expression of Chrna3 was also confined to the medial caudal part of the hippocampus  
393 (**Figure 2**). In contrast to these selective expressions of Chrna3, A4, and A7 subunits,  
394 Chrna2 and B2 were expressed equally in the dorsal and ventral hippocampus. However,  
395 Chrna5 and B4 expression levels were nearly undetectable in the hippocampus.  
396

### 397 **Expression of nAChR subunits in the midbrain and cerebellum**

398 Further investigation revealed more specializations for Chrna2–5, A7, A8, and B2–B4 in  
399 the nuclei/parts of the midbrain (**Figure 9**). Specifically, the nucleus pretectalis (Pt) and  
400 spiriform lateralis (Spl) were strongly labeled by Chrna2, A4, A5, A7, and B2. While  
401 Chrna4 and A5 were more intensely expressed both in Pt and Spl than in other midbrain  
402 nuclei, Chrna7 was selectively expressed only in Pt. Conversely, Chrna2 and B2 mRNA  
403 expressions were higher in Spl than in Pt. However, the expression of these subunits was  
404 almost completely suppressed below signal detection in the nucleus rotundus (Rt). There  
405 were exceptions, suggesting a selective cell type expression in Rt: Chrna2 and B2 were  
406 observed with low-to-moderate expression, and Chrna8, with sporadic expression. Chrna2,  
407 A5, and B2 showed low-level expression in the dorsomedial nucleus of the midbrain (DM),  
408 namely, the midbrain vocal center, and the nucleus mesencephalicus lateralis pars dorsalis  
409 (MLd), which forms the avian homologue of the central nucleus of the mammalian inferior  
410 colliculus (Boord, 1968; Woolley & Portfors, 2013). In addition, Chrna7 mRNA was

411 selectively expressed in the ventral part of MLd (near the 3<sup>rd</sup> ventricle). However, most  
412 nAChR subunits were undetected in these regions. The nuclei subpretectalis (SP) and isthmi  
413 pars parvocellularis (IPc) play crucial roles in the regulation of visual figure-ground  
414 discrimination (Schryver & Mysore, 2019; Scully, Acerbo, & Lazareva, 2014). Here, ChrnB4  
415 showed clear and specific expression in SP, while in contrast, IPc was labeled with high  
416 levels of ChrnA4, A5, and B3 expression (but ChrnA4 expression was suppressed in the  
417 lateral part of IPc; **Figure 2**). Overall, these results indicated that nAChR subunits are  
418 expressed differently in various combinations in the subnuclei/parts of the midbrain.

419

420 The layers of tectum opticum (TeO) also revealed distinct patterns of nAChR subunit  
421 distribution. According to Cajal's definition (Ramon y Cajal, 1911), there are about 15  
422 histologically identifiable layers in the avian TeO (Wylie, Gutierrez-Ibanez, Pagan, &  
423 Iwaniuk, 2009). In this study, five layers (layers 4, 6, 8, 10, and 13) were clearly differentiated  
424 according to the labeling patterns/intensities of ChrnA2, A4, A5, A7, A8, B2, and B3 mRNAs  
425 (**Figure 9**). Unlike ChrnA3 and B4, whose expression is clear in the mesopallium, these  
426 subunits were completely downregulated in all identified layers and subnuclei of TeO.  
427 ChrnA4, A7, A8, and B3 were more highly expressed in the deeper layers (layers 8–13) than  
428 in the more peripheral layers (layers 4–6), although their downregulation was not as great as  
429 that of ChrnA3 and B4. However, ChrnA2, A5, and B2 showed moderate-to-high levels of  
430 expression in all of the identified tectal layers.

431

432 We further examined the expression patterns of ChrnA2–5, A7, B2–4, D, and G in four  
433 anatomical layers of the cerebellum (the molecular, Purkinje cell, granular, and white matter  
434 layers). However, even though ChrnA2, D, and G were expressed in the granular layer, their  
435 mRNA signals were very weak (**Figure 10**), and those for ChrnA3 and B4 mRNA were  
436 almost undetectable. Moreover, whereas ChrnA4 and B2 were clearly expressed in the  
437 granular layer, ChrnA7 was selectively expressed in Purkinje cell layer. The expression of  
438 ChrnA5 was intense in both the granular and Purkinje cell layers, while ChrnB3 showed  
439 selective stronger expression at the top and bottom parts of the granular layer than in other  
440 parts of the cerebellum.

441

442 Overall, the expressions of 4 of the 15 cloned AChR subunits (ChrnA1, A6, A9, and A10)  
443 were very low or below detectable levels throughout the entire brain. However, expression  
444 of 11 subunits (ChrnA2–5, A7, A8, B2–4, D, and G) showed unique combinations of spatial



445 patterns and intensities in at least one subregion of the pallium, thalamus, midbrain, and  
446 cerebellum (**Figure 11**).

447

#### 448 **Differential expression of nAChR subunits in song nuclei**

449 Of the 15 nAChR subunits cloned from the male zebra finch, 6 (ChrA2–5, A7, and B2)  
450 were expressed in the following song nuclei at the adult stage: HVC and RA in the VMP;  
451 and LMAN, Area X, and aDLM in the AFP (Figures 2, 3, 4). Expression of ChrA2 in these  
452 song nuclei was not differentially regulated against the surrounding regions, but the five other  
453 subunits showed differential expression in one or more song nuclei compared with their  
454 surrounding regions.

455

456 Four of these differentially regulated subunits, ChrA3, A5, A7, and B2, were expressed at  
457 higher levels in the premotor song nucleus HVC than the surrounding caudal nidopallium  
458 (**Figure 12**). In particular, ChrA3 mRNA was expressed in limited HVC cells, whereas the  
459 other subunits showed a uniform expression pattern throughout HVC. In addition, the  
460 expression of ChrA5 and B2 was clearly higher in LMAN relative to the surrounding rostral  
461 nidopallium. Although ChrA7 was certainly expressed in LMAN, its expression was not  
462 specialized in comparison with that in the surrounding area (**Figure 12 (a)**). In addition,  
463 ChrA5, B2, and other subunits were not differentially expressed in the shell subregion of  
464 LMAN (Bottjer & Altenau, 2010) relative to the surrounding nidopallium.

465

466 Conversely, the expression of ChrA4 was lower in RA than in the surrounding arcopallium.  
467 Although none of the nAChR subunits exhibited higher levels of expression in RA and Area  
468 X relative to the surrounding arcopallium and striatum, respectively, low to moderate  
469 expression was observed in RA (for ChrA7 and B2) and Area X (for ChrA4 and B2)  
470 compared with the respective surrounding brain areas. In aDLM, only ChrA5 showed a  
471 higher differential expression level than the surrounding DLM.

472

473 Although differences in the expression of glutamate receptors are observed between the  
474 lateral and the medial parts of the AFP song nuclei (Wada et al., 2004), two nAChR subunits  
475 that were expressed with higher levels in LMAN (ChrA5 and B2) and in aDLM (ChrA5)  
476 relative to their respective surrounding area did not show differential expressions in the  
477 medial MAN and dorsomedial nucleus of the posterior thalamus.

478

479 **Developmental regulation of nAChR subunits during the critical period of song**  
480 **learning**

481 To examine a potential developmental change in expression of nAChR subunits in the song  
482 nuclei (HVC, RA, LMAN, Area X, and aDLM) through the critical period of song learning,  
483 we quantified the mRNA expression levels of ChrnA3–5, A7, and B2. Male zebra finches at  
484 the subsong (35–45 phd), plastic song (50–65 phd), and crystallized song (120–140 phd)  
485 stages were used. Although nAChR subunits were expressed to varying degrees among the  
486 song nuclei, only ChrnA5 showed significantly different regulation in the song nucleus  
487 LMAN, with its expression level increased from subsong to crystallized stages (one-way  
488 ANOVA followed by Scheffe's *F* tests,  $*p = 0.031$ ) (**Figure 12 (b)**). However, even though the  
489 shell subregion of LMAN is implicated in song learning in juvenile zebra finches (Bottjer &  
490 Altenau, 2010), the expressions of ChrnA5 and other subunits were not differentially  
491 regulated through the critical period of song learning. In addition, although the expression  
492 levels of ChrnA5 in Area X increased gradually from the subsong to crystallized song stage,  
493 the difference was not statistically significant due to individual variability in the mRNA  
494 expression level at the plastic and crystallized song stages. These results indicate that the  
495 expression of most nAChR subunits was consistently regulated in the song nuclei throughout  
496 song development.

497

498 **Cell type-specific expression of nAChR subunit in the song nuclei**

499 To elucidate the expression of nAChR subunits in different cell types of the vocal motor  
500 nuclei HVC and RA, in which the ACh content and related enzyme activity change markedly  
501 during the critical period for song learning (Sakaguchi & Saito, 1989), we performed single-  
502 cell RNA sequencing (scRNA-seq) with the two song nuclei from an adult male zebra finch.  
503 Based on the data obtained, we analyzed the expression of ChrnA1–10, B2–4, and D, and G  
504 mRNAs in different cell types, including glutamatergic excitatory neurons (including HVC<sub>(X)</sub>,  
505 HVC<sub>(RA)</sub>, and RA projecting neurons), GABAergic neurons, progenitor neurons, astrocytes,  
506 microglia, oligodendrocytes, OPC, and surrounding excitatory neurons in the nidopallium  
507 and arcopallium (**Figures 13, 14, 15, 16**). Consistent with earlier *in situ* hybridization results,  
508 the scRNA-seq data revealed that ChrnA1, A9, B3, B4, and D were expressed only in a few  
509 cells in both HVC and RA, while ChrnA6 mRNA was not detected. An exceptional  
510 discrepancy in mRNA detection was observed between *in situ* hybridization and scRNA-seq  
511 for ChrnA2 and ChrnA10. Although *in situ* hybridization revealed adequate expression of  
512 ChrnA2 mRNA throughout the entire brain, including HVC and RA, scRNA-seq showed no

513 ChnrA2 (+) cells in both HVC and RA. Conversely, ChnrA10 expression level was almost  
514 undetectable by *in situ* hybridization, whereas snRNA-seq showed several excitatory and  
515 inhibitory neurons and astrocytes labeled as expressing ChnrA10. Despite our best effort to  
516 carefully evaluate the specificity of the *in situ* hybridization probe and gene annotation  
517 information used for scRNA-seq analysis, the inconsistent detection of ChnrA2 and A10  
518 mRNAs remains unclear.

519

520 In contrast to those subunits with low or undetectable expression levels, ChnrA3–5, A7, A8,  
521 B2, and G were expressed in at least one cell type in these song nuclei at varying levels and  
522 in different numbers of cells (**Figures 14 and 16**). In particular, ChnrA7 and B2 were  
523 expressed in most cell types of HVC and RA. As for the results from *in situ* hybridization  
524 (**Figure 12 (a)**), ChnrA3 expression was biased in selective cell populations of HVC<sub>(RA)</sub> and  
525 HVC<sub>(X)</sub> projecting neurons and in a few RA projecting neurons. Although very few  
526 glutamatergic projecting neurons in HVC and RA expressed ChnrA4, progenitor neurons for  
527 HVC and OPC in both HVC and RA showed clear and intense expression of this subunit.  
528 ChnrA8 was selectively expressed in a subtype of astrocytes in HVC but not in RA, while  
529 ChnrG was selectively expressed in a few oligodendrocyte populations in these song nuclei.  
530 In addition, *in situ* hybridization signals for ChnrA8 and G mRNA were very subtle. Taken  
531 together, the scRNA-seq analysis revealed both nonspecific expressions of ChnrA7 and B2  
532 among various cell types and much selective expression of ChnrA3–5, A8, and G in limited  
533 cell types, suggesting that there are potentially unique nAChR subunit combinations at the  
534 single-cell level in the vocal motor song nuclei HVC and RA.

535

536 Since nAChR subunits form heteromeric or homomeric pentamers, which possess different  
537 physiological and pharmacological properties (Albuquerque, Pereira, Alkondon, & Rogers,  
538 2009; Gotti et al., 2009; M. Zoli et al., 2015), we further investigated the potential  
539 combinations of nAChR subunits coexpressed in neuronal cell types of HVC and RA by  
540 focusing on ChnrA3–5, A7, and B2 (**Figure 17**), which were detected in the song nuclei by  
541 *in situ* hybridization. The results revealed that limited populations of each neuron type  
542 expressed only specific nAChR subunits. For instance, although ChnrA3, A5, A7, and B2  
543 were expressed in HVC<sub>(RA)</sub> neurons, 55% of HVC<sub>(RA)</sub> neurons showed no expression of  
544 nAChR subunits. In addition, most of the remaining HVC<sub>(RA)</sub> neurons expressed only a single  
545 type of nAChR subunit. The selective expression of nAChR subunits was similarly observed  
546 in other neuron types in HVC and RA: HVC<sub>(X)</sub> neurons, interneurons, and progenitor neurons

547 in HVC and projecting neurons and interneurons in RA. ChrnA7 subunits are known to form  
548 homomeric nAChRs, while other  $\alpha$  subunits (ChrnA2–6) combine with  $\beta$  subunits to form  
549 heteromeric receptors (Gotti et al., 2009; M. Zoli et al., 2015). Indeed, we found that ChrnA7  
550 was expressed in some populations of all neuron types in HVC and RA (29% of HVC<sub>(RA)</sub>,  
551 62% of HVC<sub>(X)</sub>, 12% of HVC interneurons, 5% of HVC progenitor neurons, 32% of RA  
552 projecting neurons, and 10% of RA interneurons), suggesting the potential existence of  
553 ChrnA7-homomeric receptors in these neural cell types. Because the expressions of ChrnB3  
554 and B4 were detected only in a few cells in HVC and RA (**Figures 4, 14, 16**), ChrnB2 must  
555 be the main  $\beta$  subunit of heteromeric nAChRs in the song nuclei. Our snRNA-seq data  
556 revealed that 10%–22% of the neural cell types in HVC and RA expressed ChrnB2 (**Figure**  
557 **17 (a), (b)**). It is necessary to recognize potential technical limitations of scRNA-seq in  
558 detecting the transcribed mRNAs at low levels; even though we counted at least 1 UMI of  
559 the scRNA-seq reads as a positive expression of each nAChR subunit, cells coexpressing  
560 ChnB2 and other  $\alpha$  subunits comprised only a 2%–20% fraction of each neural cell type in  
561 HVC and RA. When we focused especially on ChrnB2-expressing cells, ChrnA7 was the  
562 main  $\alpha$  subunit coexpressed with ChrnB2 in 31%, 66%, and 33% of ChrnB2(+)-HVC<sub>(RA)</sub>, -  
563 HVC<sub>(X)</sub>, and -RA projecting neurons, respectively (arrowheads in **Figure 17 (a)-(c)**). This  
564 information on coexpression suggests the presence of a ChrnA7/B2 heteromeric receptor,  
565 which was recently found in rodent and human brains (Qiang Liu, Huang, Shen, Steffensen,  
566 & Wu, 2012; Q. Liu et al., 2009; Thomsen et al., 2015). These findings demonstrated that  
567 nAChR subunits were expressed in a limited cell population of each cell type in the vocal  
568 motor nuclei HVC and RA. Furthermore, nAChR may form ChrnA7-homomeric or ChrnB2-  
569 containing heteromeric receptors in these cell populations. However, compared with the more  
570 abundant expression of ChrnA7-homomeric receptors, far fewer neuronal cells expressed  
571 ChrnB2-containing receptors.

572

573

## 574 **Discussion**

575 To comprehensively investigate the expression of nAChR subunits in an oscine songbird  
576 brain, including the neural circuits for acquiring and producing birdsong, we cloned 15  
577 nAChR subunits, ChrnA1–10, B2–4, D, and G, from the zebra finch brain and highlighted  
578 their unique expression patterns in the telencephalon, thalamus, midbrain, and cerebellum.  
579 Whether the developmental origin of the hyperpallium is distinct or similar to regions below  
580 it remains an unsolved problem in avian pallial organization (Jarvis et al., 2005; Medina &  
581 Reiner, 2000; Reiner et al., 2004). The results of this study have shown that all 6 nAChR  
582 subunits expressed in the telencephalon were similarly expressed in both the hyperpallium  
583 and nidopallium across the mesopallium. The concordant expression of these nAChRs  
584 between the hyperpallium and nidopallium is consistent with the hypothesis that these two  
585 pallium subdivisions have a common origin (Gedman et al., 2021; Jarvis et al., 2013).

586

587 Five of the subunits (ChrnA3–5, A7, and B2) were expressed at varying levels in one or  
588 more song nuclei in the zebra finch brain. Of these, only ChrnA5 mRNA was differently  
589 regulated in the AFP song nucleus LMAN throughout the critical period of song development.  
590 These findings indicated that, in contrast to the change in ACh concentration and the activity  
591 of ChAT and AChE in the song nuclei through the critical period of song learning (Sakaguchi  
592 & Saito, 1989, 1991), the expression of most nAChR subunits was consistently maintained  
593 in the song nuclei during song acquisition. Furthermore, scRNA-seq analysis revealed the  
594 potential expression of ChrnA7-homomeric and ChrnB2-containing heteromeric nAChRs in  
595 limited cell populations of most neuronal cell types in the vocal premotor nuclei HVC and  
596 RA.

597

## 598 **Comparison of nAChR subunit expression between avian and mammalian species**

599 A similar number of nAChR subunits are expressed in the CNS of avian and mammalian  
600 species (Han et al., 2000; Nicolas Le Novere, Zoli, & Changeux, 1996; Lein et al., 2007;  
601 Lovell et al., 2018; Morris et al., 1990). However, the expression patterns and levels of  
602 nAChRs in the brain are not conserved between them. For example, the pattern of expression  
603 of four nAChR subunits (ChrnA1–3, A5) was apparently different in the pallium of zebra  
604 finches and the cortex of the mouse (**Figures 2, 3, 4, 18**). Specifically, ChrnA3 and ChrnA5  
605 were expressed in the mesopallium and entire pallial subregions, of the zebra finch,  
606 respectively (**Figures 2, 5**). In contrast, there was no detectable expression of the mRNAs of  
607 these subunits in the mouse cortex (**Figure 18**). Conversely, ChrnA1 and ChrnA2 were

608 consistently expressed throughout the entire mouse brain, the expression levels of these two  
609  $\alpha$  subunits were undetectable in the zebra finch brain. Furthermore, some of the nAChR  
610 subunits, such as ChnrA2 and A4, were differentially expressed in the cortical layers of the  
611 mice and marmoset (**Figure 19**), suggesting that nAChRs expression in the telencephalic  
612 regions is species-specifically diversified. The discrepancies thus identified in the pattern of  
613 expression of nAChR subunits are in sharp contrast to highly conserved expression patterns  
614 of the glutamate and dopamine receptor subunits between the avian pallium and mammalian  
615 cortical regions (Kubikova, Wada, & Jarvis, 2010; Wada et al., 2004).

616

### 617 **The potential functional contribution of nAChR subunits in the vocal motor nuclei**

618 Multiple lines of studies in songbirds have suggested potential contributions of the  
619 cholinergic system to vocal learning and production. For example, stimulating the cholinergic  
620 basal forebrain, a region homologous to the nucleus basalis of Meynert in mammals (R. Li  
621 & Sakaguchi, 1997; Reiner et al., 2004), suppresses auditory responses to the bird's own  
622 song in HVC and RA neurons in anesthetized zebra finches (Shea & Margoliash, 2003).  
623 Furthermore, the direct injection of nicotine into HVC produces a strong and consistent  
624 suppression of auditory responses in HVC neurons. Arousal state-dependent changes in  
625 auditory responses in HVC are an essential modulator of auditory input to the vocal motor  
626 region during song learning (Cardin & Schmidt, 2003; Schmidt & Konishi, 1998; Shea &  
627 Margoliash, 2003, 2010). However, the precise HVC neuron type responsible for nicotine-  
628 induced auditory suppression has not been determined physiologically.

629

630 Our scRNA-seq analysis revealed that in HVC, ChrnA3, A5, A7, and B2 were expressed in  
631 three neuron types in HVC: HVC<sub>(RA)</sub> neurons, HVC<sub>(X)</sub> neurons, and interneurons (**Figure 14**).  
632 However, the populations of cells that expressed these nAChR subunits differed among the  
633 neural cell-type classes in HVC. We found that 45% of HVC<sub>(RA)</sub> neurons and 30% of HVC  
634 interneurons expressed at least one type of nAChR subunits, mainly ChrnA7 or B2. In  
635 contrast, 77% of HVC<sub>(X)</sub> neurons expressed one or more of the ChrnA3, A5, A7, and B2  
636 subunits. In particular, 63% of HVC<sub>(X)</sub> neurons expressed ChrnA7 subunits, which can form  
637 functional homomeric receptors. Thus, ChrnA7 subunits may play an important role in  
638 modulating the activity of HVC<sub>(X)</sub> neurons in an arousal state-dependent manner. Further  
639 gene manipulation studies of these nAChR subunits at the cell-type level will be crucial to  
640 investigate the direct functional contribution of nAChRs in HVC to song learning and  
641 production.

642

643 In RA, the chronic infusion of a mixture of mAChR and nAChR antagonists during the  
644 critical period of song learning induces abnormal song development, characterized by the  
645 absence of stereotyped syllable sequences (Puzerey, Maher, Prasad, & Goldberg, 2018).  
646 Acute infusion of the AChR antagonist mixture into RA of juvenile zebra finches does not  
647 affect the syllable acoustics or the timing of early plastic songs, suggesting that not  
648 cholinergic modulation of fast synaptic transmission but rather cell signaling in RA is crucial  
649 for normal song learning (Puzerey et al., 2018). In addition, tetanic stimulation of LMAN to  
650 RA axon fibers induces long-term potentiation (LTP) in RA in the presence of nicotine;  
651 however, without nicotine it does not produce LTP (Salgado-Commissariat, Rosenfield, &  
652 Helekar, 2004). This nicotine-mediated LTP in RA is blocked by selective antagonists to  
653 ChrnA7-homomeric and ChrnA4/B2-heteromeric nAChRs. Our scRNA-seq findings  
654 revealed that ChrnA7 was identified in approximately 30% of RA projecting neurons, which  
655 could be a sensitive site to ChrnA7 homomeric receptor-specific antagonists in RA. However,  
656 although 15% of RA projecting neurons expressed ChrnB2, cells coexpressing ChrnB2 and  
657 other  $\alpha$  subunits including ChrnA4 accounted for only 0.1%–1.2% of RA projecting neurons.  
658 These expression data are contrary to the observed pharmacological effect of ChrnA4/B2  
659 heteromeric nAChR antagonists in RA. Although ChrnA4/B2 coexpression in RA was sparse,  
660 we found that 5% of RA projecting neurons coexpressed ChrnA7 and B2. Thus, instead of a  
661 ChrnA4/B2 combination, ChrnA7/B2 heteromeric receptors may contribute to the induction  
662 of nicotine-mediated LTP. Notably, approximately half of RA projecting neurons did not  
663 express any nAChR subunits. Thus, concerning nAChRs, RA projecting neurons are  
664 composed of heterogeneous populations, which may elicit differential responses to nAChR  
665 activation by nicotine (Meng, Wang, Yao, Zhang, & Li, 2017; Salgado-Commissariat et al.,  
666 2004).

667

### 668 **The potential functional contribution of nAChR subunits in the AFP nuclei**

669 Similar to the VMP song nuclei, we found that limited nAChR subunits were expressed in  
670 the AFP song nuclei, Area X (ChrnA2–5, A7, and B2), aDLM (ChrnA2, A4, A5, A7, and  
671 B2), and LMAN (ChrnA2, A5, A7, and B2). Particularly, the expressions of ChrnA5 and B2  
672 were higher in LMAN than in the surrounding nidopallium. Furthermore, ChrnA5 was the  
673 only subunit that showed a significant difference in expression during the critical period of  
674 song learning. Although physiological and pharmacological analyses of these subunits have  
675 not been performed in the AFP nuclei, our findings suggest that ChrnA7-homomeric and

676 Chrnb2-containing heteromeric nAChRs exist in the AFP song nuclei, as speculated for HVC  
677 and RA. The AFP is a crucial neural circuit in the regulation of song learning and  
678 maintenance by generating vocal variability (Andalman & Fee, 2009; Aronov, Andalman, &  
679 Fee, 2008; Brainard & Doupe, 2000; Kao et al., 2005; Ölveczky, Andalman, & Fee, 2005).  
680 The concentration of ACh and the activity of ChAT and AChE are increased and maintained  
681 in LMAN during the critical period of song learning (Sakaguchi & Saito, 1989, 1991). Thus,  
682 specific agonists/antagonists of ChrnA7-homomeric and Chrnb2-containing heteromeric  
683 nAChRs could be used to examine whether vocal variability can be modulated during song  
684 development. Further studies focusing on particular cell types and nAChR subtype  
685 combinations in the song nuclei will be crucial to elucidating cholinergic contributions via  
686 the nAChRs involved in neural plasticity and song learning.

687



688

689 **Table 1. Cloned partial cDNA information of nAChR subunits in this study<sup>1</sup>**

690 <sup>1</sup> The primers listed were used for cloning the cDNA fragments. Accession numbers are for  
691 record in GenBank. The last three columns list the similarity of amino acid sequences,  
692 expressed as percentages between cloned fragments and the corresponding nAChRs in zebra  
693 finch, chicken, and human, respectively. Human chrnA8 does not exist.

694

695 **Table 2. Sequence similarities between cDNAs and the protein-coding regions of 15**  
696 **nAChR subunits in the zebra finch<sup>1</sup>**

697 <sup>1</sup> Matching base-pair sequences as a fraction of the length of cDNAs are shown as percentages.  
698 High similarity values ( $\geq 98.5\%$ ) on the diagonal (cells highlighted in red) shown on-target  
699 identity. Perfect dissimilarity with off-target subunits is represented by a zero in an off-  
700 diagonal entry. Because the full-length transcript is expected to be expressed in cells, non-  
701 zero off-diagonal similarity values indicate the potential for *in situ* cross-hybridization of  
702 each subunit cDNA fragment to 14 off-target subunits. The low off-diagonal similarity values  
703 ( $\leq 76.8\%$ ) indicate that the potential for such confounds was low.

704

705

706 **Acknowledgments**

707 We appreciate Mrs. Keiko Sumida for her great contribution toward breeding our  
708 experimental birds. This research was supported by the Ministry of Education, Culture,  
709 Sports, Science and Technology Scholarship #153033 to C. N. A., and MEXT/JSPS  
710 KAKENHI Grant Number #4903-JP17H06380, JP19H04888, JP21H02456, JP21K18265,  
711 and the Takeda Science Foundation to K.W.

712

713 **Availability of data and materials**

714 The authors confirm that all of the data underlying the reported findings are included in the  
715 manuscript. All raw data are available to the corresponding author on request.

716

717 **Authors' contributions**

718 NCA and KW designed the research. NCA, NT, ZH, and KW performed the experiments.  
719 NCA, NT, and KW performed the analysis. CS, YS, ST, HI, and YG contributed to critical  
720 support for experiments and analysis. NCA, NT, and KW wrote the paper. The authors  
721 declare no competing financial interests. All authors read and approved the final manuscript.

722

723 **Figures & Figure Legends**

724

725 **Figure 1. Phylogram of nicotinic acetylcholine receptor subunits and brain diagram of**  
726 **the neural circuits for song learning and production**

727 (a) Phylogenetic relationship of nAChR subunits in the zebra finch, chicken, and human,  
728 generated with full-length protein-coding sequences using Molecular Evolutionary Genetics  
729 Analysis software (<https://www.megasoftware.net/>). Local bootstrap probabilities from the  
730 maximum-likelihood analysis are shown for branches below the terminals. All subunit types  
731 show closer homologies to each other across species than they do to different receptor types  
732 within species.

733 (b) The vocal motor circuit and the anterior forebrain pathway (pallial–basal ganglia–  
734 thalamic loop circuit) are represented as solid and dotted black lines, respectively. HVC  
735 (proper name); RA, robust nucleus of the arcopallium; Area X, Area X of the striatum; aDLM,  
736 anterior dorsal lateral nucleus of the medial thalamus; LMAN, lateral magnocellular nucleus  
737 of the anterior nidopallium; nXIIIts, the tracheosyringeal part of the 12th cranial nerve nuclei;  
738 H, hyperpallium; M, mesopallium; N, nidopallium; A, arcopallium; L, field L; St, Striatum;  
739 P, pallidum; Hp, hippocampus.

740

741 **Figure 2. Expression of nicotinic acetylcholine receptor A subunits (ChrnA1–5) in the**  
742 **male zebra finch brain**

743 Expression images for each subunit are in a different row, and within rows, images of  
744 parasagittal brain sections are organized by medial (left) to lateral (right) progression.  
745 Sections are oriented with rostral side to the right, and dorsal side up. Levels of brightness  
746 represents levels of the mRNA signal. A camera lucida drawing at the top of each column  
747 identifies the brain areas represented in the sections in the column below. Scale bar = 1 mm.

748

749 **Figure 3. Expression of nicotinic acetylcholine receptor A subunits (ChrnA6–10) in the**  
750 **male zebra finch brain**

751 Expression images are arranged as in Figure 2. Scale bar = 1 mm.

752

753 **Figure 4. Expression of nicotinic acetylcholine receptor B (ChrnB2–4), D, and G**  
754 **subunits in the male zebra finch brain**

755 Expression images are arranged as in Figure 2. Scale bar = 1 mm.

756

757 **Figure 5. Expression of nAChR subunits in subdivisions of the anterior pallial regions**  
758 *In situ* hybridization images for ChrnA2–5, A7, B2, and B4. Camera lucida drawing (bottom  
759 right panel) shows boundaries of the major subdivisions (H, hyperpallium; M, mesopallium;  
760 N, nidopallium; Str, Striatum) of these brain regions in exact correspondence to the orange  
761 dotted lines in the ChrnB4 image, and approximately for all others. Scale bar = 3 mm, for all  
762 images.

763

764 **Figure 6. Expression of nAChR subunits in subdivisions of the posterior medial pallial**  
765 **regions**

766 *In situ* hybridization images for ChrnA2–5, A7, B2, and B4. Bottom right: camera lucida  
767 drawing showing major subdivisions (Hp, hippocampus; NCM, caudomedial nidopallium;  
768 CMM, caudomedial mesopallium of the brain) of these brain regions. Scale bar = 3 mm.

769

770 **Figure 7. Expression of nAChR subunits in subdivisions of the arcopallium**

771 (a) *In situ* hybridization images for ChrnA2–5, A7, B2, and B4 in the lateral arcopallial  
772 regions. Camera lucida drawing (lower right) shows major subdivisions of this region of the  
773 brain. Orange dotted lines represent the borders of brain subdivisions: the anterior, posterior,  
774 dorsal, and intermediate arcopallium denoted by AA, AP, AD, and AI, respectively. AI<sub>d</sub> and  
775 AI<sub>v</sub>: dorsal and ventral subdivisions of AI, respectively. cN: caudal nidopallium.

776 (b) Specific expression of ChrnA8 in the intermediate part of the medial ventral arcopallium  
777 (AMVi), also called nucleus taenia (TnA).

778

779 **Figure 8. Expression of nAChR subunits in subdivisions of the hippocampus**

780 *In situ* hybridization images for ChrnA2–5, A7, B2, and B4. Camera lucida drawing (lower  
781 right panel) shows the dorsal (Hp<sub>d</sub>) and ventral (Hp<sub>v</sub>) subdivisions of the hippocampus. cN:  
782 caudal nidopallium. Scale bar = 3 mm.

783

784 **Figure 9. Expression of nAChR subunits in the midbrain**

785 *In situ* hybridization images for ChrnA2–5, A7, A8, and B2–4. Orange dotted lines show the  
786 borders of nuclei/parts in the midbrain. Right bottom: Nissl-stained brain image showing  
787 midbrain nuclei: Pt, nucleus pretectalis; Spl, nucleus spiriform lateralis; Rt, nucleus rotundus;  
788 DM, nucleus dorsomedialis of the midbrain; ML<sub>d</sub>, nucleus mesencephalicus lateralis, pars  
789 dorsalis; SP, nucleus; IP<sub>c</sub>, nucleus isthmi pars parvocellularis. Arabic numerals represent  
790 clearly identified layers of the tectum opticum. Scale bar = 3 mm.

791

792 **Figure 10. Expression of nAChR subunits in the cerebellum**

793 *In situ* hybridization images for ChrnA2–5, A7, B2–4, D, and G. Camera lucida showing  
794 sublayers of the cerebellum; p = Purkinje layer, m = molecular layer, g = granular layer, w =  
795 white matter, dn = deep nucleus. Scale bar = 3 mm.

796

797 **Figure 11. Heatmap summarizing the expression of nAChR subunits in subregions of**  
798 **the zebra finch brain**

799 Levels of expression were measured by image pixel intensity and represented in the heatmap  
800 by 5-grading colors (color bar).

801

802 **Figure 12. Expression of nAChR subunits in the song nuclei of adult male zebra finches**

803 (a) ChrnA3–5, A7, and B2 expression in song nuclei, HVC, RA, LMAN, Area X, and aDLM.  
804 Brains are sagittal, white color represents mRNA signal. Right panels: Camera lucida  
805 drawings depicting each song nucleus. Dotted dark lines show the borders of the song nuclei.  
806 (b) nAChR subunit expression in the song nuclei during song development. ChrnA3–5, A7,  
807 and B2 expression in HVC, RA, LMAN, Area X, and aDLM during the subsong (35–45 phd,  
808 orange), plastic song (50–65 phd, blue), and crystallized song (120–140 phd, red) stages of  
809 song development. Bars: mean ± SEM. n = 6 birds/each stage. One-way analysis of variance,  
810 ANOVA, \* $p < 0.05$ .

811

812 **Figure 13. Expression of marker genes at each cell-type in HVC**

813 Violin (left side panel) and UMAP (right side panel) plots of cell clusters expressing major  
814 cell type marker genes (a) and sub-type marker of glutamatergic neuron (b).

815

816 **Figure 14. Expression of nAChR subunits in various cell types in HVC**

817 UMAP (Uniform Manifold Approximation and Projection) plots of cells expressing  
818 ChrnA1–5, A7–10, B2–4, D, and G in HVC (n = 6,510 cells). Red dots in each panel  
819 represent cells expressing the subunit indicated at the top left. The color gradation represents  
820 the intensity of expression. In the reference UMAP panel at the top, each color represents a  
821 class of cell types.

822

823 **Figure 15. Expression of marker genes at each cell-type in RA**

824 Violin (left side panel) and UMAP (right side panel) plots of cell clusters expressing major  
825 cell type marker genes **(a)** and sub-type marker of glutamatergic neuron **(b)**.

826

827 **Figure 16. Expression of nAChR subunits in various cell types in RA**

828 UMAP (Uniform Manifold Approximation and Projection) plots of cells expressing  
829 ChrnA1–5, A7–10, B2–4, D, and G in RA (n = 6,977 cells). Red dots in each panel represent  
830 cells expressing the subunit indicated at the top left. The color gradation represents the  
831 intensity of expression. In the reference UMAP panels (upper), each color represents a class  
832 of cell types.

833

834 **Figure 17. Expression of nAChR subunits in various neuron types in HVC and RA**

835 UMAP plots of neuronal cell types (organized by row) expressing each of the ChrnA3–5, A7,  
836 and B2 subunits (organized by column) in HVC **(a)** and RA **(b)**. Each colored dot represents  
837 one neuron expressing the corresponding subunit gene. The color gradation represents the  
838 intensity of expression.  $HVC_{(RA)}$  and  $HVC_{(X)}$  are projecting neurons from HVC to RA and  
839 Area X, respectively.  $HVC_{(RA)}$ ,  $HVC_{(X)}$ , and RA projecting neurons are glutamatergic  
840 excitatory neurons.  $HVC_{(RA)} = 1,715$  cells;  $HVC_{(X)} = 326$  cells; interneurons in HVC and RA  
841 = 896 and 959 cells, respectively; HVC progenitor cells = 275 cells; and RA projecting  
842 neurons = 892 cells. Arrowheads indicate cells coexpressing ChrnA7 and B2 subunits.  
843 Percentage at the bottom of each UMAP plot is the fraction of the total cell population  
844 expressing the corresponding nAChR subunit in the corresponding neural cell type. **(c)**  
845 Coexpression rates of ChrnB2 (+) neurons with ChrnA3 (green), A4 (light blue), A5 (cream-  
846 yellow), and A7 (pink). Gray represents negatives (no expression of any of the ChrnA3–5,  
847 and A7 subunits).

848

849 **Figure 18. nAChRs mRNA expression in the mouse brain**

850 All images are adapted from Allen Brain Atlas mouse *in situ* hybridization data  
851 (<https://mouse.brain-map.org/search/index>).

852

853 **Figure 19. Differential expressions of ChrnA2 and A4 between mouse and marmoset**  
854 **cortices**

855 **(a)** ChrnA2 expression in the mouse (left) and marmoset (right) cortices. **(b)** ChrnA4  
856 expression in the mouse (left) and marmoset (right) cortices. Panels below are enlarged

857 from enclosed dotted square parts in the above panels. *In situ* hybridization images are  
858 adapted from Allen Brain Atlas mouse ISH data (<https://mouse.brain-map.org/search/index>)  
859 and the Marmoset Gene Atlas (<https://gene-atlas.brainminds.riken.jp/>).  
860

## 861 **References**

- 862 Albuquerque, E. X., Pereira, E. F., Alkondon, M., & Rogers, S. W. (2009). Mammalian nicotinic  
863 acetylcholine receptors: from structure to function. *Physiol Rev*, *89*(1), 73-120.  
864 doi:10.1152/physrev.00015.2008
- 865 Anagnostaras, S. G., Murphy, G. G., Hamilton, S. E., Mitchell, S. L., Rahnama, N. P., Nathanson, N. M.,  
866 & Silva, A. J. (2003). Selective cognitive dysfunction in acetylcholine M1 muscarinic receptor  
867 mutant mice. *Nat Neurosci*, *6*(1), 51-58. doi:10.1038/nn992
- 868 Andalman, A. S., & Fee, M. S. (2009). A basal ganglia-forebrain circuit in the songbird biases motor  
869 output to avoid vocal errors. *Proc Natl Acad Sci U S A*, *106*(30), 12518-12523.  
870 doi:10.1073/pnas.0903214106
- 871 Aronov, D., Andalman, A. S., & Fee, M. S. (2008). A specialized forebrain circuit for vocal babbling in  
872 the juvenile songbird. *Science*, *320*(5876), 630-634. doi:10.1126/science.1155140
- 873 Aronov, D., Veit, L., Goldberg, J. H., & Fee, M. S. (2011). Two distinct modes of forebrain circuit  
874 dynamics underlie temporal patterning in the vocalizations of young songbirds. *J Neurosci*,  
875 *31*(45), 16353-16368. doi:10.1523/JNEUROSCI.3009-11.2011
- 876 Asogwa, N. C., Mori, C., Sanchez-Valpuesta, M., Hayase, S., & Wada, K. (2018). Inter- and intra-  
877 specific differences in muscarinic acetylcholine receptor expression in the neural pathways  
878 for vocal learning in songbirds. *J Comp Neurol*, *526*(17), 2856-2869. doi:10.1002/cne.24532
- 879 Bell, Z. W., Lovell, P., Mello, C. V., Yip, P. K., George, J. M., & Clayton, D. F. (2019). Urotensin-related  
880 gene transcripts mark developmental emergence of the male forebrain vocal control system  
881 in songbirds. *Sci Rep*, *9*(1), 816. doi:10.1038/s41598-018-37057-w
- 882 Boord, R. L. (1968). Ascending projections of the primary cochlear nuclei and nucleus laminaris in  
883 the pigeon. *Journal of Comparative Neurology*, *133*(4), 523-541.
- 884 Bottjer, S. W., & Altenau, B. (2010). Parallel pathways for vocal learning in basal ganglia of songbirds.  
885 *Nat Neurosci*, *13*(2), 153-155. doi:10.1038/nn.2472
- 886 Bottjer, S. W., Miesner, E. A., & Arnold, A. P. (1984). Forebrain lesions disrupt development but not  
887 maintenance of song in passerine birds. *Science*, *224*(4651), 901-903.
- 888 Brainard, M. S., & Doupe, A. J. (2000). Interruption of a basal ganglia-forebrain circuit prevents  
889 plasticity of learned vocalizations. *Nature*, *404*(6779), 762-766. doi:10.1038/35008083
- 890 Brenowitz, E. A., & Beecher, M. D. (2005). Song learning in birds: diversity and plasticity,  
891 opportunities and challenges. *Trends Neurosci*, *28*(3), 127-132.  
892 doi:10.1016/j.tins.2005.01.004



893 Cardin, J. A., & Schmidt, M. F. (2003). Song system auditory responses are stable and highly tuned  
894 during sedation, rapidly modulated and unselective during wakefulness, and suppressed by  
895 arousal. *J Neurophysiol*, *90*(5), 2884-2899.

896 Colquitt, B. M., Merullo, D. P., Konopka, G., Roberts, T. F., & Brainard, M. S. (2021). Cellular  
897 transcriptomics reveals evolutionary identities of songbird vocal circuits. *Science*, *371*(6530).  
898 doi:10.1126/science.abd9704

899 Conner, J. M., Culbertson, A., Packowski, C., Chiba, A. A., & Tuszynski, M. H. (2003). Lesions of the  
900 basal forebrain cholinergic system impair task acquisition and abolish cortical plasticity  
901 associated with motor skill learning. *Neuron*, *38*(5), 819-829.

902 Couturier, S., Bertrand, D., Matter, J.-M., Hernandez, M.-C., Bertrand, S., Millar, N., . . . Ballivet, M.  
903 (1990). A neuronal nicotinic acetylcholine receptor subunit ( $\alpha 7$ ) is developmentally  
904 regulated and forms a homo-oligomeric channel blocked by  $\alpha$ -BTX. *Neuron*, *5*(6), 847-856.

905 Dajas-Bailador, F., & Wonnacott, S. (2004). Nicotinic acetylcholine receptors and the regulation of  
906 neuronal signalling. *Trends Pharmacol Sci*, *25*(6), 317-324. doi:10.1016/j.tips.2004.04.006

907 Dineley-Miller, K., & Patrick, J. (1992). Gene transcripts for the nicotinic acetylcholine receptor  
908 subunit, beta4, are distributed in multiple areas of the rat central nervous system. *Molecular*  
909 *Brain Research*, *16*(3), 339-344. doi:[https://doi.org/10.1016/0169-328X\(92\)90244-6](https://doi.org/10.1016/0169-328X(92)90244-6)

910 Doupe, A. J., & Kuhl, P. K. (1999). Birdsong and human speech: common themes and mechanisms.  
911 *Annu Rev Neurosci*, *22*, 567-631. doi:10.1146/annurev.neuro.22.1.567

912 Fu, Y., Tucciarone, J. M., Espinosa, J. S., Sheng, N., Darcy, D. P., Nicoll, R. A., . . . Stryker, M. P. (2014).  
913 A cortical circuit for gain control by behavioral state. *Cell*, *156*(6), 1139-1152.  
914 doi:10.1016/j.cell.2014.01.050

915 Gedman, G., Haase, B., Durieux, G., Biegler, M. T., Fedrigo, O., & Jarvis, E. D. (2021). As above, so  
916 below: Whole transcriptome profiling demonstrates strong molecular similarities between  
917 avian dorsal and ventral pallial subdivisions. *J Comp Neurol*. doi:10.1002/cne.25159

918 Gotti, C., & Clementi, F. (2004). Neuronal nicotinic receptors: from structure to pathology. *Prog*  
919 *Neurobiol*, *74*(6), 363-396. doi:10.1016/j.pneurobio.2004.09.006

920 Gotti, C., Clementi, F., Fornari, A., Gaimarri, A., Guiducci, S., Manfredi, I., . . . Zoli, M. (2009).  
921 Structural and functional diversity of native brain neuronal nicotinic receptors. *Biochem*  
922 *Pharmacol*, *78*(7), 703-711. doi:10.1016/j.bcp.2009.05.024

923 Halvorsen, S. W., & Berg, D. K. (1990). Subunit composition of nicotinic acetylcholine receptors from  
924 chick ciliary ganglia. *Journal of Neuroscience*, *10*(6), 1711-1718.

925 Han, Z.-Y., Le Novère, N., Zoli, M., Hill Jr, J. A., Champtiaux, N., & Changeux, J.-P. (2000). Localization  
926 of nAChR subunit mRNAs in the brain of *Macaca mulatta*. *European Journal of Neuroscience*,  
927 12(10), 3664-3674. doi:<https://doi.org/10.1046/j.1460-9568.2000.00262.x>

928 Hasselmo, M. E. (2006). The role of acetylcholine in learning and memory. *Curr Opin Neurobiol*, 16(6),  
929 710-715. doi:10.1016/j.conb.2006.09.002

930 Herrero, J. L., Roberts, M. J., Delicato, L. S., Gieselmann, M. A., Dayan, P., & Thiele, A. (2008).  
931 Acetylcholine contributes through muscarinic receptors to attentional modulation in V1.  
932 *Nature*, 454(7208), 1110-1114. doi:10.1038/nature07141

933 Jarvis, E. D., Gunturkun, O., Bruce, L., Csillag, A., Karten, H., Kuenzel, W., . . . Butler, A. B. (2005).  
934 Avian brains and a new understanding of vertebrate brain evolution. *Nat Rev Neurosci*, 6(2),  
935 151-159. doi:10.1038/nrn1606

936 Jarvis, E. D., Yu, J., Rivas, M. V., Horita, H., Feenders, G., Whitney, O., . . . Wada, K. (2013). Global  
937 view of the functional molecular organization of the avian cerebrum: mirror images and  
938 functional columns. *J Comp Neurol*, 521(16), 3614-3665. doi:10.1002/cne.23404

939 Kao, M. H., Doupe, A. J., & Brainard, M. S. (2005). Contributions of an avian basal ganglia-forebrain  
940 circuit to real-time modulation of song. *Nature*, 433(7026), 638-643.  
941 doi:10.1038/nature03127

942 Kruse, A. C., Kobilka, B. K., Gautam, D., Sexton, P. M., Christopoulos, A., & Wess, J. (2014). Muscarinic  
943 acetylcholine receptors: novel opportunities for drug development. *Nat Rev Drug Discov*,  
944 13(7), 549-560. doi:10.1038/nrd4295

945 Kubikova, L., Wada, K., & Jarvis, E. D. (2010). Dopamine receptors in a songbird brain. *J Comp Neurol*,  
946 518(6), 741-769. doi:10.1002/cne.22255

947 Le Novere, N., Corringier, P. J., & Changeux, J. P. (2002). The diversity of subunit composition in  
948 nAChRs: evolutionary origins, physiologic and pharmacologic consequences. *J Neurobiol*,  
949 53(4), 447-456. doi:10.1002/neu.10153

950 Le Novere, N., Zoli, M., & Changeux, J. P. (1996). Neuronal nicotinic receptor  $\alpha 6$  subunit mRNA is  
951 selectively concentrated in catecholaminergic nuclei of the rat brain. *European Journal of*  
952 *Neuroscience*, 8(11), 2428-2439.

953 Lein, E. S., Hawrylycz, M. J., Ao, N., Ayres, M., Bensinger, A., Bernard, A., . . . Jones, A. R. (2007).  
954 Genome-wide atlas of gene expression in the adult mouse brain. *Nature*, 445(7124), 168-  
955 176. doi:10.1038/nature05453

956 Li, H. Q., & Spitzer, N. C. (2020). Exercise enhances motor skill learning by neurotransmitter  
957 switching in the adult midbrain. *Nat Commun*, 11(1), 2195. doi:10.1038/s41467-020-16053-  
958 7

959 Li, R., & Sakaguchi, H. (1997). Cholinergic innervation of the song control nuclei by the ventral  
960 paleostriatum in the zebra finch: a double-labeling study with retrograde fluorescent tracers  
961 and choline acetyltransferase immunohistochemistry. *Brain Res*, 763(2), 239-246.

962 Liu, Q., Huang, Y., Shen, J., Steffensen, S., & Wu, J. (2012). Functional  $\alpha 7\beta 2$  nicotinic acetylcholine  
963 receptors expressed in hippocampal interneurons exhibit high sensitivity to pathological  
964 level of amyloid  $\beta$  peptides. *BMC Neurosci*, 13(1), 155. doi:10.1186/1471-2202-13-155

965 Liu, Q., Huang, Y., Xue, F., Simard, A., DeChon, J., Li, G., . . . Wu, J. (2009). A novel nicotinic  
966 acetylcholine receptor subtype in basal forebrain cholinergic neurons with high sensitivity  
967 to amyloid peptides. *J Neurosci*, 29(4), 918-929. doi:10.1523/JNEUROSCI.3952-08.2009

968 Lovell, P. V., Clayton, D. F., Replogle, K. L., & Mello, C. V. (2008). Birdsong "transcriptomics":  
969 neurochemical specializations of the oscine song system. *PLoS One*, 3(10), e3440.  
970 doi:10.1371/journal.pone.0003440

971 Lovell, P. V., Huizinga, N. A., Friedrich, S. R., Wirthlin, M., & Mello, C. V. (2018). The constitutive  
972 differential transcriptome of a brain circuit for vocal learning. *BMC Genomics*, 19(1), 231.  
973 doi:10.1186/s12864-018-4578-0

974 Lovell, P. V., Wirthlin, M., Kaser, T., Buckner, A. A., Carleton, J. B., Snider, B. R., . . . Mello, C. V. (2020).  
975 ZEBRA: Zebra finch Expression Brain Atlas-A resource for comparative molecular  
976 neuroanatomy and brain evolution studies. *J Comp Neurol*, 528(12), 2099-2131.  
977 doi:10.1002/cne.24879

978 Luo, M., Ding, L., & Perkel, D. J. (2001). An avian basal ganglia pathway essential for vocal learning  
979 forms a closed topographic loop. *J Neurosci*, 21(17), 6836-6845.

980 Marler, P., & Slabbekoorn, H. (2004). *Nature's Music: The Science of Birdsong*: Elsevier Academic  
981 Press.

982 Medina, L., & Reiner, A. (2000). Do birds possess homologues of mammalian primary visual,  
983 somatosensory and motor cortices? *Trends Neurosci*, 23(1), 1-12.

984 Mello, C. V., Kaser, T., Buckner, A. A., Wirthlin, M., & Lovell, P. V. (2019). Molecular architecture of  
985 the zebra finch arcopallium. *J Comp Neurol*. doi:10.1002/cne.24688

986 Meng, W., Wang, S., Yao, L., Zhang, N., & Li, D. (2017). Muscarinic Receptors Are Responsible for the  
987 Cholinergic Modulation of Projection Neurons in the Song Production Brain Nucleus RA of  
988 Zebra Finches. *Front Cell Neurosci*, 11, 51. doi:10.3389/fncel.2017.00051

989 Morris, B. J., Hicks, A. A., Wisden, W., Darlison, M. G., Hunt, S. P., & Barnard, E. A. (1990). Distinct  
990 regional expression of nicotinic acetylcholine receptor genes in chick brain. *Molecular Brain  
991 Research*, 7(4), 305-315. doi:[https://doi.org/10.1016/0169-328X\(90\)90081-N](https://doi.org/10.1016/0169-328X(90)90081-N)

992 Nottebohm, F., Stokes, T. M., & Leonard, C. M. (1976). Central control of song in the canary, *Serinus*  
993 *canarius*. *J Comp Neurol*, *165*(4), 457-486. doi:10.1002/cne.901650405

994 Noudoost, B., & Moore, T. (2011). The role of neuromodulators in selective attention. *Trends Cogn*  
995 *Sci*, *15*(12), 585-591. doi:10.1016/j.tics.2011.10.006

996 Ölveczky, B. P., Andalman, A. S., & Fee, M. S. (2005). Vocal Experimentation in the Juvenile Songbird  
997 Requires a Basal Ganglia Circuit. *PLoS Biol.*, *3*(5), e153.  
998 doi:10.1371/journal.pbio.0030153.g001

999 Parikh, V., Kozak, R., Martinez, V., & Sarter, M. (2007). Prefrontal acetylcholine release controls cue  
1000 detection on multiple timescales. *Neuron*, *56*(1), 141-154.

1001 Pedersen, J. E., Bergqvist, C. A., & Larhammar, D. (2019). Evolution of vertebrate nicotinic  
1002 acetylcholine receptors. *BMC Evol Biol*, *19*(1), 38. doi:10.1186/s12862-018-1341-8

1003 Puzerey, P. A., Maher, K., Prasad, N., & Goldberg, J. H. (2018). Vocal learning in songbirds requires  
1004 cholinergic signaling in a motor cortex-like nucleus. *J Neurophysiol*, *120*(4), 1796-1806.

1005 Ramon y Cajal, S. (1911). Histologie du système nerveux de l'homme et des vertébrés. *Maloine, Paris*,  
1006 *2*, 153-173.

1007 Reiner, A., Perkel, D. J., Bruce, L. L., Butler, A. B., Csillag, A., Kuenzel, W., . . . Avian Brain  
1008 Nomenclature, F. (2004). Revised nomenclature for avian telencephalon and some related  
1009 brainstem nuclei. *J Comp Neurol*, *473*(3), 377-414. doi:10.1002/cne.20118

1010 Role, L. W., & Berg, D. K. (1996). Nicotinic Receptors in the Development and Modulation of CNS  
1011 Synapses. *Neuron*, *16*(6), 1077-1085. doi:10.1016/s0896-6273(00)80134-8

1012 Ryan, S. M., & Arnold, A. P. (1981). Evidence for cholinergic participation in the control of bird song;  
1013 acetylcholinesterase distribution and muscarinic receptor autoradiography in the zebra  
1014 finch brain. *J Comp Neurol*, *202*(2), 211-219. doi:10.1002/cne.902020207

1015 Sadananda, M. (2004). Acetylcholinesterase in central vocal control nuclei of the zebra finch  
1016 (*Taeniopygia guttata*). *J Biosci*, *29*(2), 189-200.

1017 Sakaguchi, H., & Saito, N. (1989). The acetylcholine and catecholamine contents in song control  
1018 nuclei of zebra finch during song ontogeny. *Developmental Brain Research*, *47*(2), 313-317.

1019 Sakaguchi, H., & Saito, N. (1991). Developmental change of cholinergic activity in the forebrain of  
1020 the zebra finch during song learning. *Developmental Brain Research*, *62*(2), 223-228.

1021 Salgado-Commissariat, D., Rosenfield, D. B., & Helekar, S. A. (2004). Nicotine-mediated plasticity in  
1022 robust nucleus of the archistriatum of the adult zebra finch. *Brain Res*, *1018*(1), 97-105.  
1023 doi:10.1016/j.brainres.2004.05.051

1024 Sargent, P. B. (1993). The diversity of neuronal nicotinic acetylcholine receptors. *Annual Review of*  
1025 *Neuroscience*, *16*(1), 403-443.

1026 Sarter, M., Bruno, J. P., & Turchi, J. (1999). Basal forebrain afferent projections modulating cortical  
1027 acetylcholine, attention, and implications for neuropsychiatric disorders. *Ann N Y Acad Sci*,  
1028 877, 368-382.

1029 Saunders, A., Macosko, E. Z., Wysoker, A., Goldman, M., Krienen, F. M., de Rivera, H., . . . McCarroll,  
1030 S. A. (2018). Molecular Diversity and Specializations among the Cells of the Adult Mouse  
1031 Brain. *Cell*, 174(4), 1015-1030 e1016. doi:10.1016/j.cell.2018.07.028

1032 Scharff, C., & Nottebohm, F. (1991). A comparative study of the behavioral deficits following lesions  
1033 of various parts of the zebra finch song system: implications for vocal learning. *J Neurosci*,  
1034 11(9), 2896-2913.

1035 Schmidt, M. F., & Konishi, M. (1998). Gating of auditory responses in the vocal control system of  
1036 awake songbirds. *Nat Neurosci*, 1(6), 513.

1037 Schryver, H. M., & Mysore, S. P. (2019). Spatial dependence of stimulus competition in the avian  
1038 nucleus isthmi pars magnocellularis. *Brain Behav Evol*, 93(2-3), 137-151.

1039 Scully, E. N., Acerbo, M. J., & Lazareva, O. F. (2014). Bilateral lesions of nucleus  
1040 subpretectalis/interstitio-pretecto-subpretectalis (SP/IPS) selectively impair figure-ground  
1041 discrimination in pigeons. *Vis Neurosci*, 31(1), 105-110. doi:10.1017/S0952523813000424

1042 Shea, S. D., Koch, H., Baleckaitis, D., Ramirez, J. M., & Margoliash, D. (2010). Neuron-specific  
1043 cholinergic modulation of a forebrain song control nucleus. *J Neurophysiol*, 103(2), 733-745.  
1044 doi:10.1152/jn.00803.2009

1045 Shea, S. D., & Margoliash, D. (2003). Basal forebrain cholinergic modulation of auditory activity in  
1046 the zebra finch song system. *Neuron*, 40(6), 1213-1226. doi:10.1016/s0896-6273(03)00723-  
1047 2

1048 Shea, S. D., & Margoliash, D. (2010). Behavioral state-dependent reconfiguration of song-related  
1049 network activity and cholinergic systems. *J Chem Neuroanat*, 39(2), 132-140.  
1050 doi:10.1016/j.jchemneu.2009.10.002

1051 Stuart, T., Butler, A., Hoffman, P., Hafemeister, C., Papalexi, E., Mauck, W. M., 3rd, . . . Satija, R.  
1052 (2019). Comprehensive Integration of Single-Cell Data. *Cell*, 177(7), 1888-1902 e1821.  
1053 doi:10.1016/j.cell.2019.05.031

1054 Tasic, B., Menon, V., Nguyen, T. N., Kim, T. K., Jarsky, T., Yao, Z., . . . Zeng, H. (2016). Adult mouse  
1055 cortical cell taxonomy revealed by single cell transcriptomics. *Nat Neurosci*, 19(2), 335-346.  
1056 doi:10.1038/nn.4216

1057 Tasic, B., Yao, Z., Graybuck, L. T., Smith, K. A., Nguyen, T. N., Bertagnolli, D., . . . Zeng, H. (2018).  
1058 Shared and distinct transcriptomic cell types across neocortical areas. *Nature*, 563(7729),  
1059 72-78. doi:10.1038/s41586-018-0654-5

1060 Thomsen, M. S., Zwart, R., Ursu, D., Jensen, M. M., Pinborg, L. H., Gilmour, G., . . . Mikkelsen, J. D.  
1061 (2015). alpha7 and beta2 Nicotinic Acetylcholine Receptor Subunits Form Heteromeric  
1062 Receptor Complexes that Are Expressed in the Human Cortex and Display Distinct  
1063 Pharmacological Properties. *PLoS One*, *10*(6), e0130572. doi:10.1371/journal.pone.0130572  
1064 Thouvarecq, R., Protais, P., Jouen, F., & Caston, J. (2001). Influence of cholinergic system on motor  
1065 learning during aging in mice. *Behav Brain Res*, *118*(2), 209-218.  
1066 Wada, K., Ballivet, M., Boulter, J., Connolly, J., Wada, E., Deneris, E. S., . . . Patrick, J. (1988).  
1067 Functional expression of a new pharmacological subtype of brain nicotinic acetylcholine  
1068 receptor. *Science*, *240*(4850), 330-334. doi:10.1126/science.2832952  
1069 Wada, K., Sakaguchi, H., Jarvis, E. D., & Hagiwara, M. (2004). Differential expression of glutamate  
1070 receptors in avian neural pathways for learned vocalization. *J Comp Neurol*, *476*(1), 44-64.  
1071 doi:10.1002/cne.20201  
1072 Wallace, T. L., & Bertrand, D. (2013). Importance of the nicotinic acetylcholine receptor system in  
1073 the prefrontal cortex. *Biochem Pharmacol*, *85*(12), 1713-1720.  
1074 doi:10.1016/j.bcp.2013.04.001  
1075 Watson, J. T., Adkins - Regan, E., Whiting, P., Lindstrom, J. M., & Podleski, T. R. (1988).  
1076 Autoradiographic localization of nicotinic acetylcholine receptors in the brain of the zebra  
1077 finch (*Poephila guttata*). *Journal of Comparative Neurology*, *274*(2), 255-264.  
1078 Whiting, P., Schoepfer, R., Conroy, W., Gore, M., Keyser, K., Shimasaki, S., . . . Lindstrom, J. (1991).  
1079 Expression of nicotinic acetylcholine receptor subtypes in brain and retina. *Molecular Brain*  
1080 *Research*, *10*(1), 61-70.  
1081 Winzer-Serhan, U. H., & Leslie, F. M. (1997). Codistribution of nicotinic acetylcholine receptor  
1082 subunit  $\alpha 3$  and  $\beta 4$  mRNAs during rat brain development. *Journal of Comparative Neurology*,  
1083 *386*(4), 540-554. doi:[https://doi.org/10.1002/\(SICI\)1096-9861\(19971006\)386:4<540::AID-](https://doi.org/10.1002/(SICI)1096-9861(19971006)386:4<540::AID-CNE2>3.0.CO;2-2)  
1084 [CNE2>3.0.CO;2-2](https://doi.org/10.1002/(SICI)1096-9861(19971006)386:4<540::AID-CNE2>3.0.CO;2-2)  
1085 Wonnacott, S. (1997). Presynaptic nicotinic ACh receptors. *Trends Neurosci*, *20*(2), 92-98.  
1086 doi:[https://doi.org/10.1016/S0166-2236\(96\)10073-4](https://doi.org/10.1016/S0166-2236(96)10073-4)  
1087 Woolley, S. M., & Portfors, C. V. (2013). Conserved mechanisms of vocalization coding in mammalian  
1088 and songbird auditory midbrain. *Hear Res*, *305*, 45-56. doi:10.1016/j.heares.2013.05.005  
1089 Wylie, D. R., Gutierrez-Ibanez, C., Pakan, J. M., & Iwaniuk, A. N. (2009). The optic tectum of birds:  
1090 mapping our way to understanding visual processing. *Can J Exp Psychol*, *63*(4), 328-338.  
1091 doi:10.1037/a0016826  
1092 Zhang, Y., Chen, K., Sloan, S. A., Bennett, M. L., Scholze, A. R., O'Keeffe, S., . . . Wu, J. Q. (2014). An  
1093 RNA-sequencing transcriptome and splicing database of glia, neurons, and vascular cells of

1094 the cerebral cortex. *J Neurosci*, 34(36), 11929-11947. doi:10.1523/JNEUROSCI.1860-  
1095 14.2014

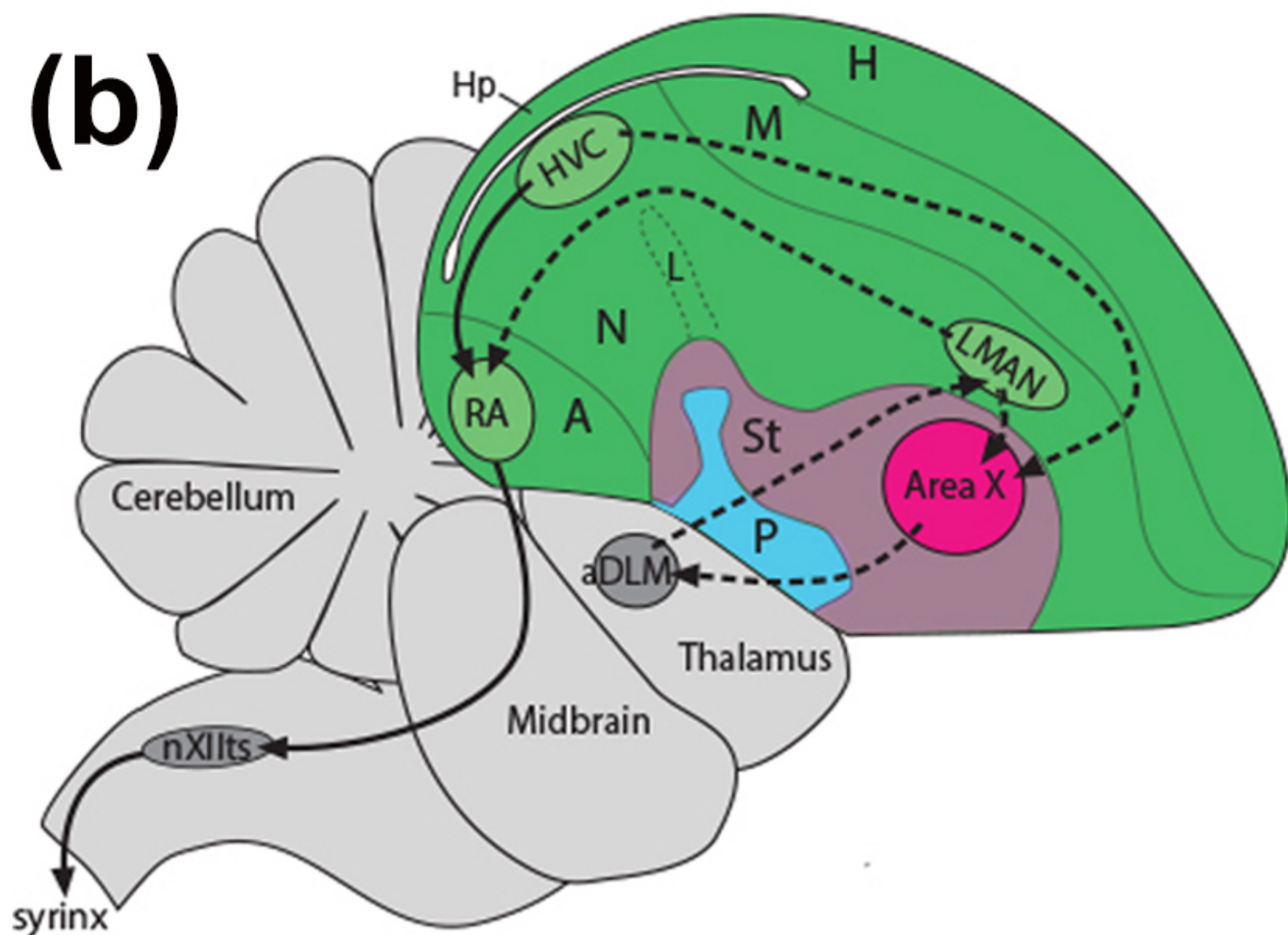
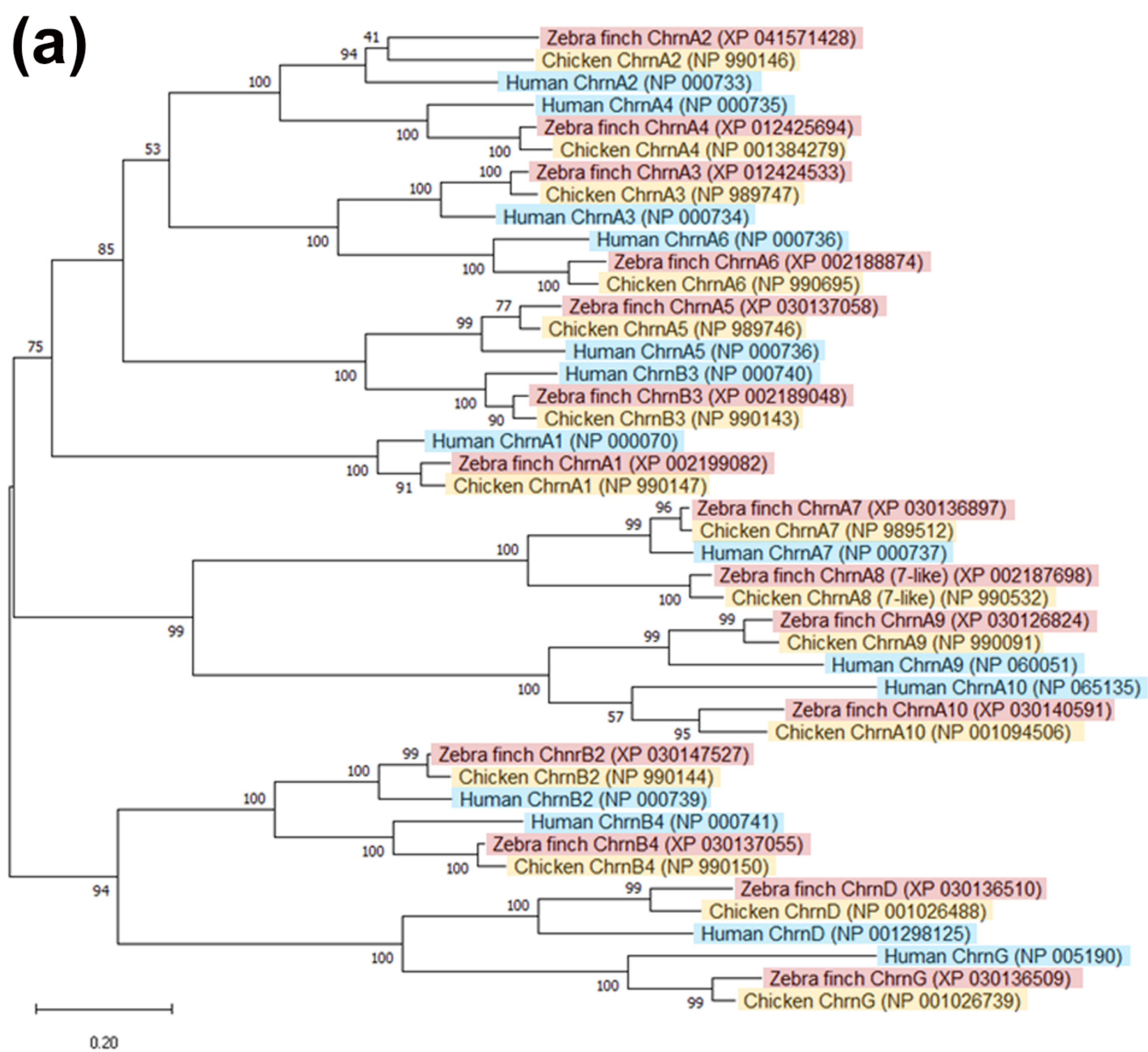
1096 Zoli, M., Le Novere, N., Hill, J. A., & Changeux, J.-P. (1995). Developmental regulation of nicotinic  
1097 ACh receptor subunit mRNAs in the rat central and peripheral nervous systems. *Journal of*  
1098 *Neuroscience*, 15(3), 1912-1939.

1099 Zoli, M., Pistillo, F., & Gotti, C. (2015). Diversity of native nicotinic receptor subtypes in mammalian  
1100 brain. *Neuropharmacology*, 96(Pt B), 302-311. doi:10.1016/j.neuropharm.2014.11.003

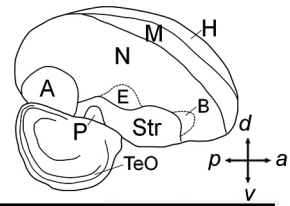
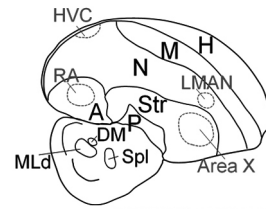
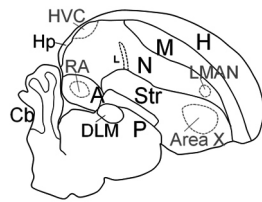
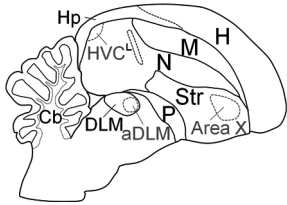
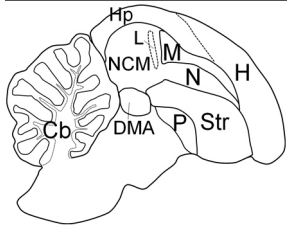
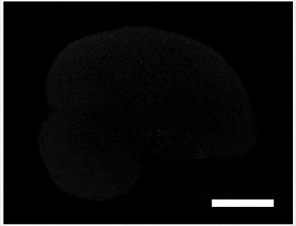
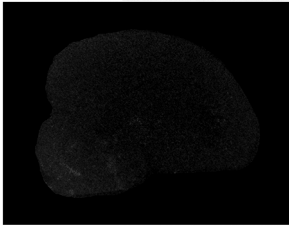
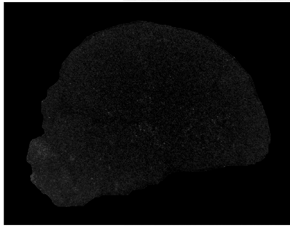
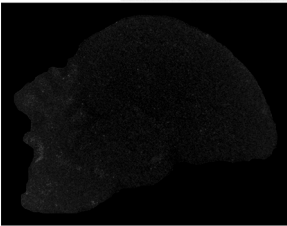
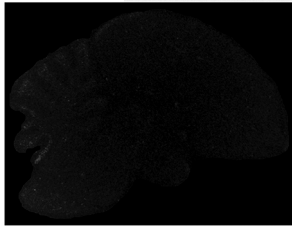
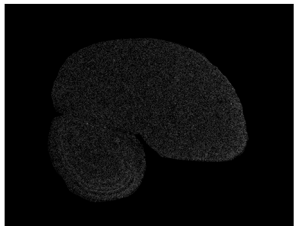
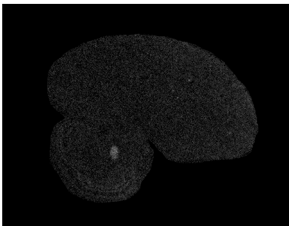
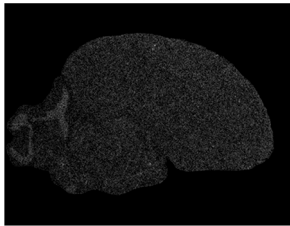
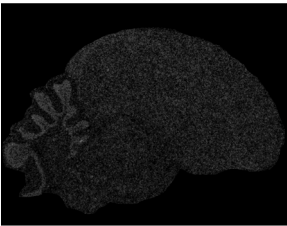
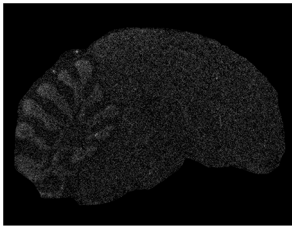
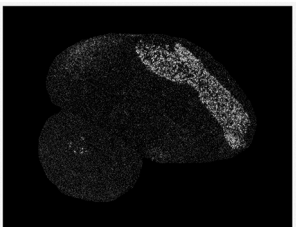
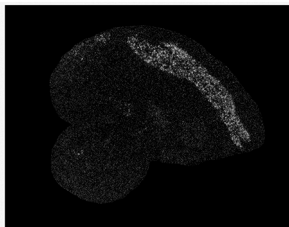
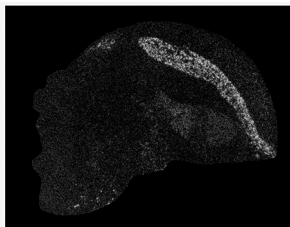
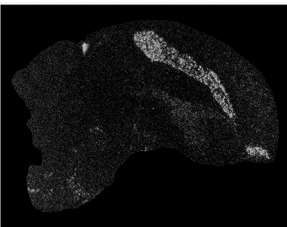
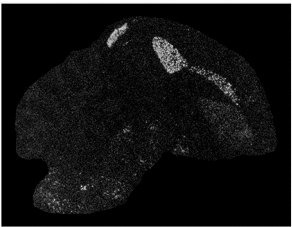
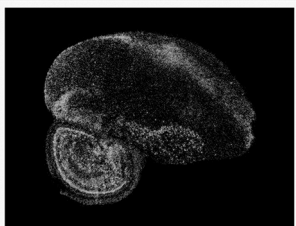
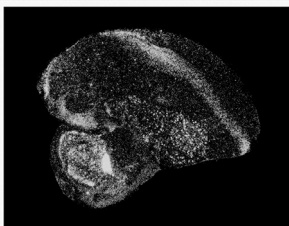
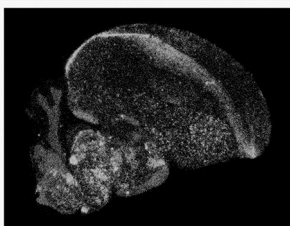
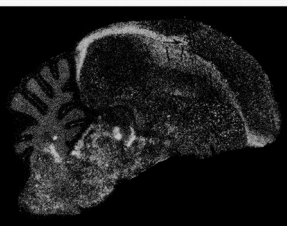
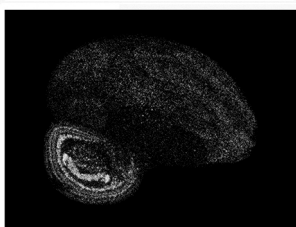
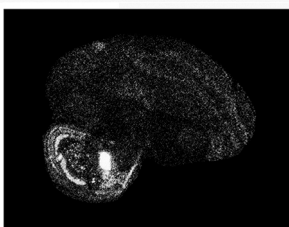
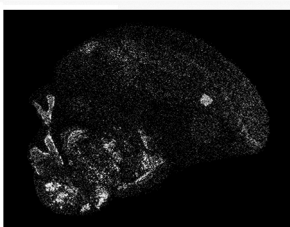
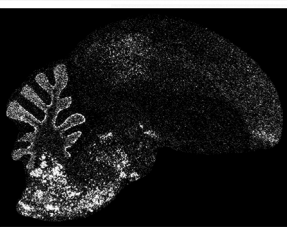
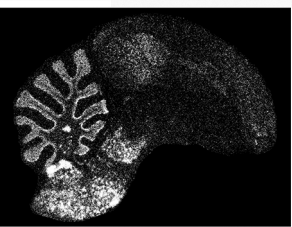
1101 Zoli, M., Pucci, S., Vilella, A., & Gotti, C. (2018). Neuronal and Extraneuronal Nicotinic Acetylcholine  
1102 Receptors. *Curr Neuropharmacol*, 16(4), 338-349.  
1103 doi:10.2174/1570159X15666170912110450

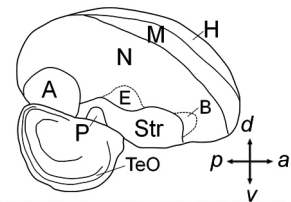
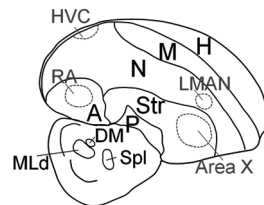
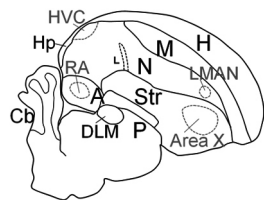
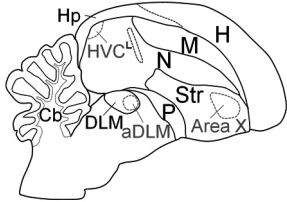
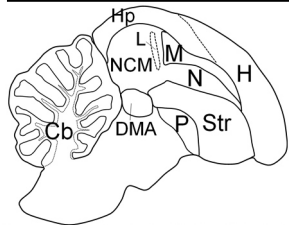
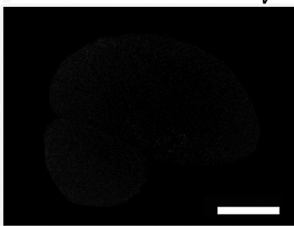
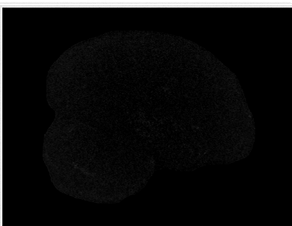
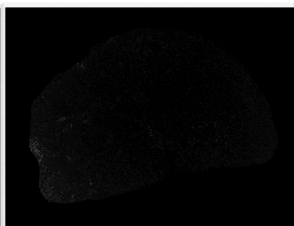
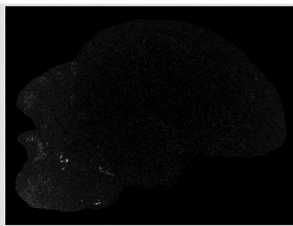
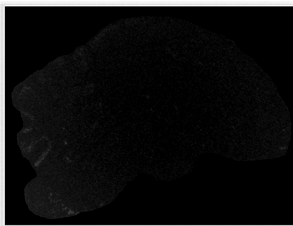
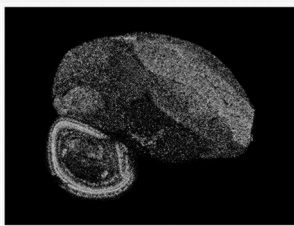
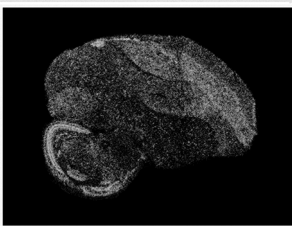
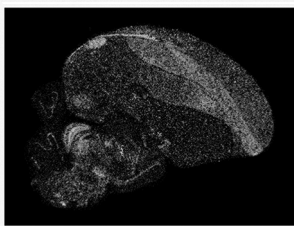
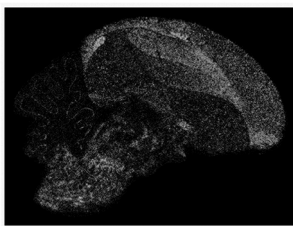
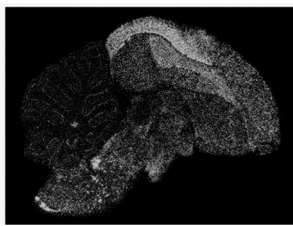
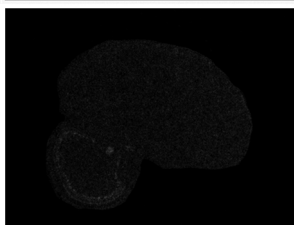
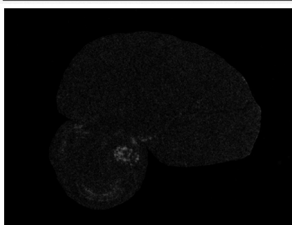
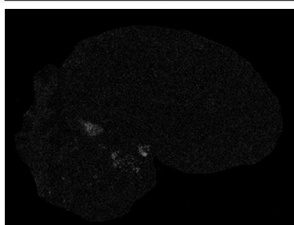
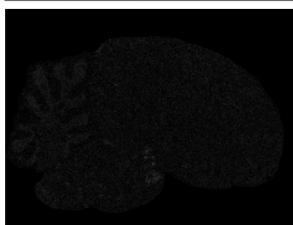
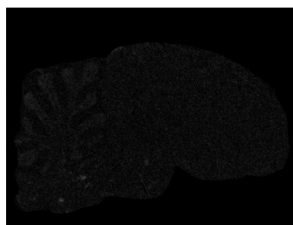
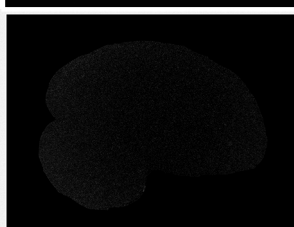
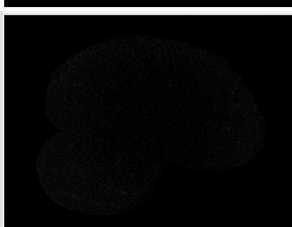
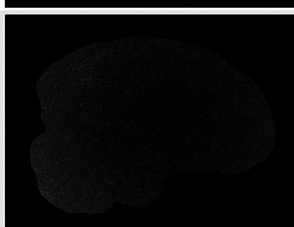
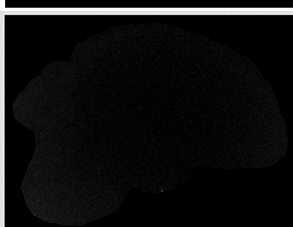
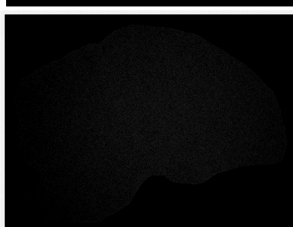
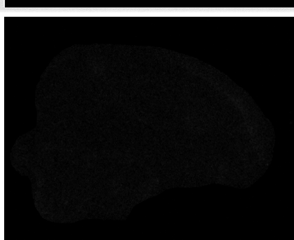
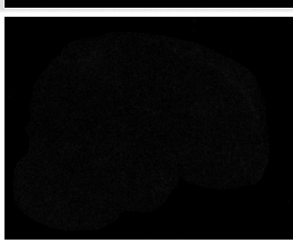
1104 Zuschratter, W., & Scheich, H. (1990). Distribution of choline acetyltransferase and  
1105 acetylcholinesterase in the vocal motor system of zebra finches. *Brain Res*, 513(2), 193-201.  
1106 doi:[https://doi.org/10.1016/0006-8993\(90\)90457-M](https://doi.org/10.1016/0006-8993(90)90457-M)

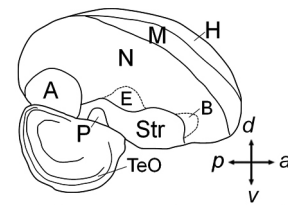
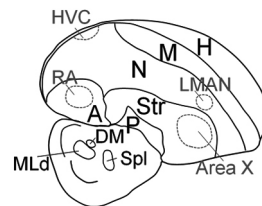
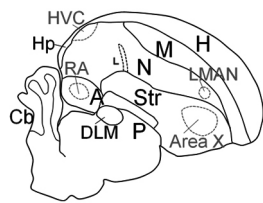
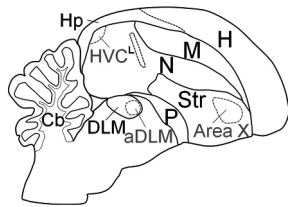
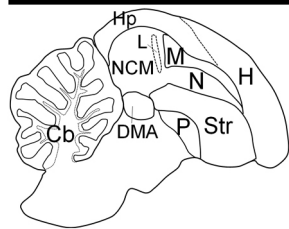
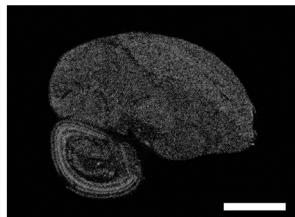
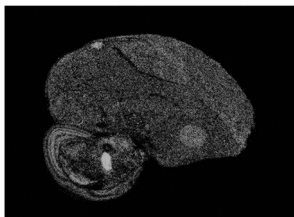
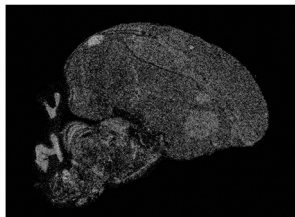
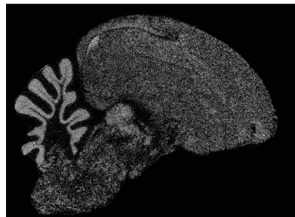
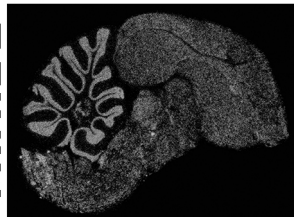
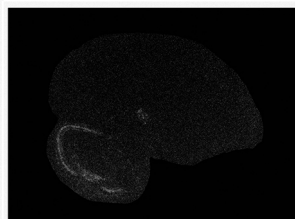
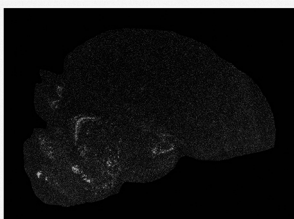
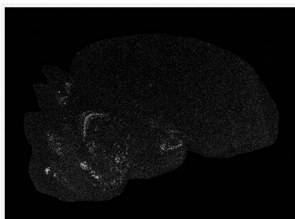
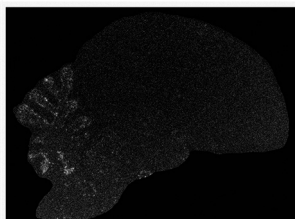
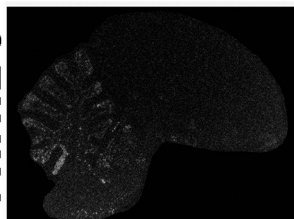
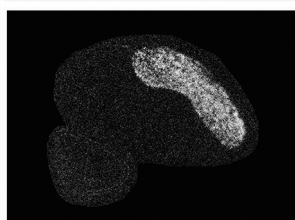
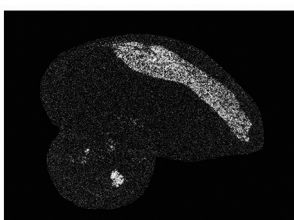
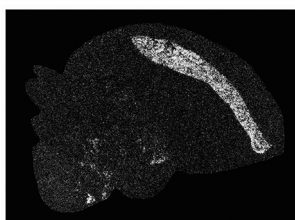
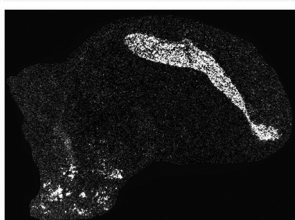
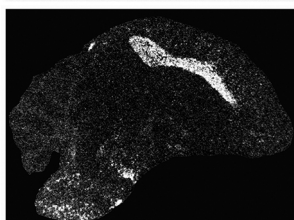
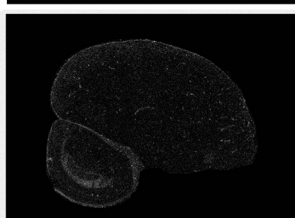
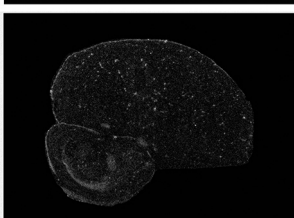
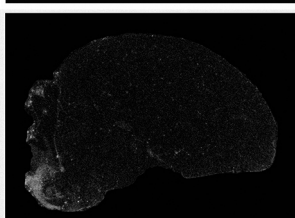
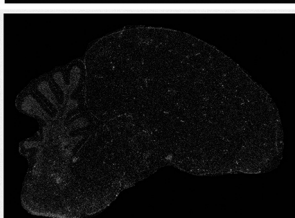
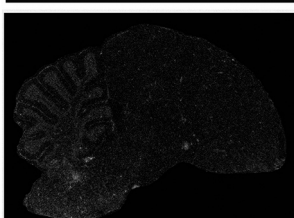
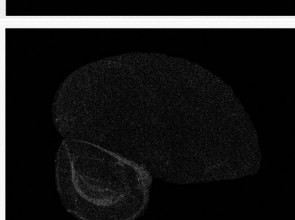
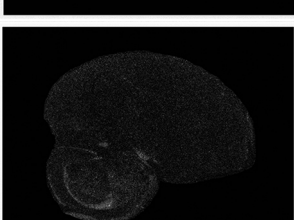
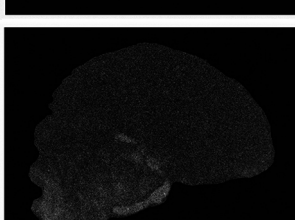
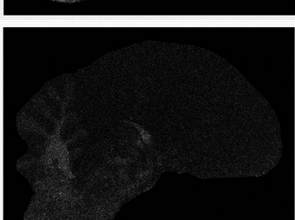
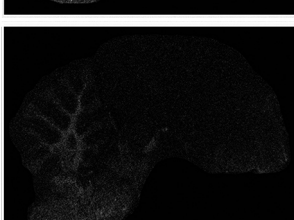
1107  
1108

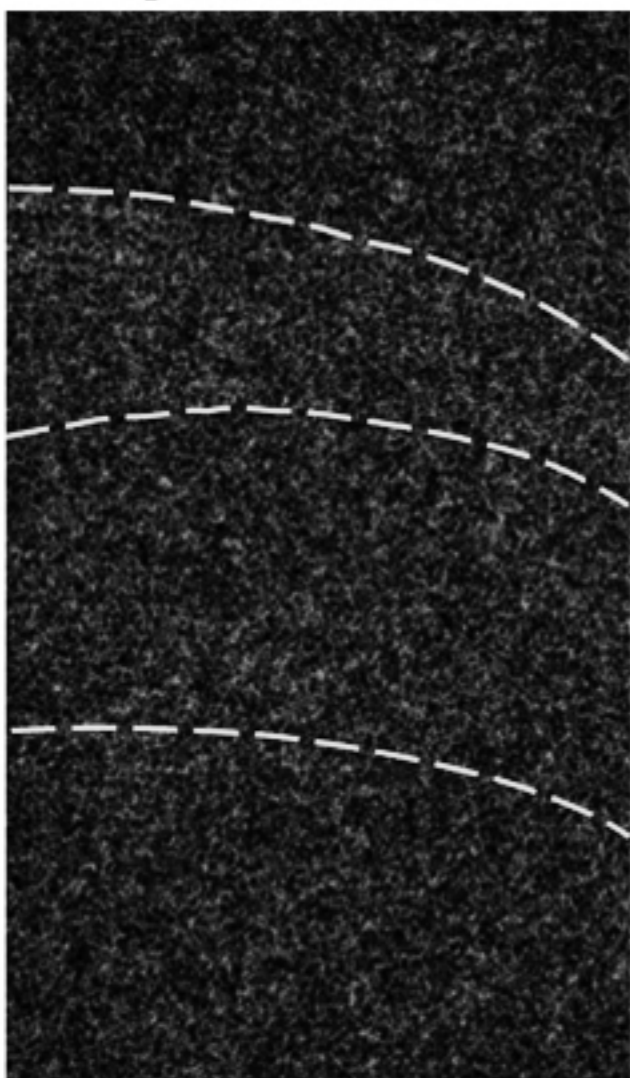
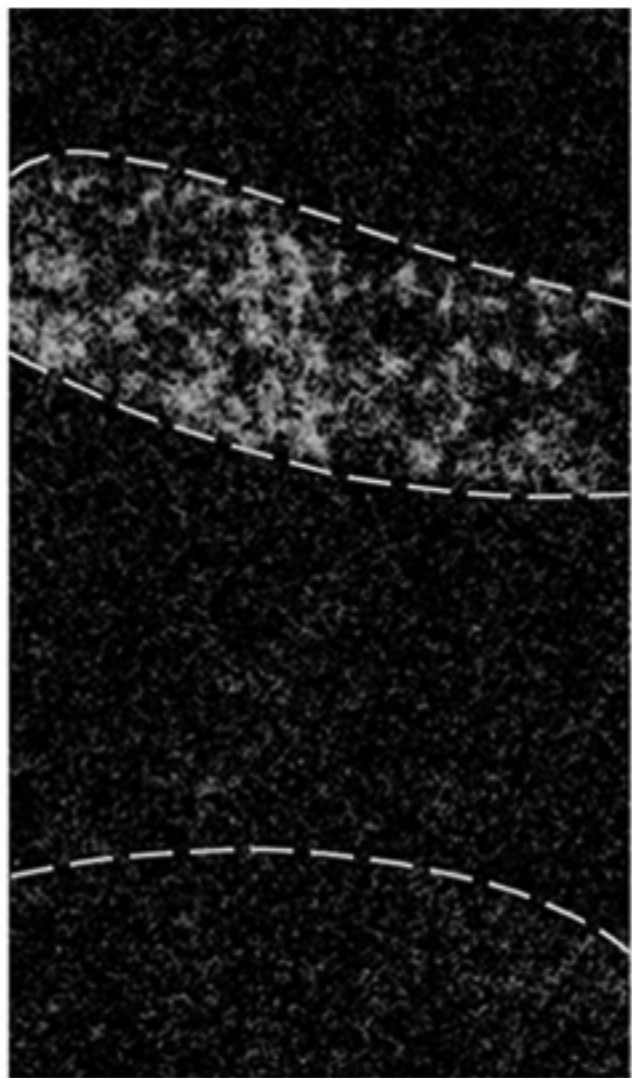
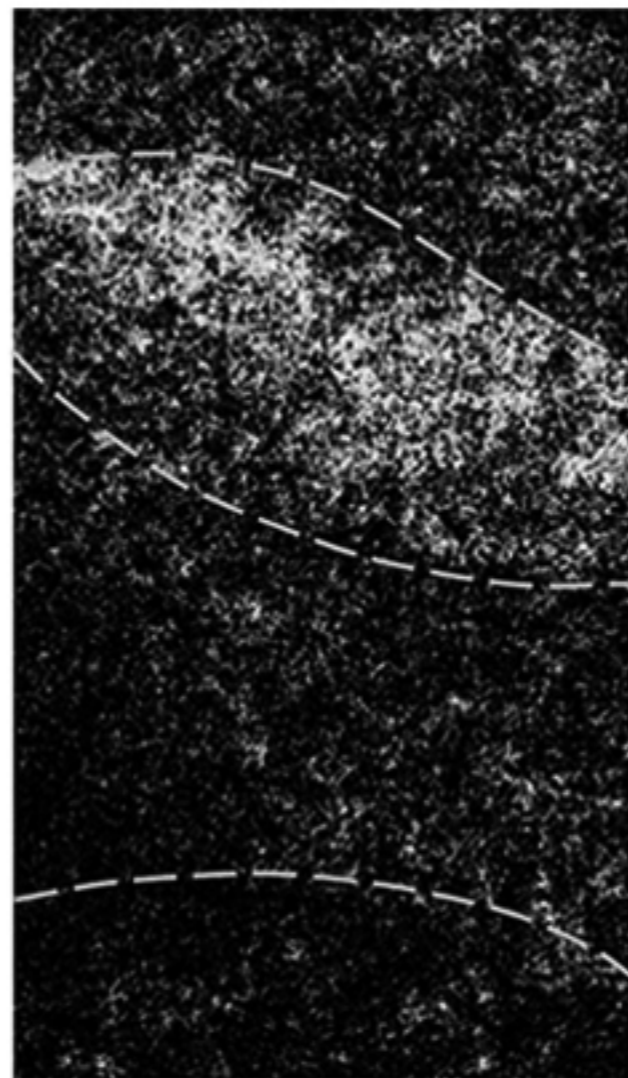
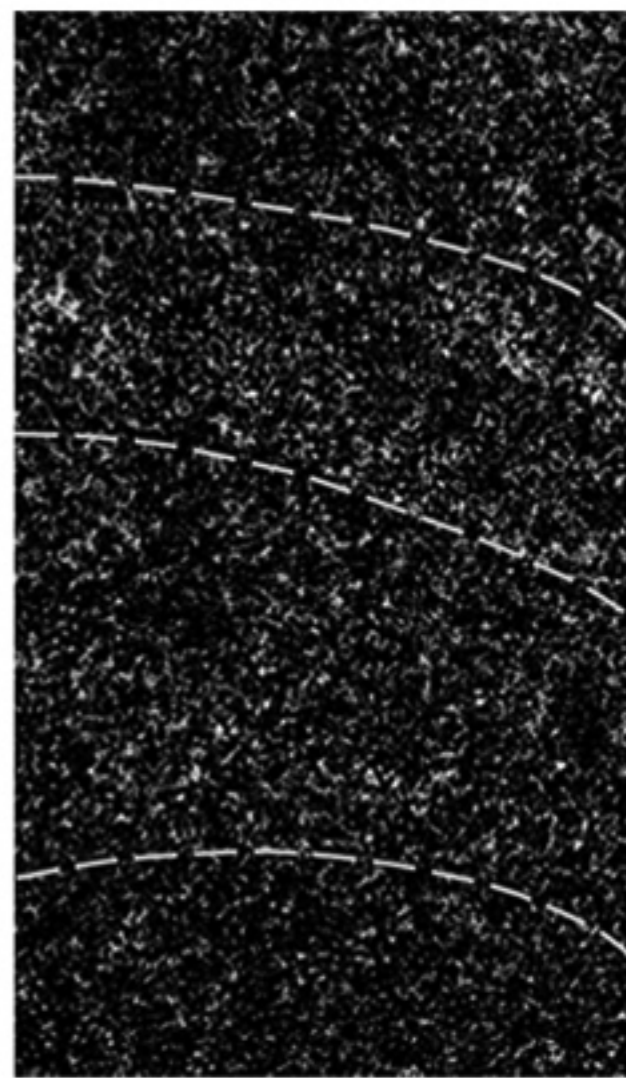
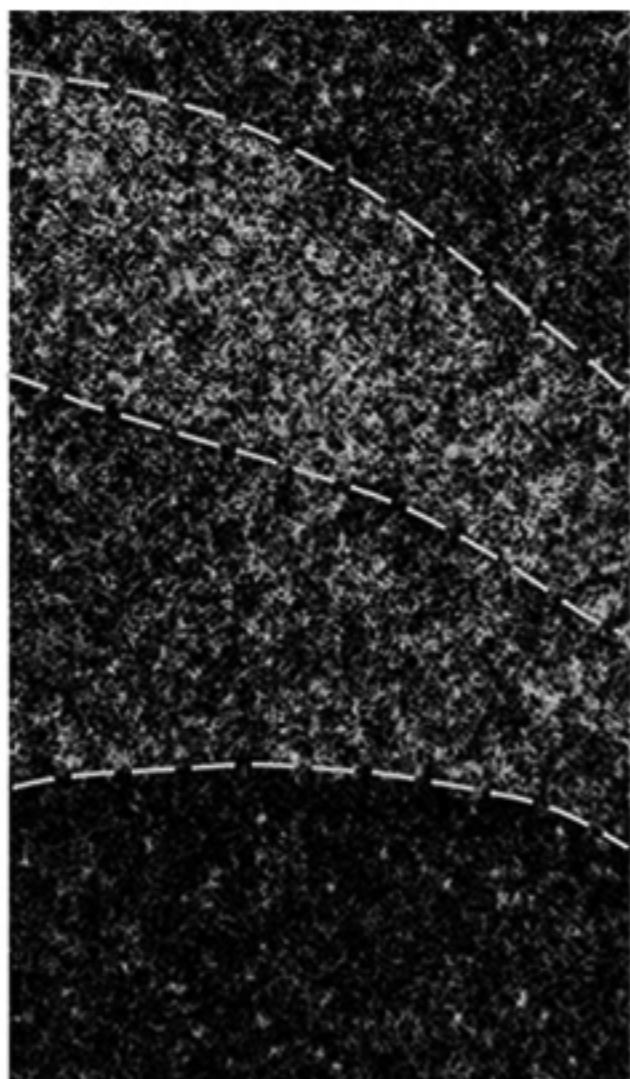
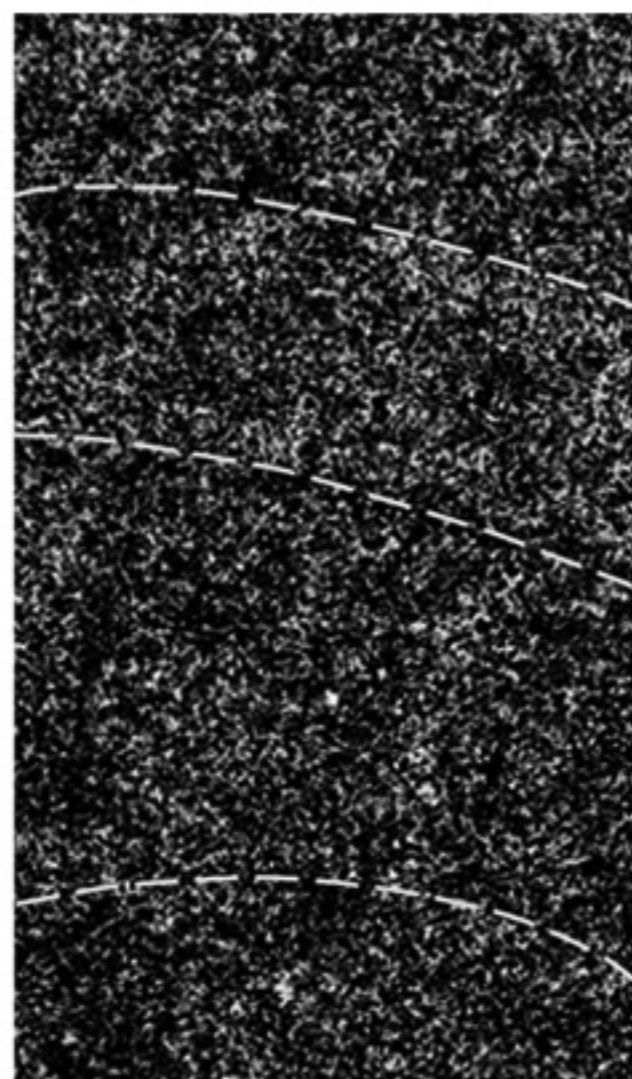
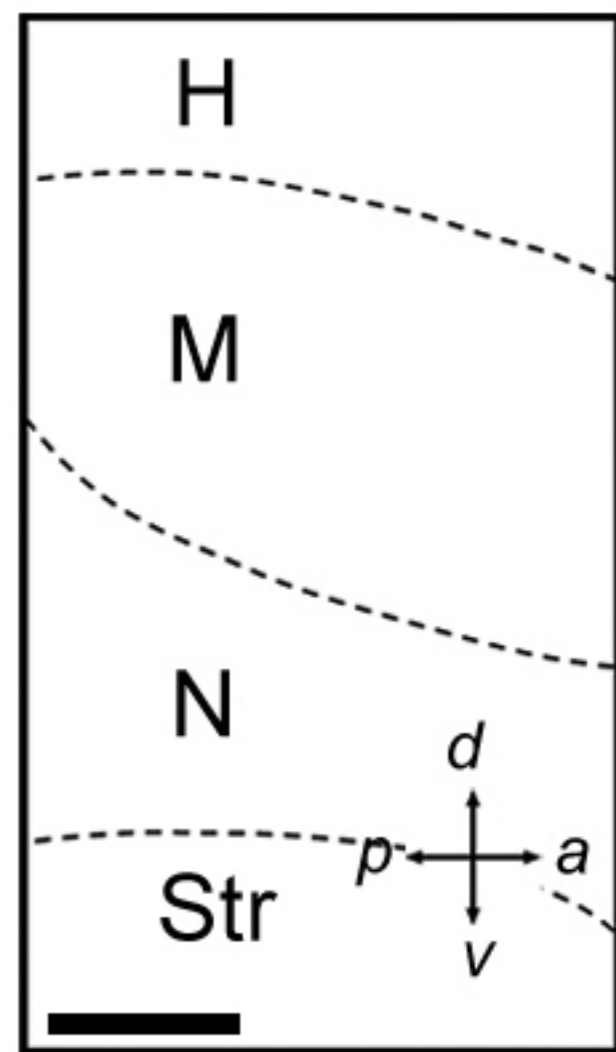
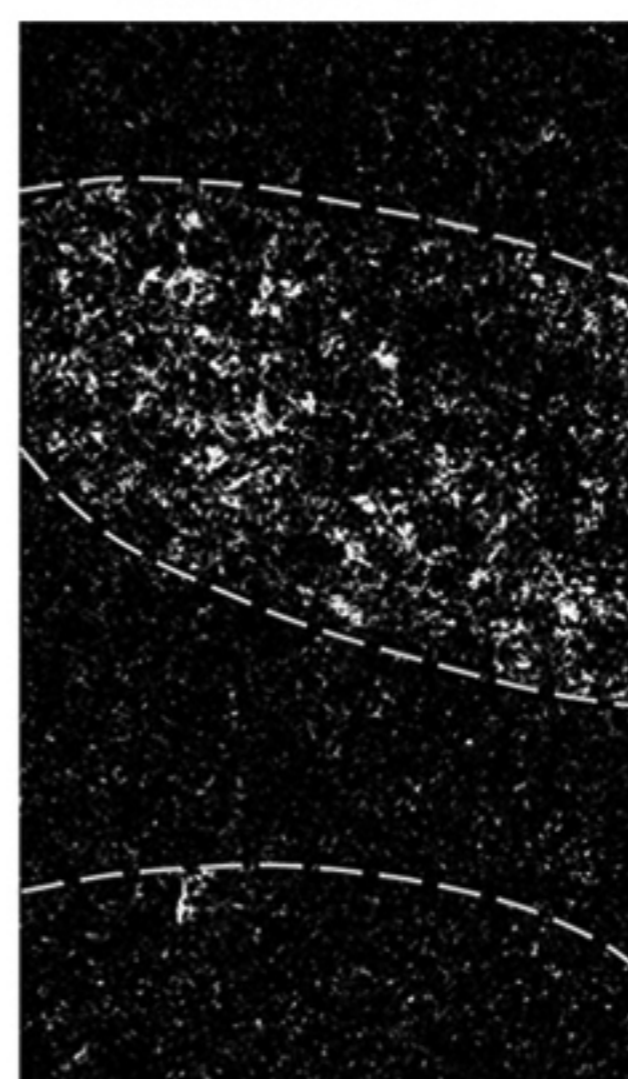


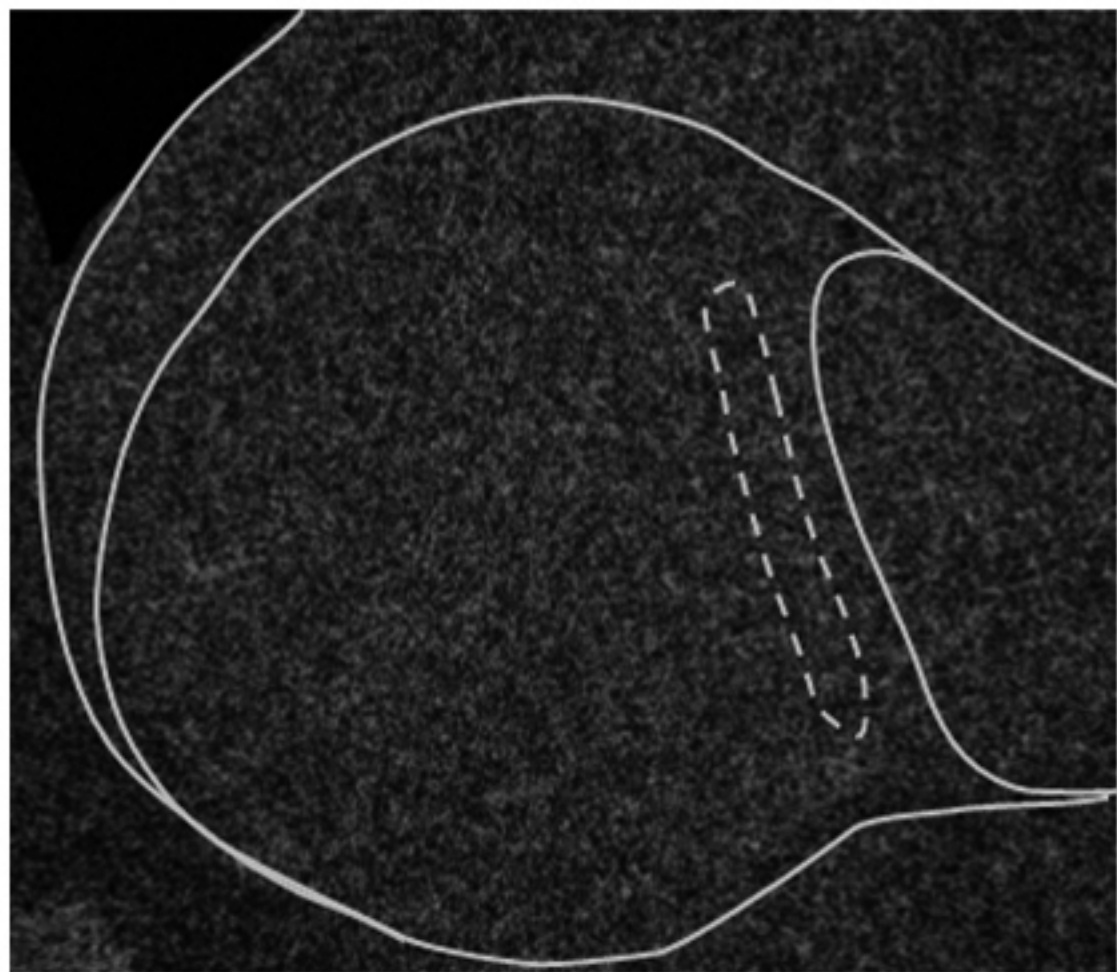
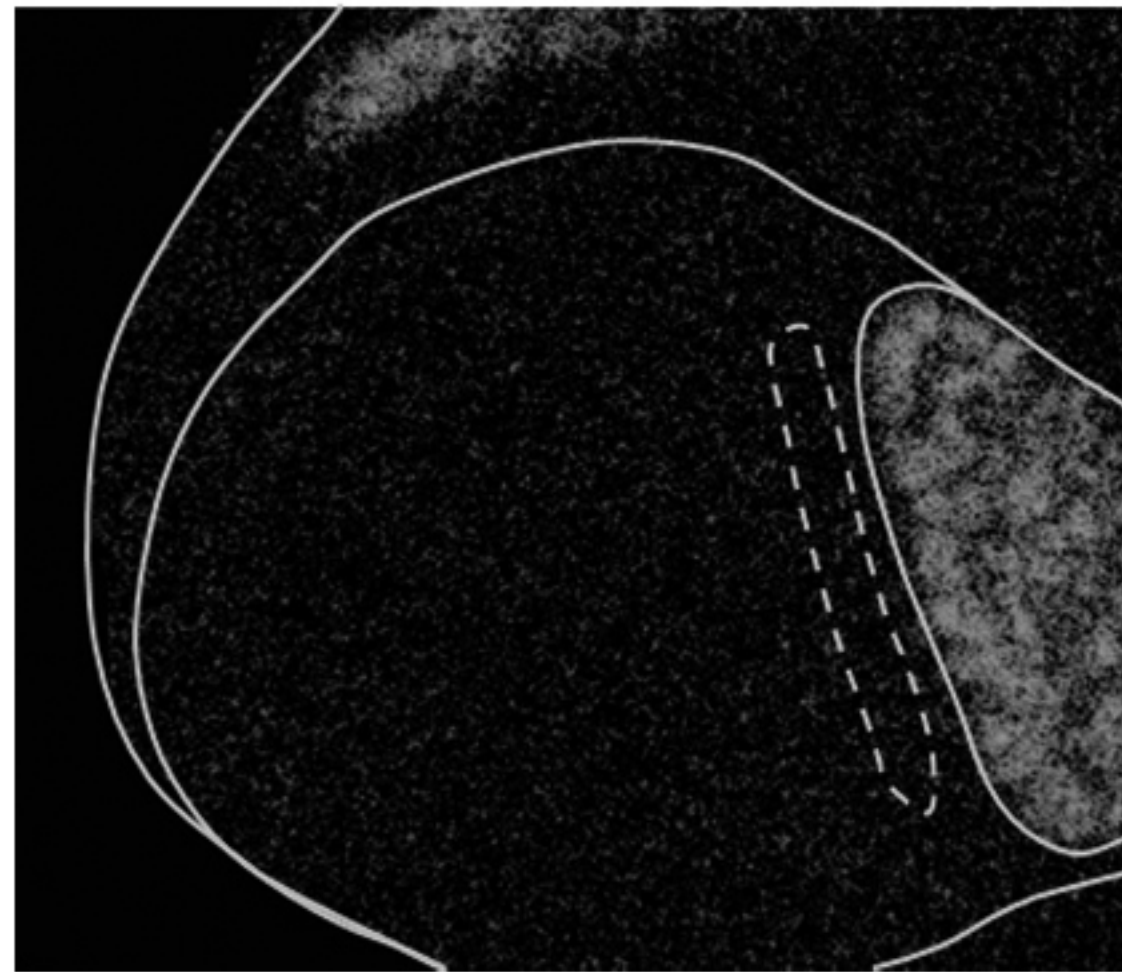
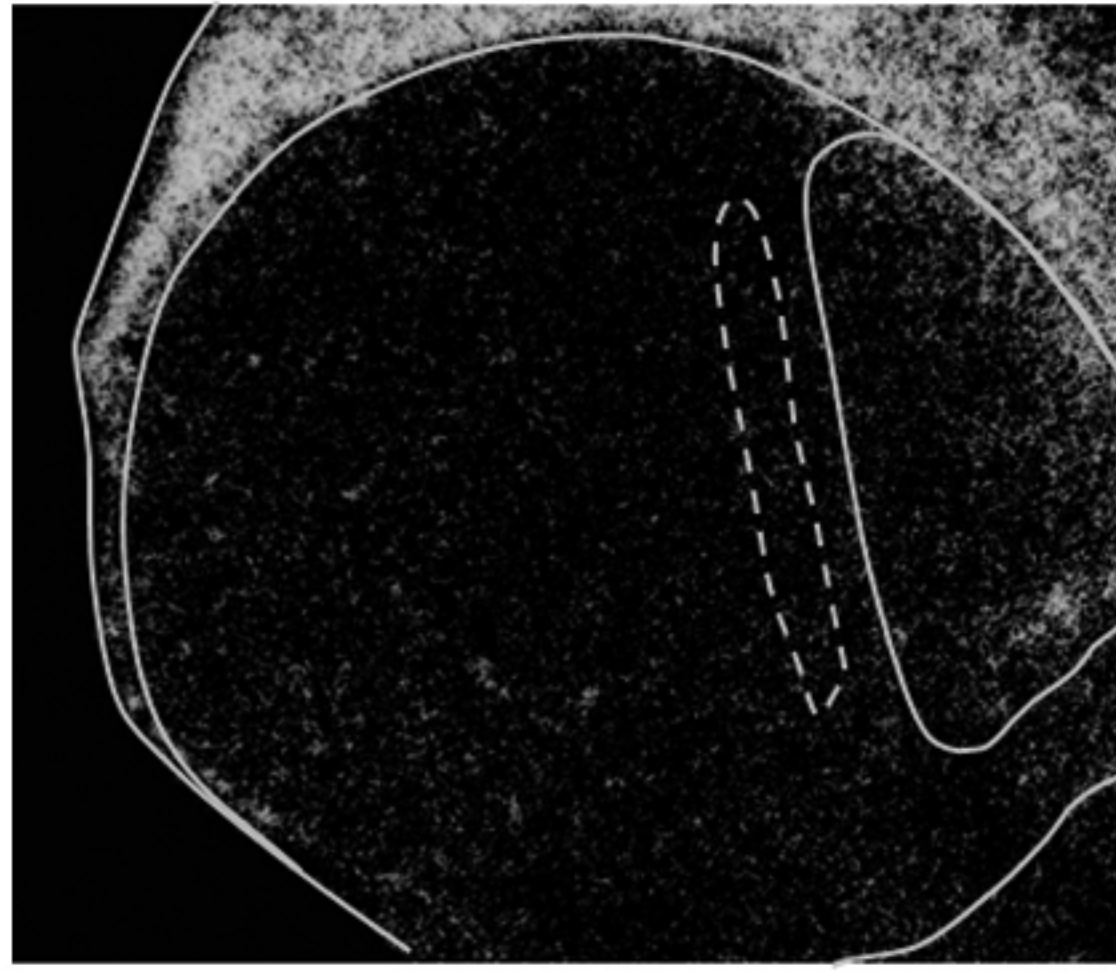
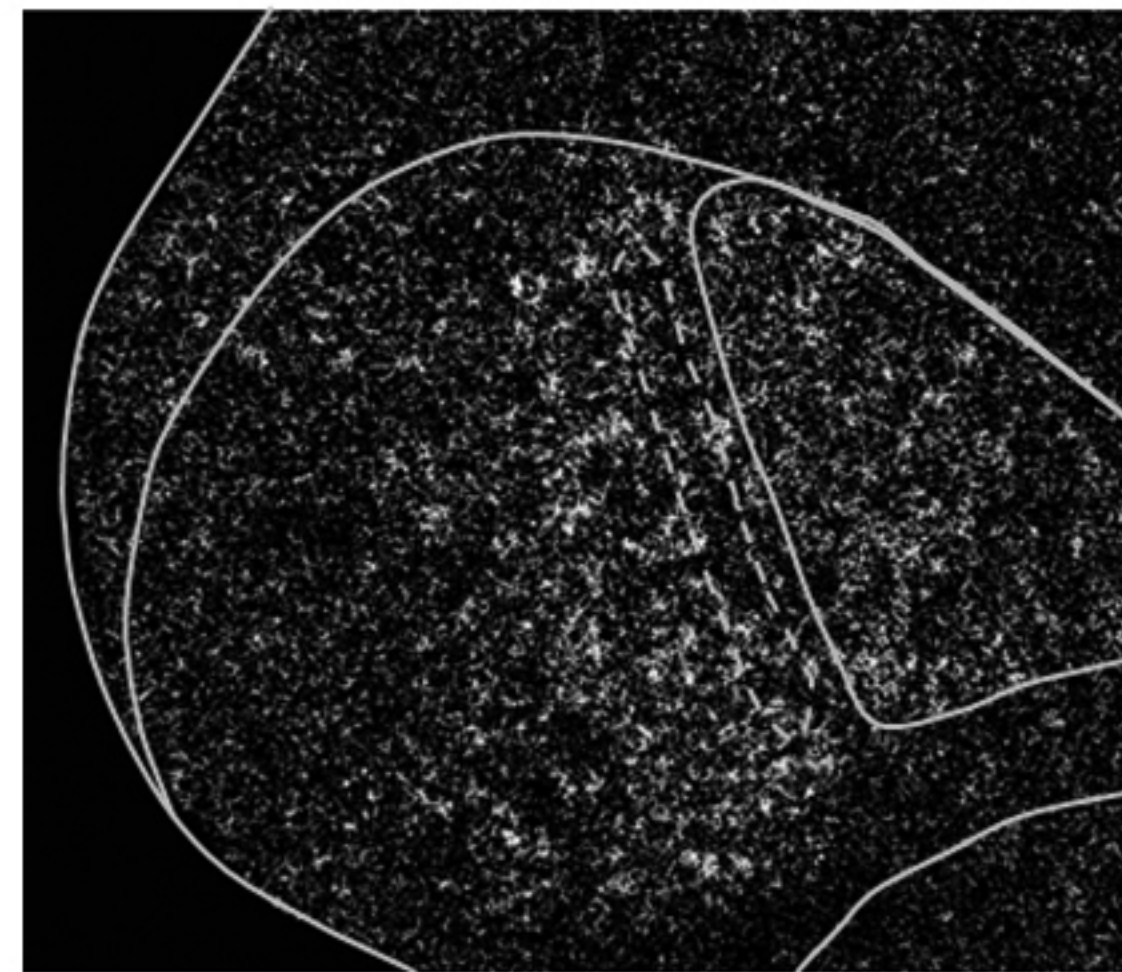
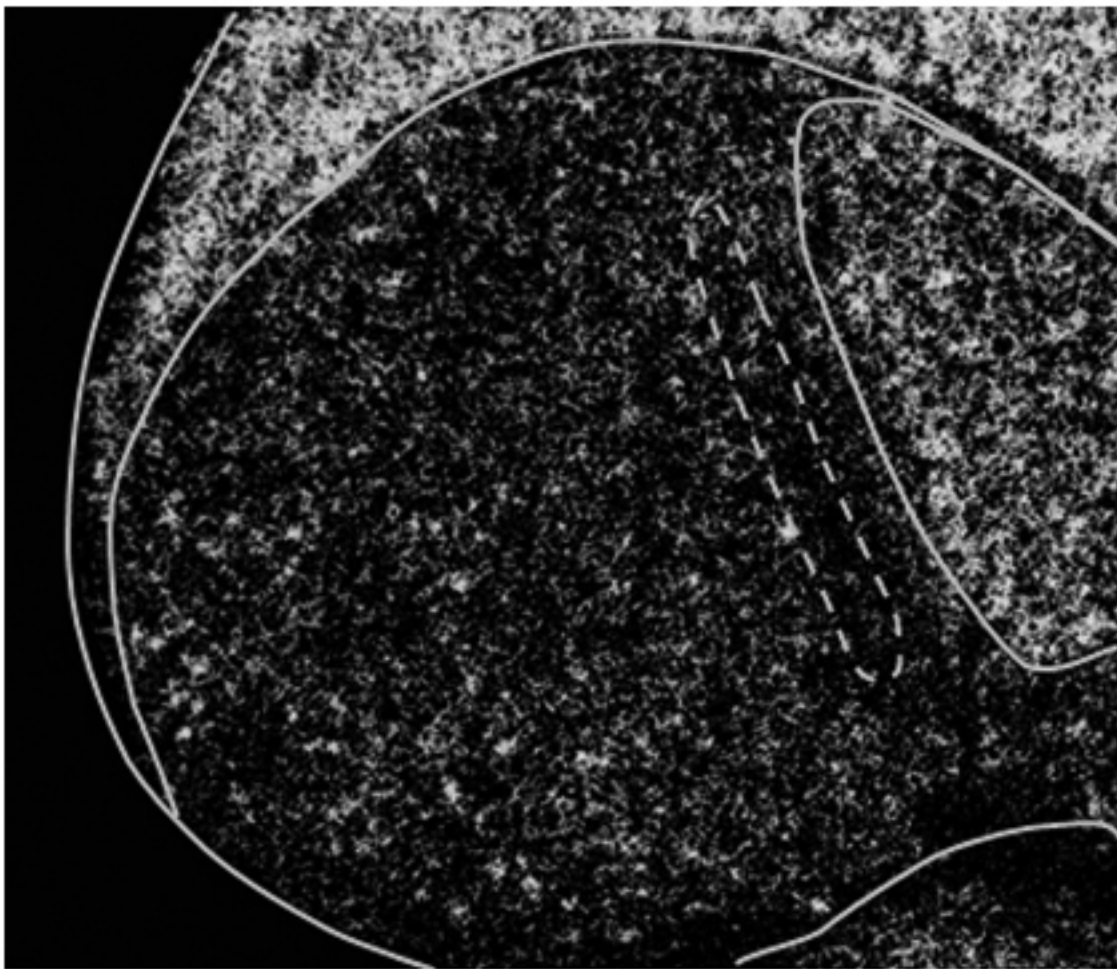
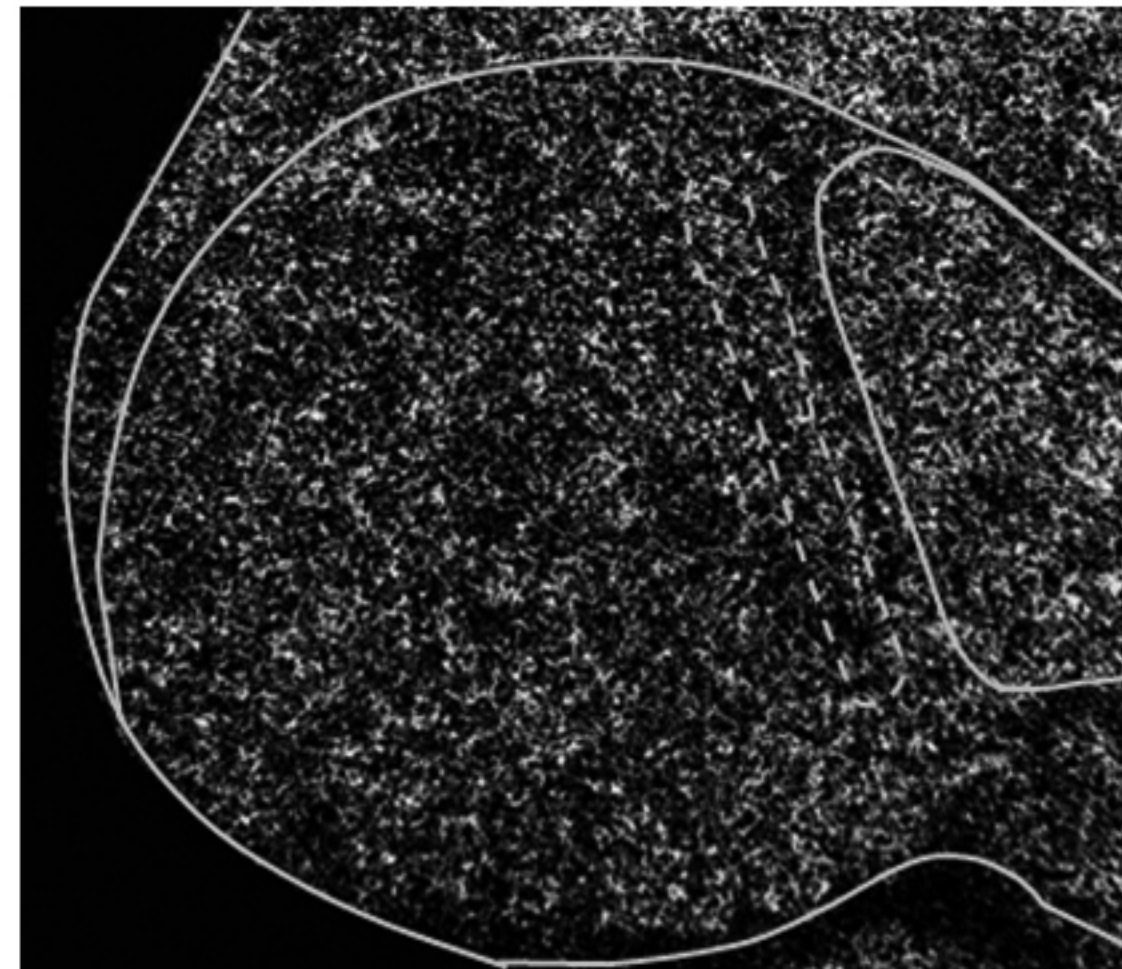
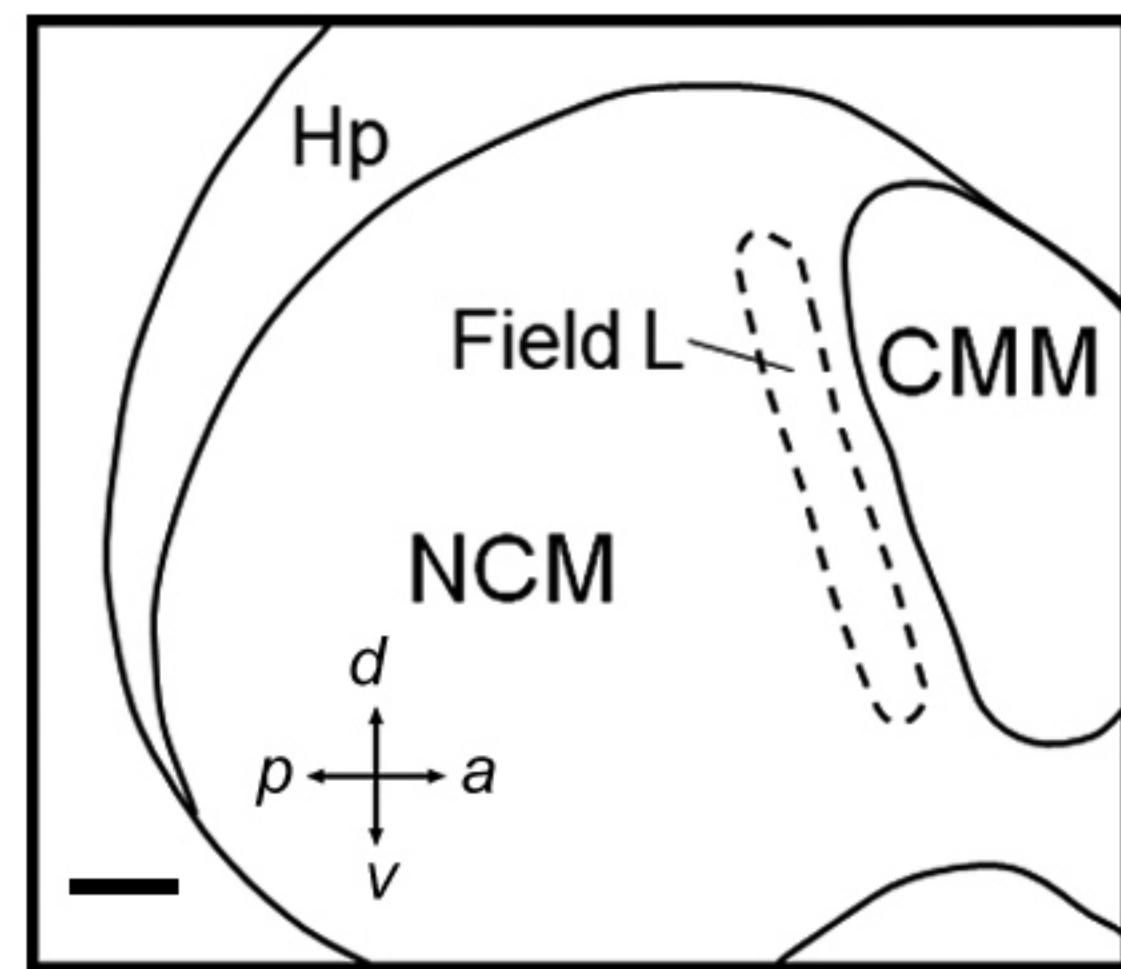
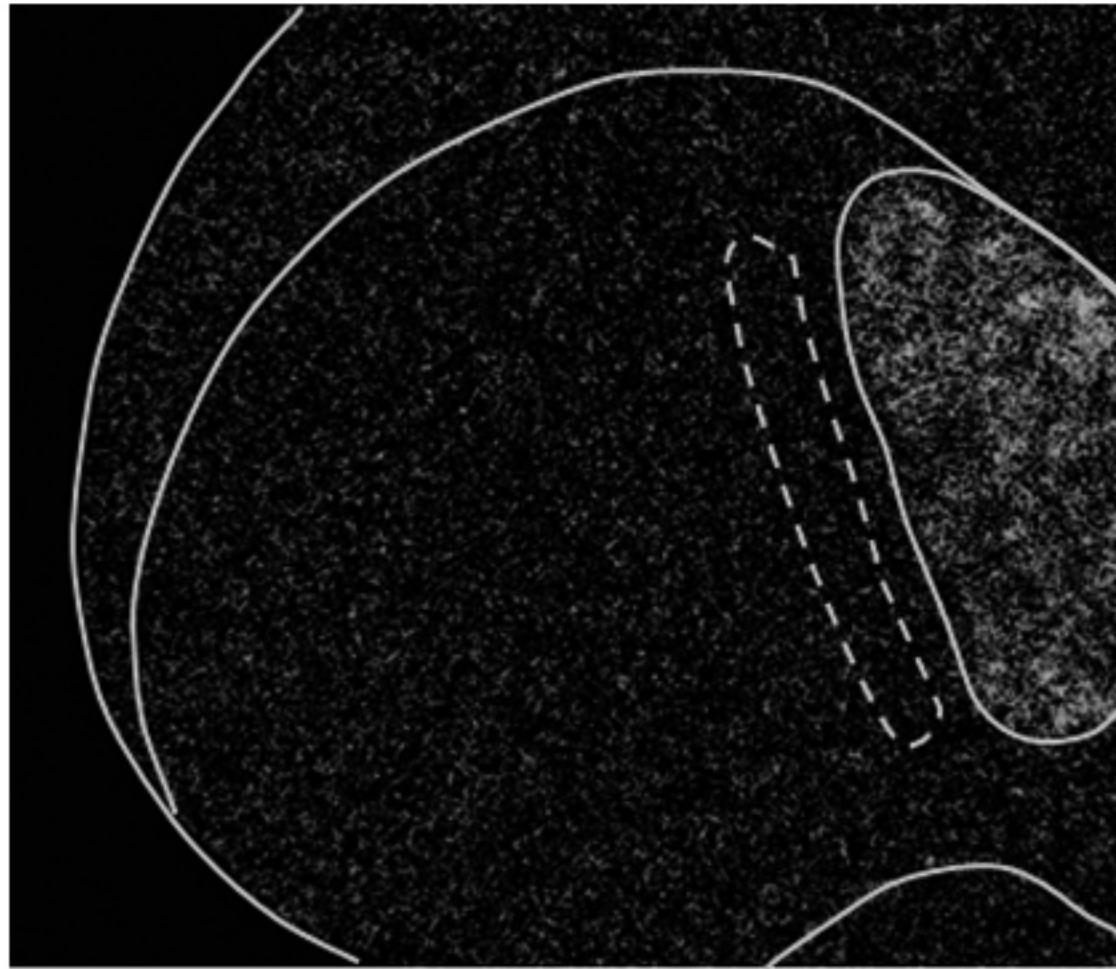


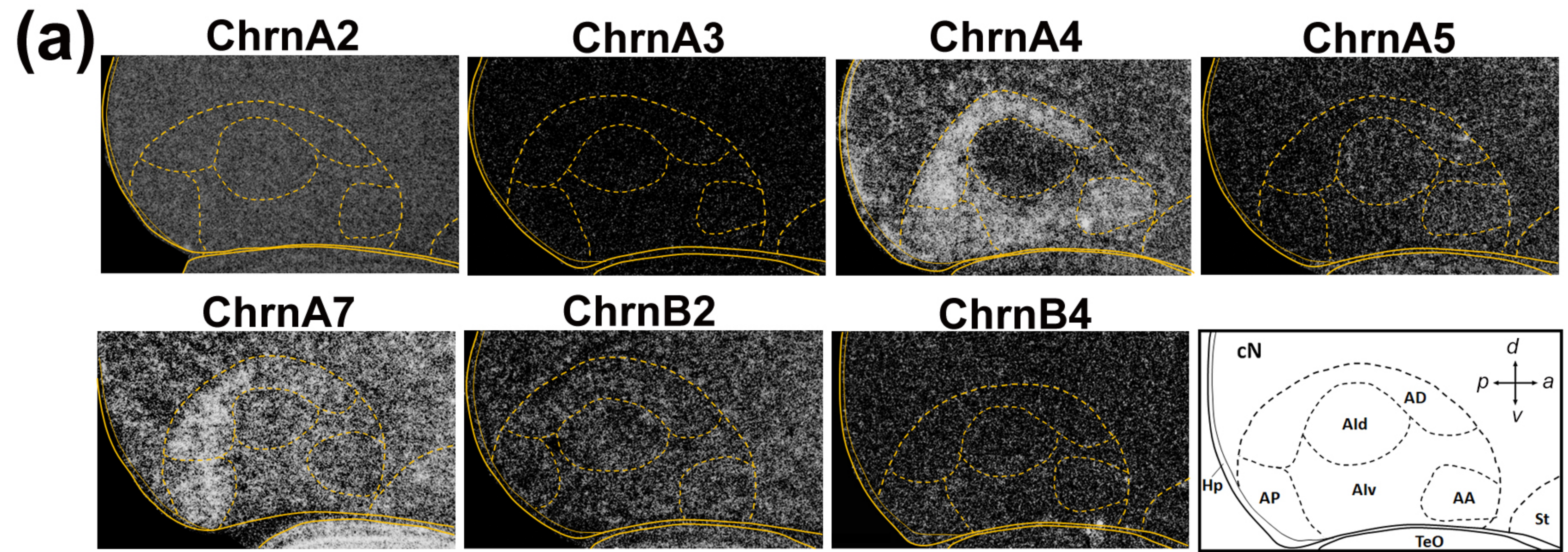
**Medial****Lateral****ChrA1****ChrA2****ChrA3****ChrA4****ChrA5**

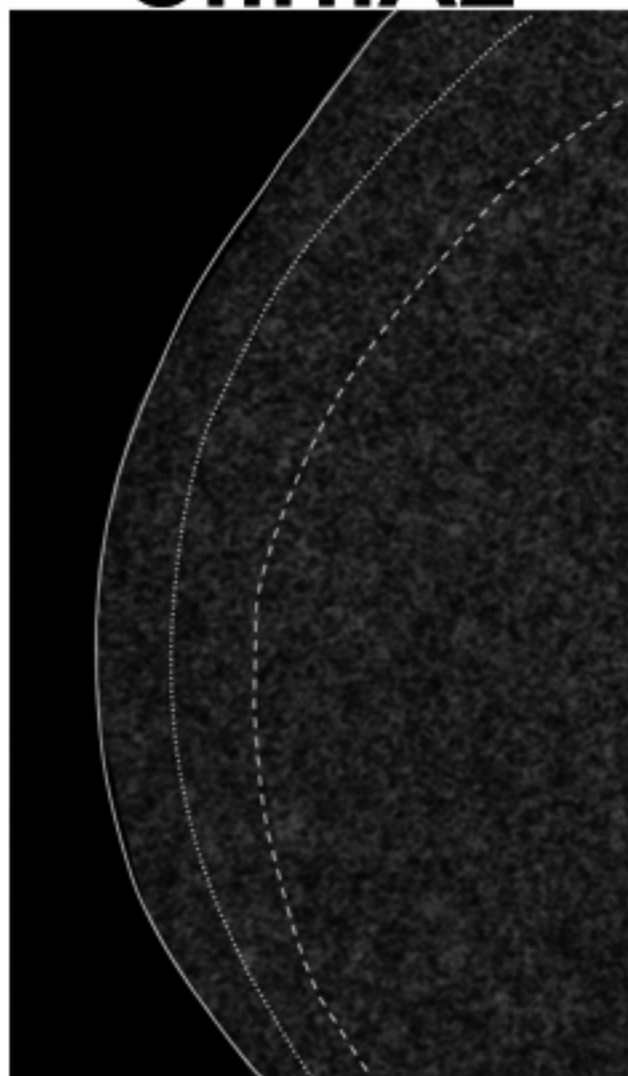
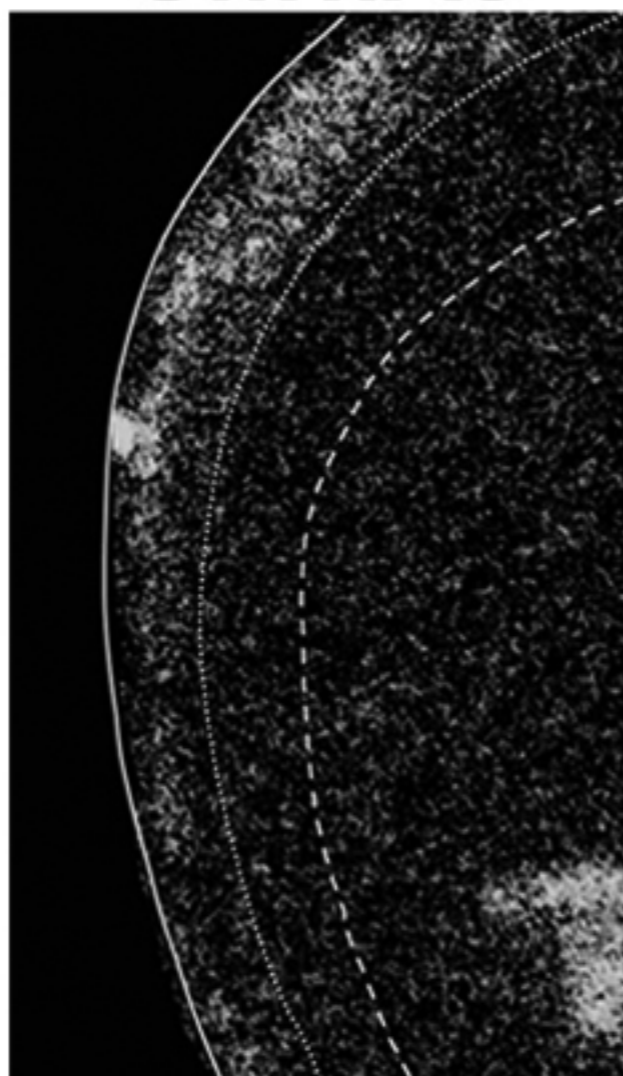
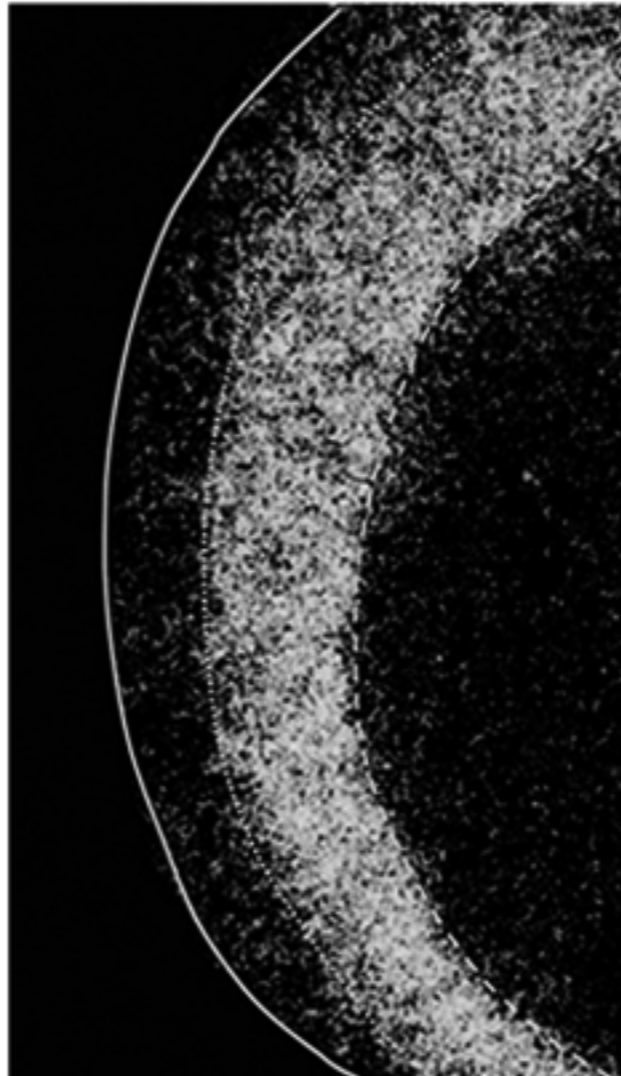
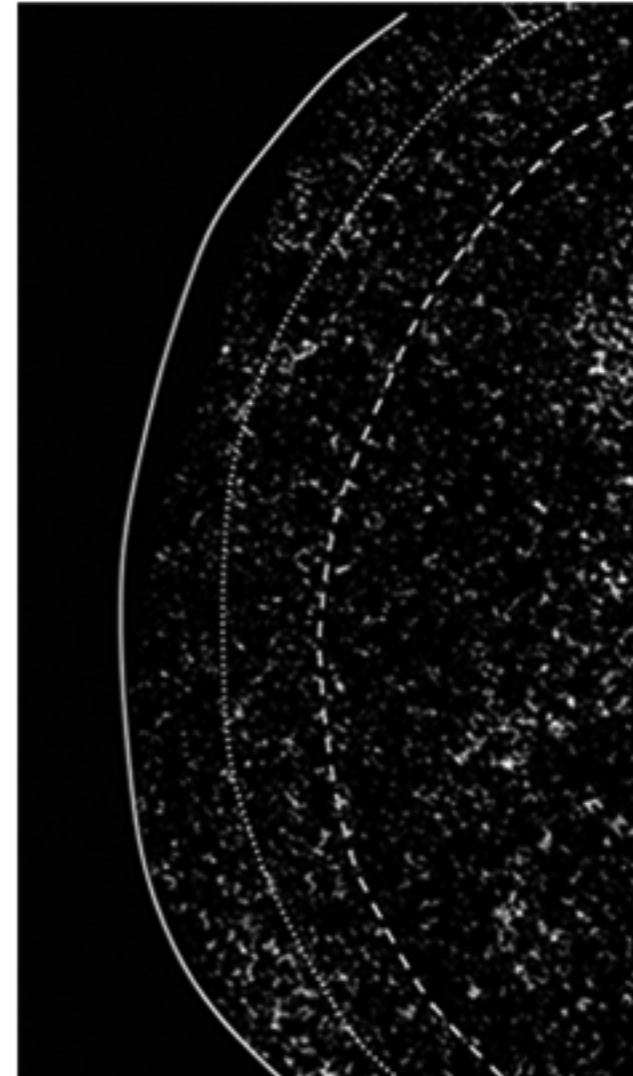
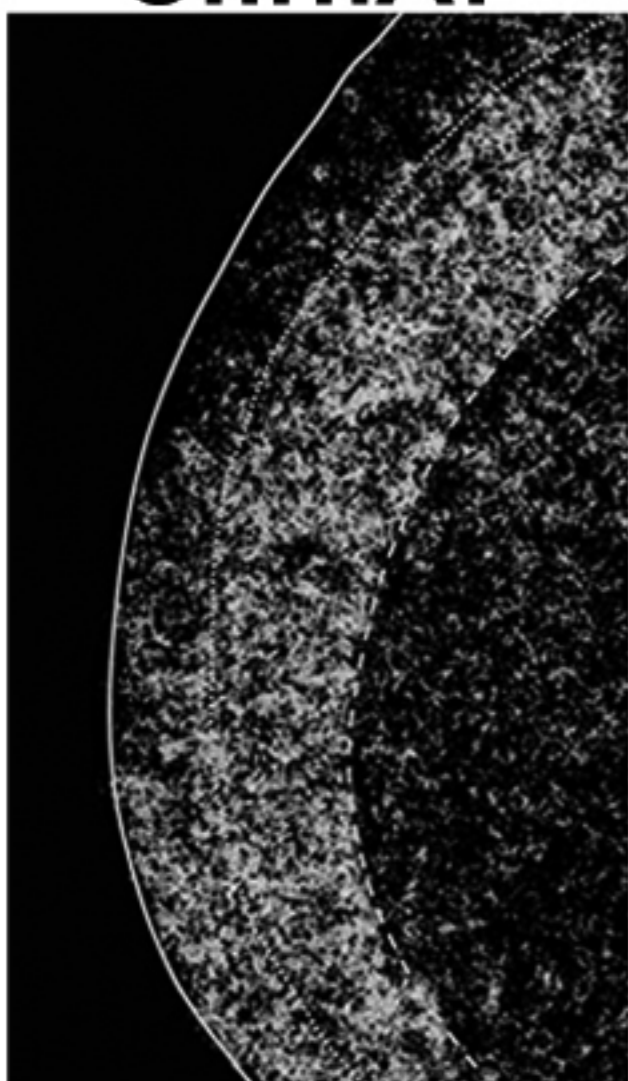
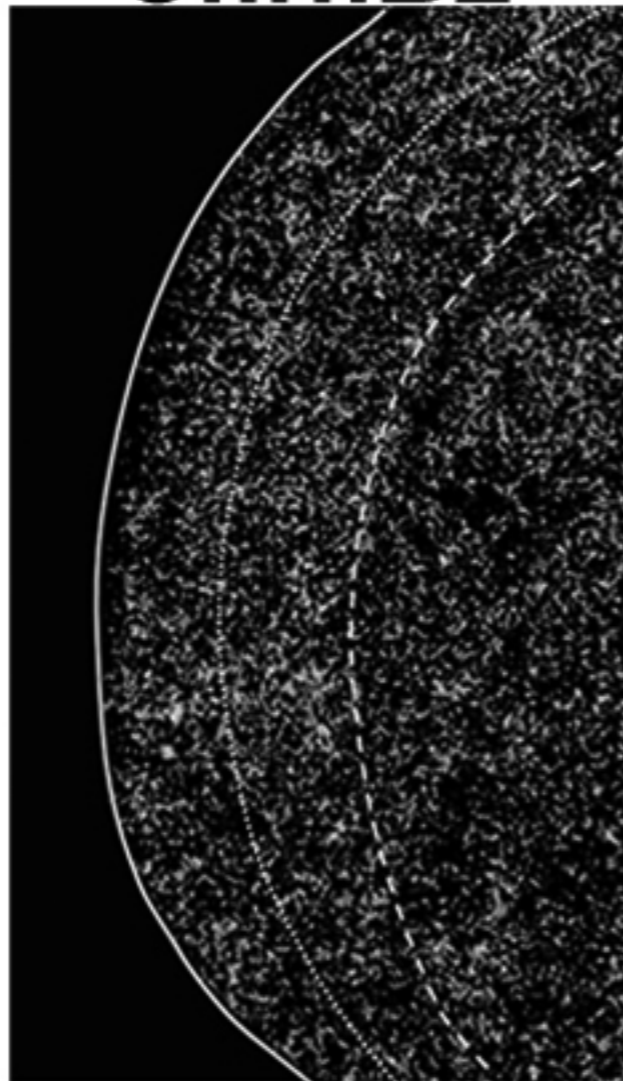
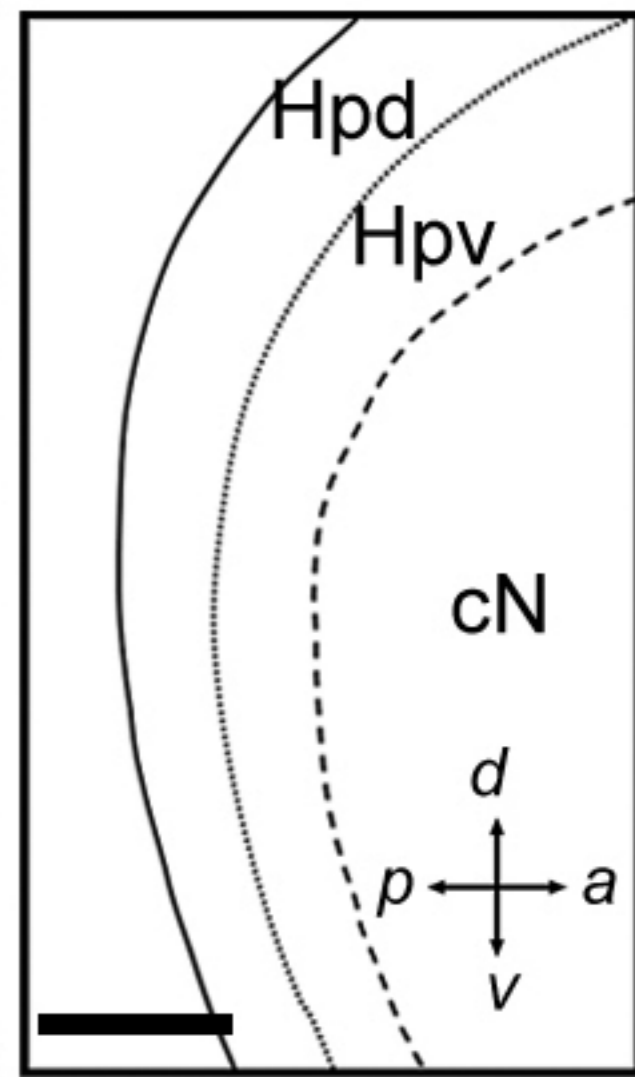
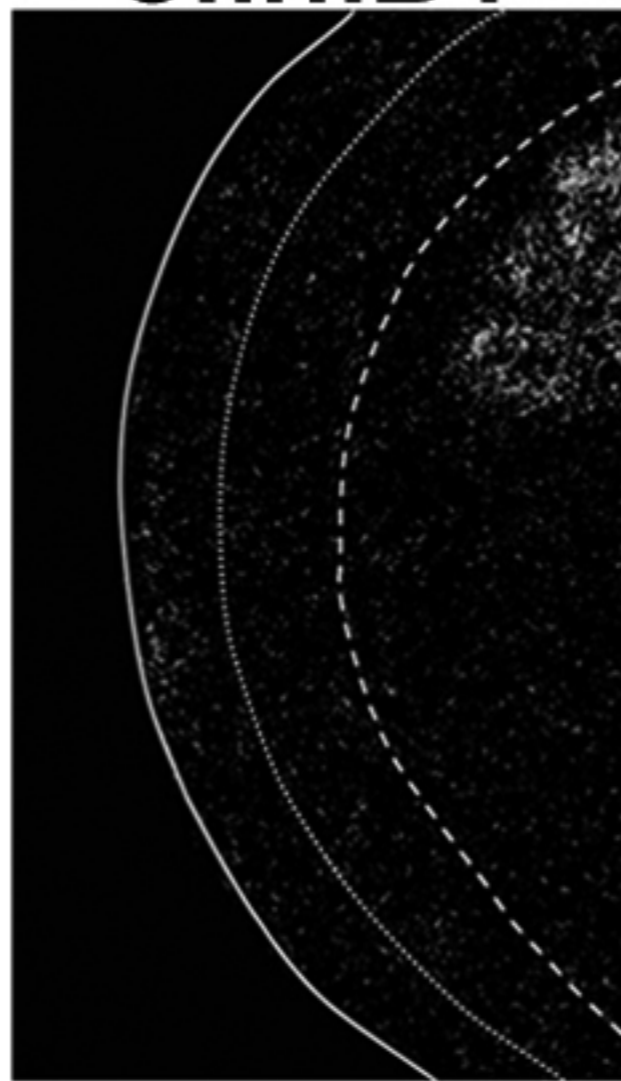
**Medial****Lateral****ChrA6****ChrA7****ChrA8****ChrA9****ChrA10**

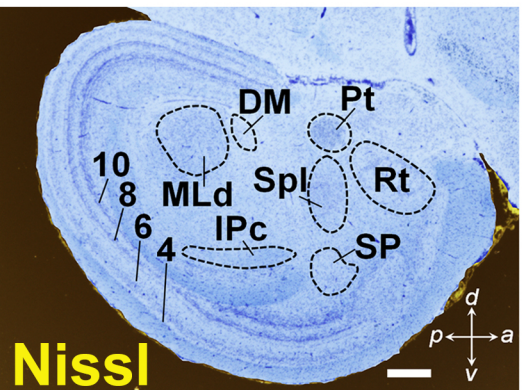
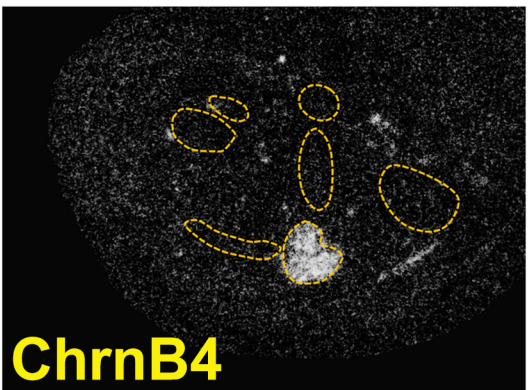
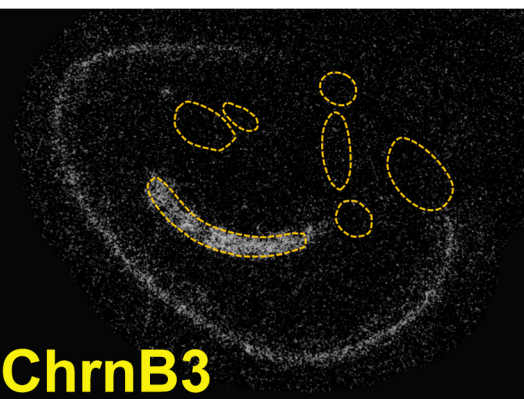
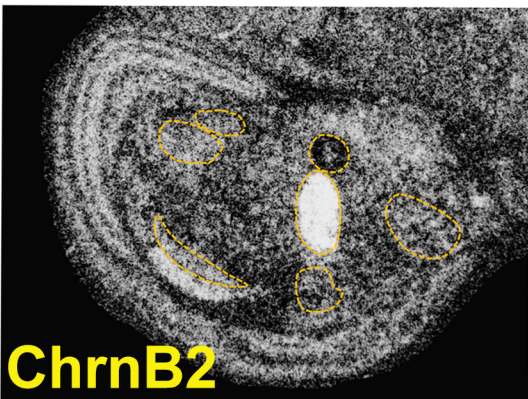
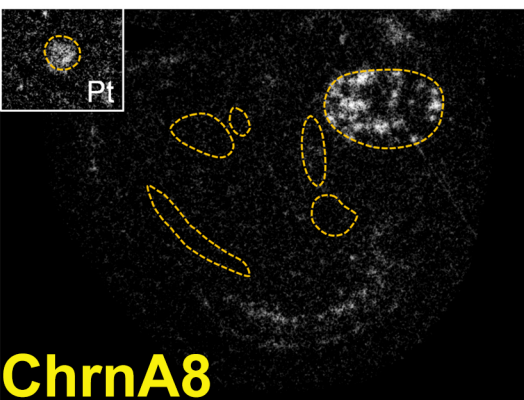
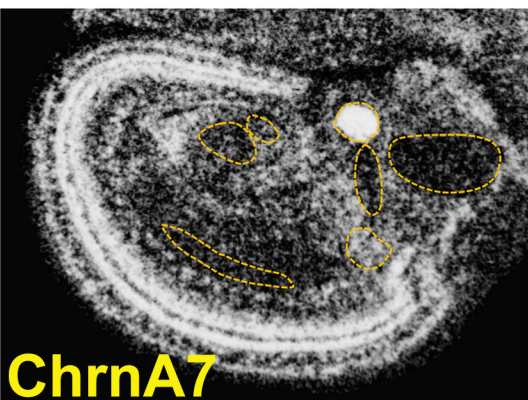
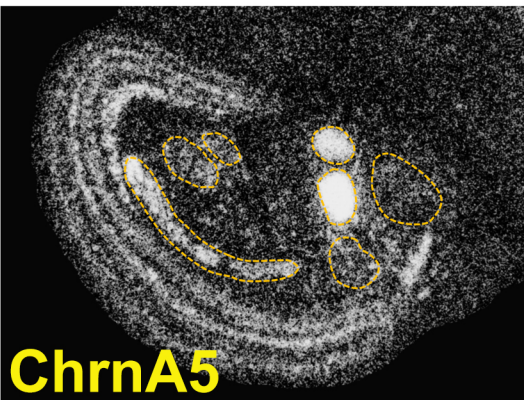
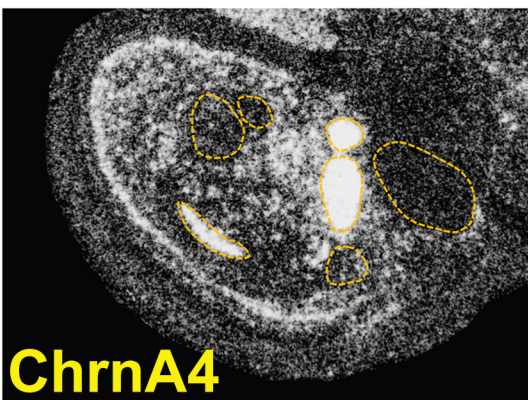
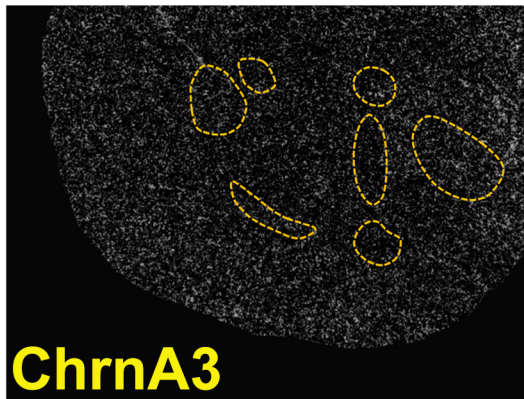
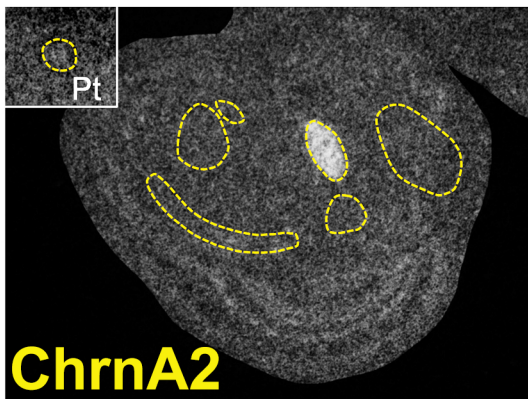
**Medial****Lateral****Chrnb2****Chrnb3****Chrnb4****ChrnD****ChrnG**

**ChrnA2****ChrnA3****ChrnA4****ChrnA5****ChrnA7****ChrnB2****ChrnB4**

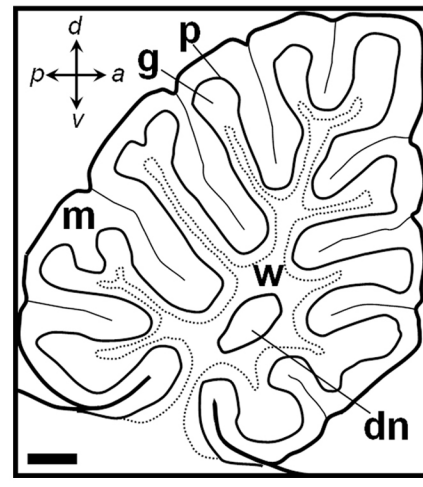
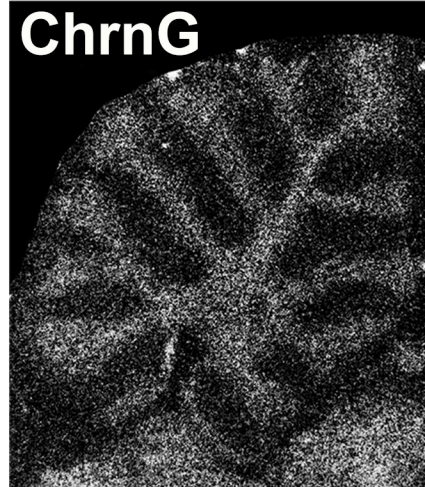
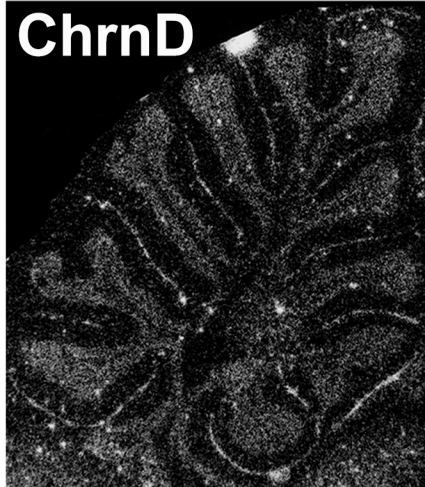
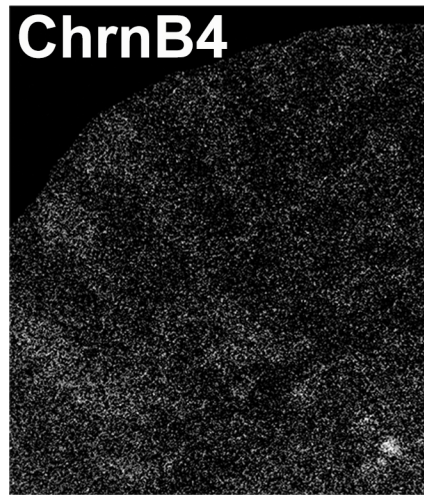
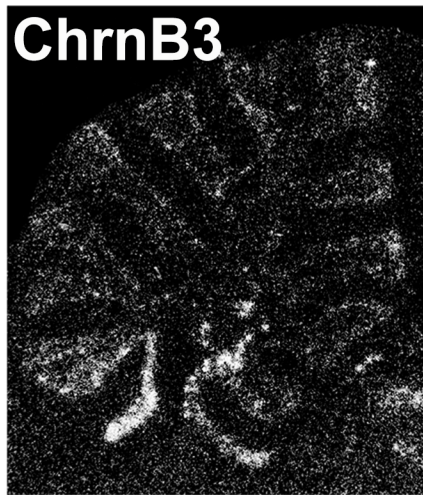
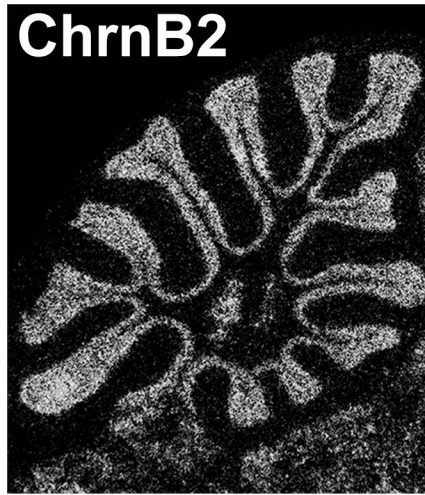
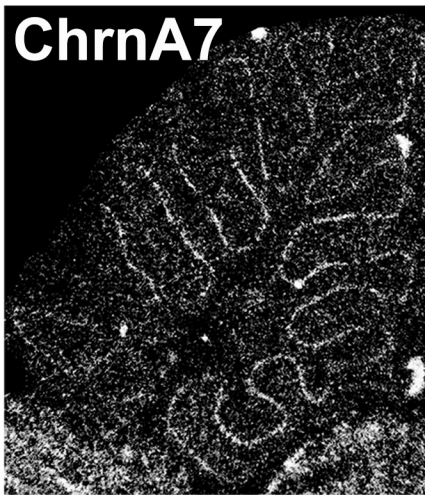
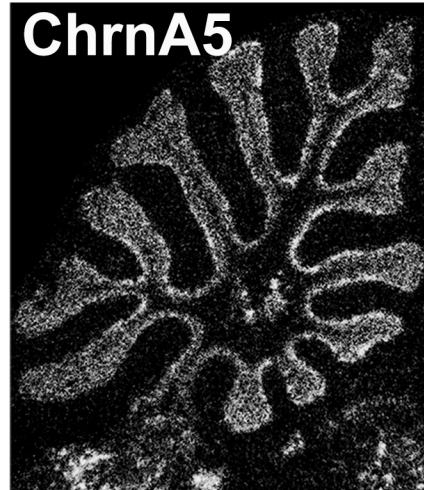
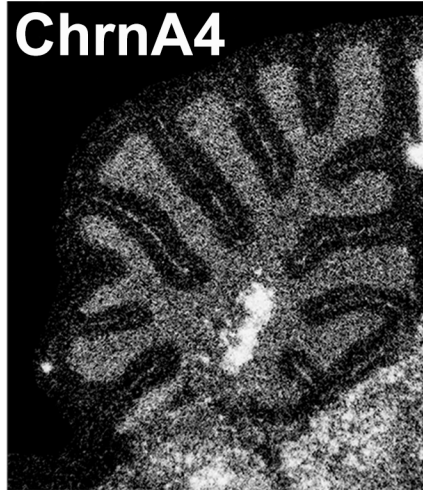
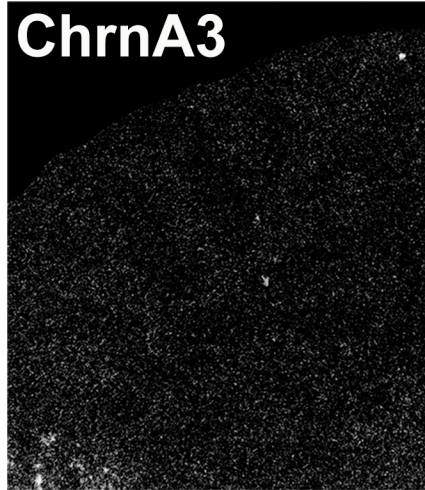
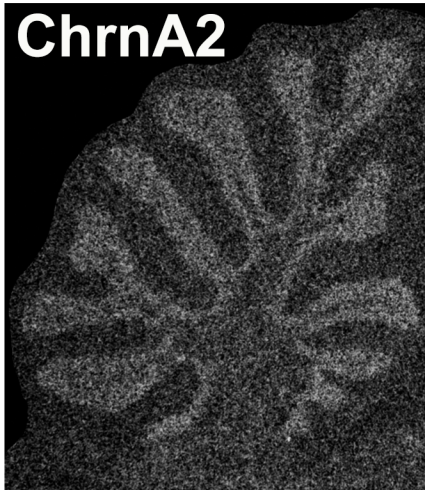
**ChrnA2****ChrnA3****ChrnA4****ChrnA5****ChrnA7****ChrnB2****ChrnB4**

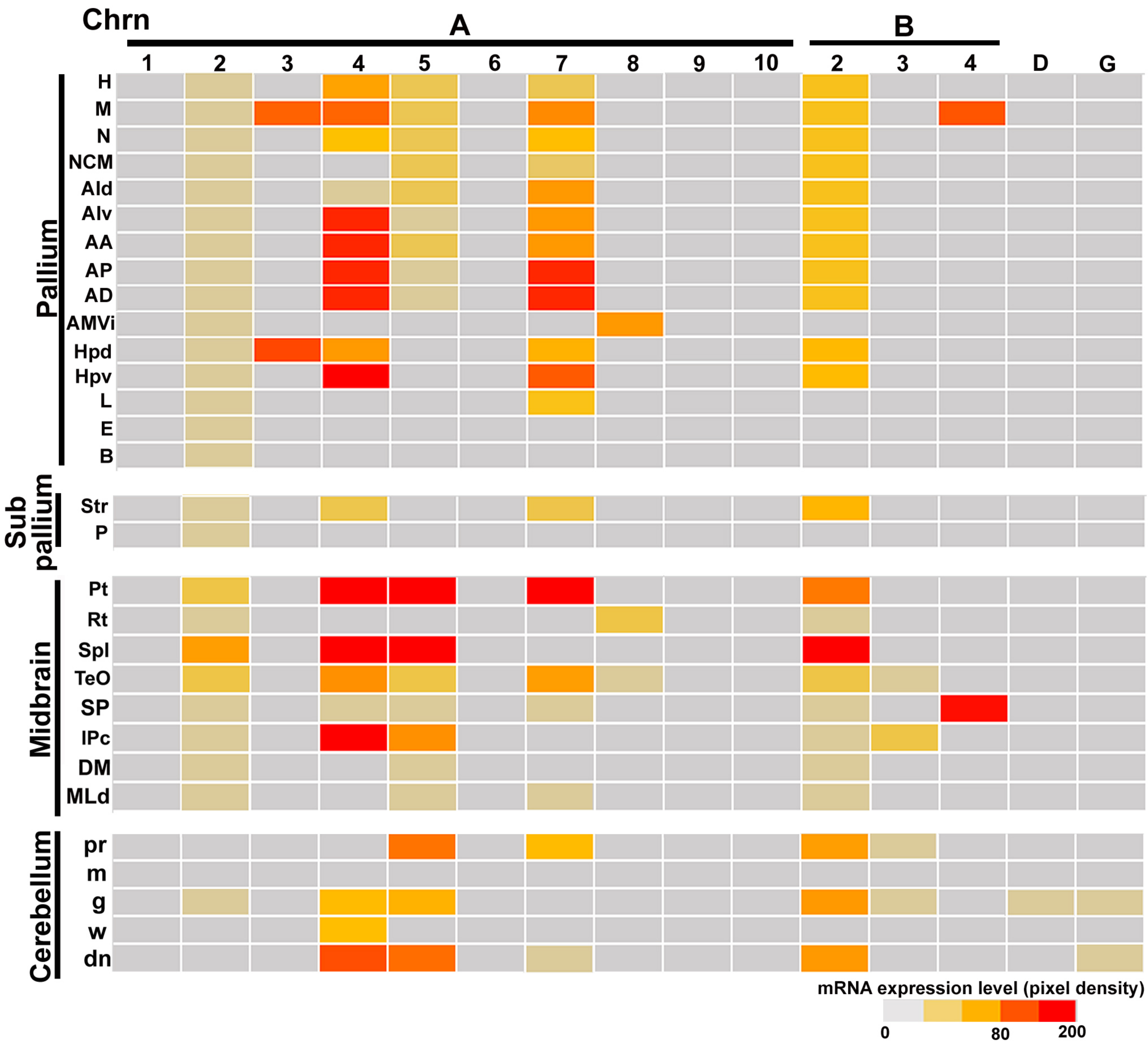


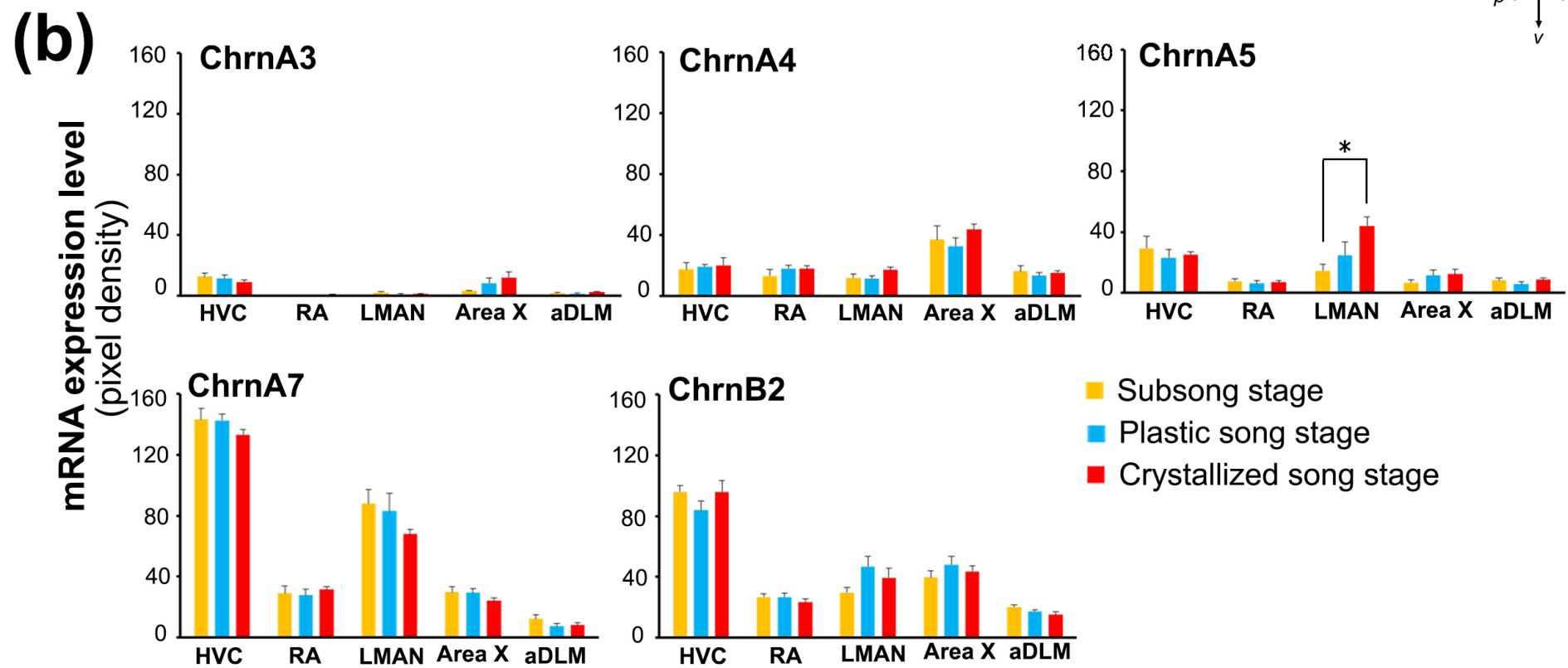
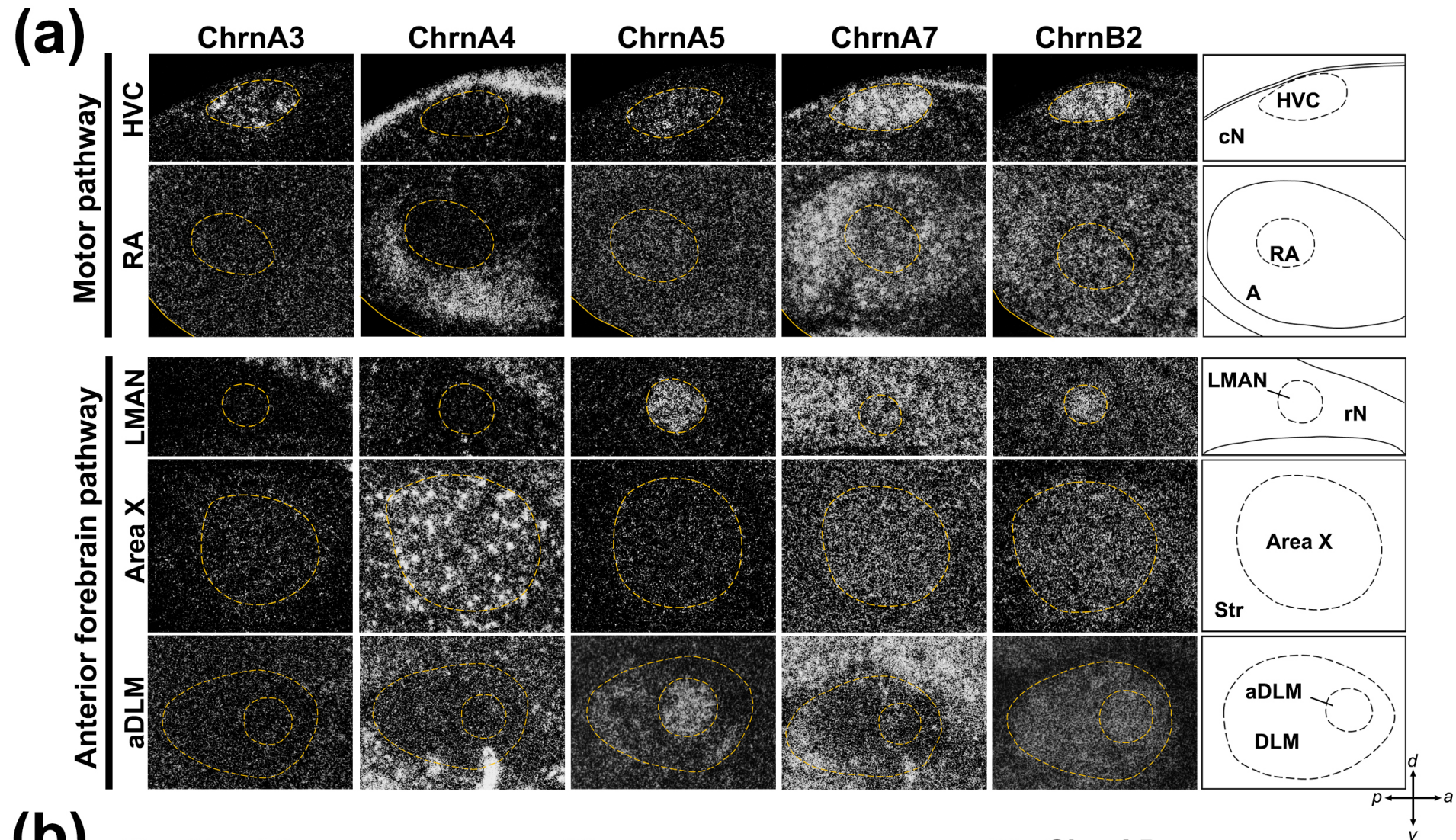
**ChrnA2****ChrnA3****ChrnA4****ChrnA5****ChrnA7****ChrnB2****ChrnB4**

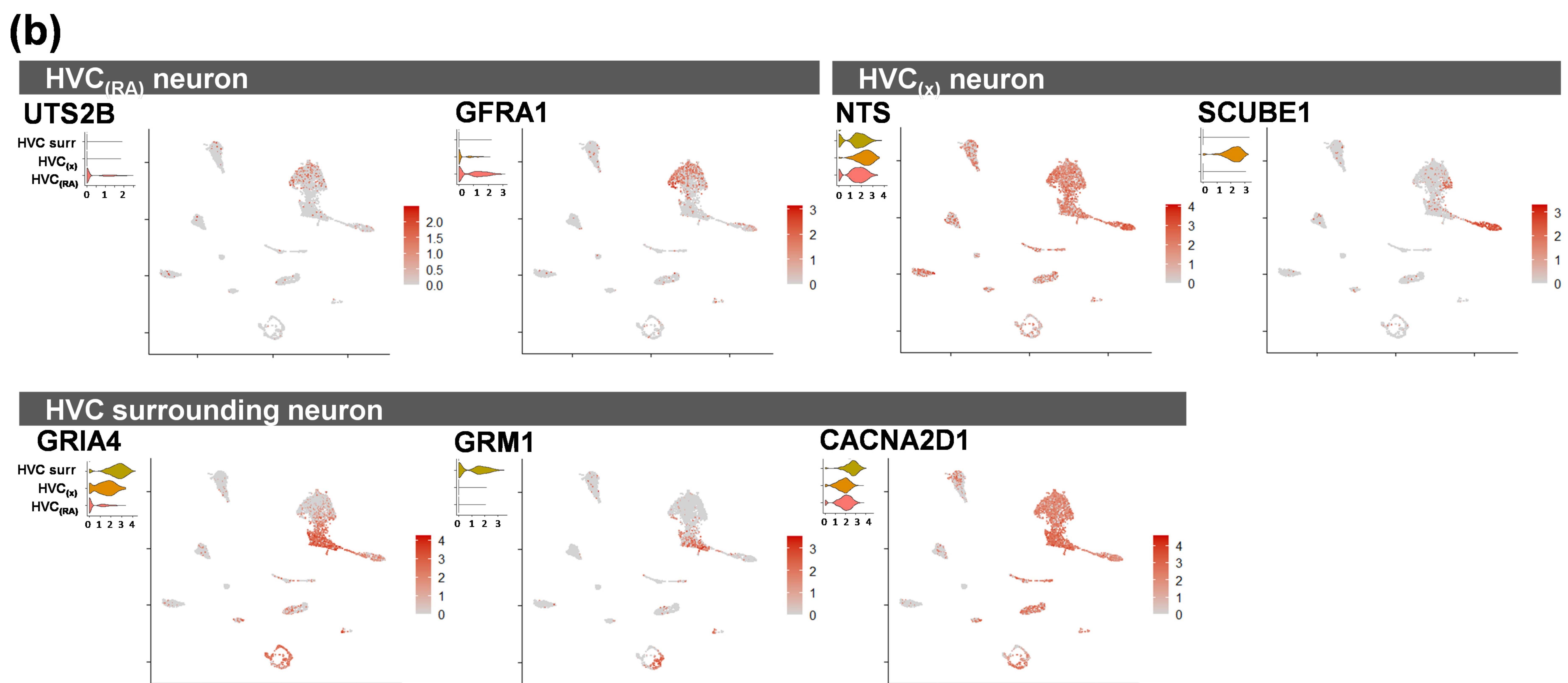
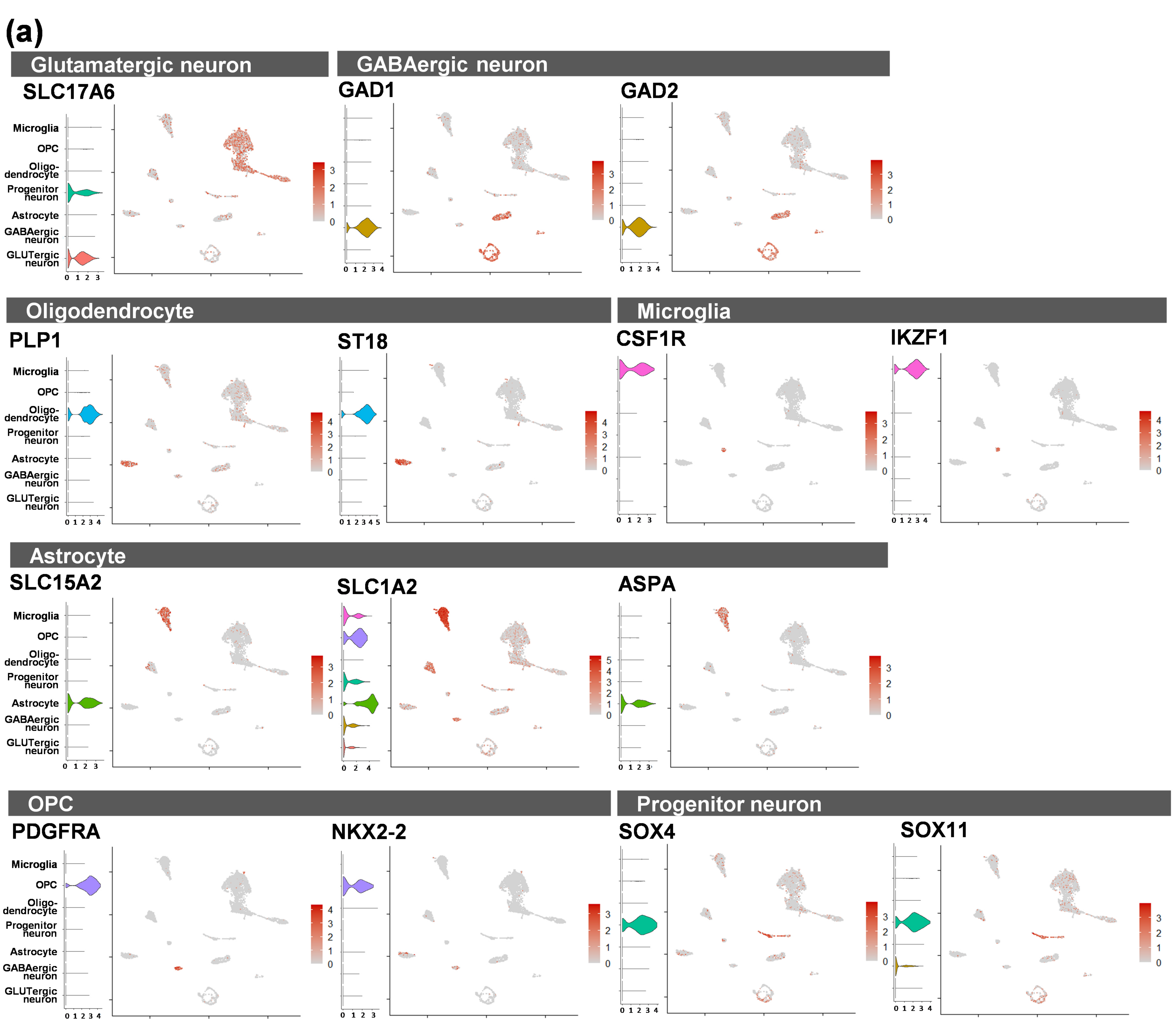


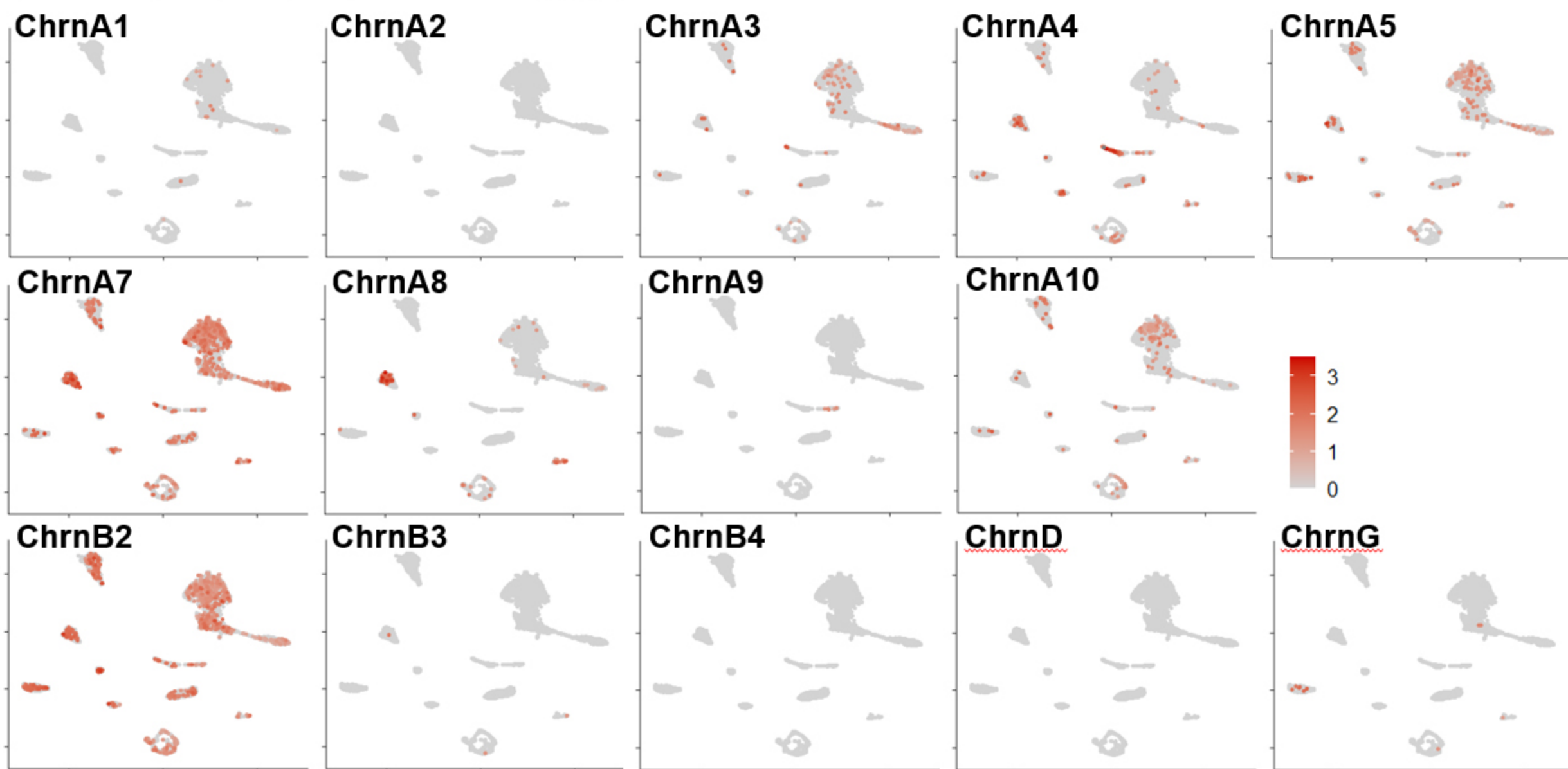
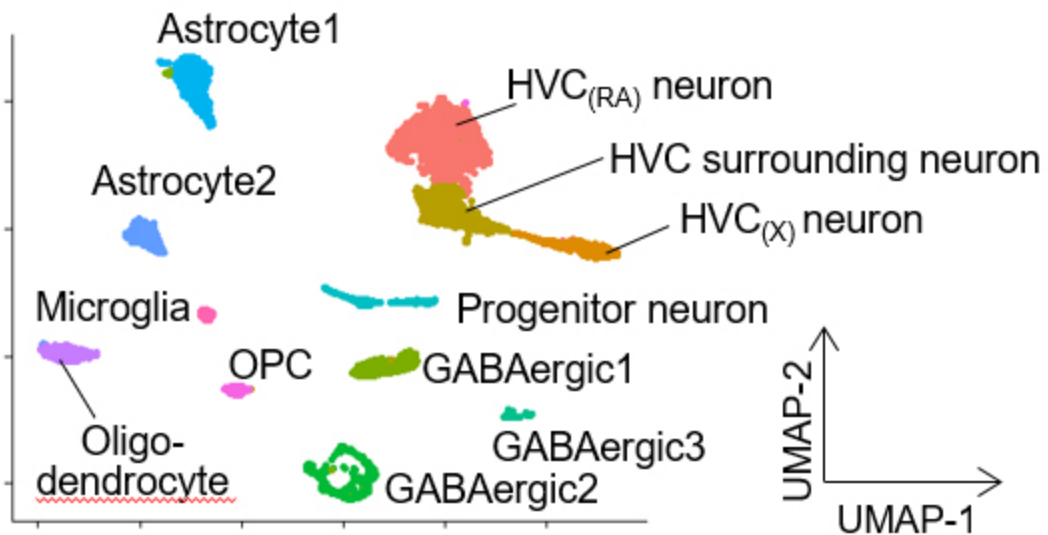


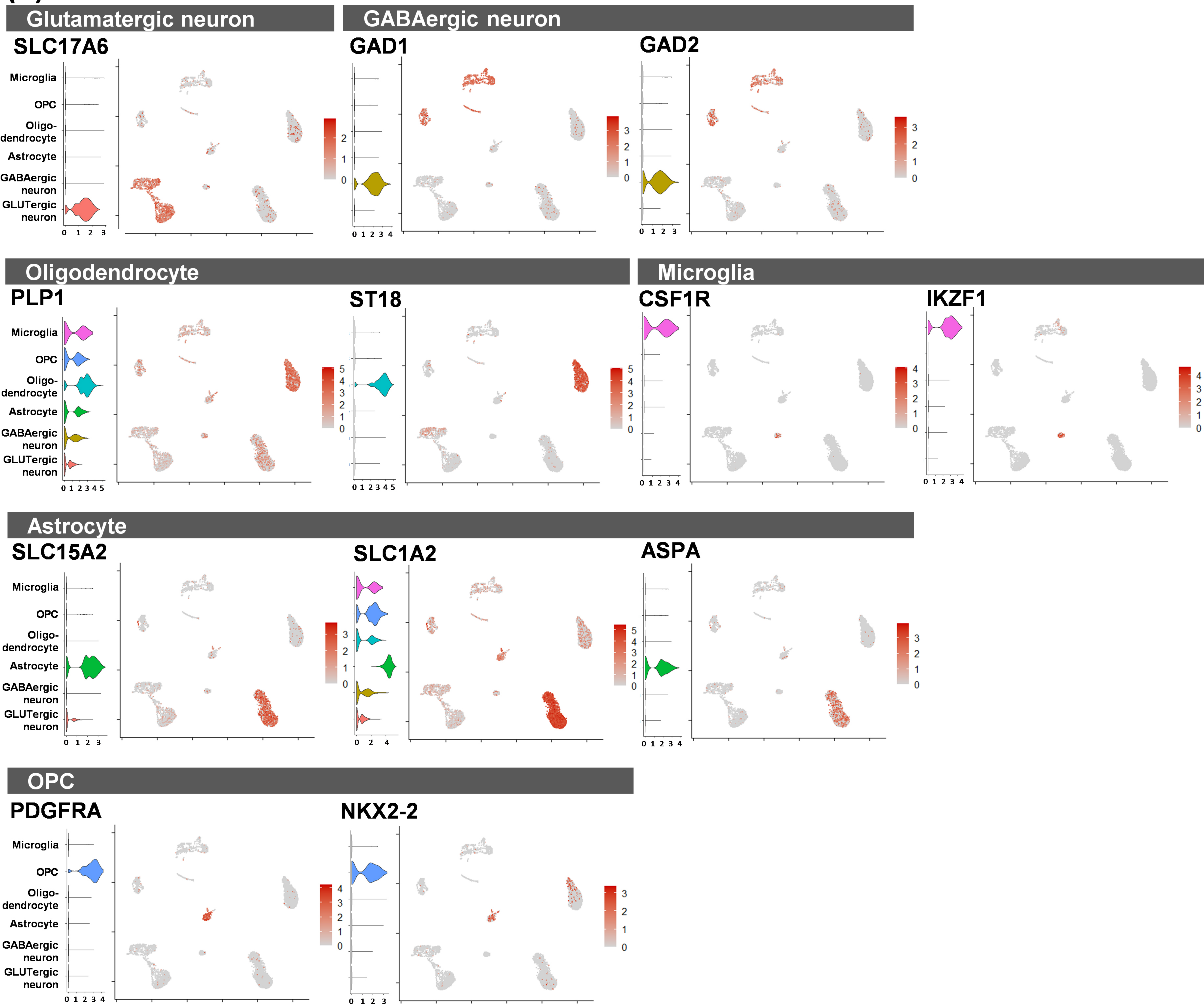
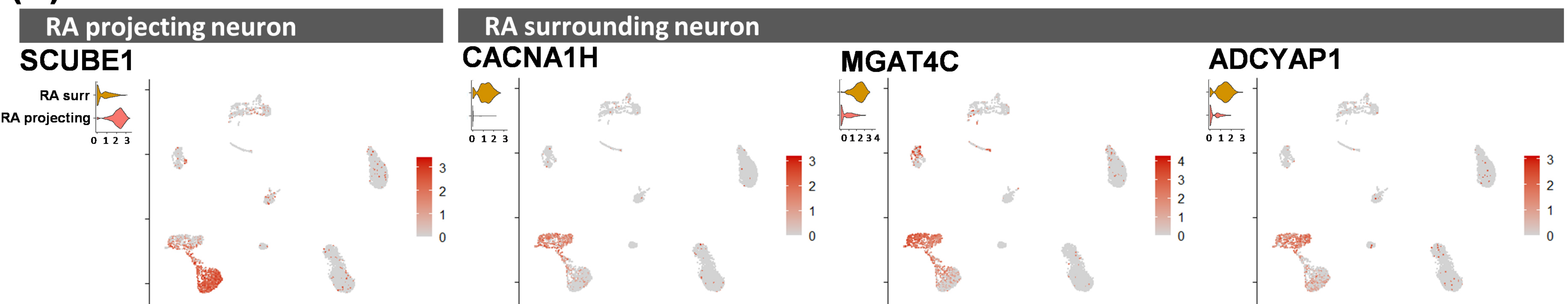


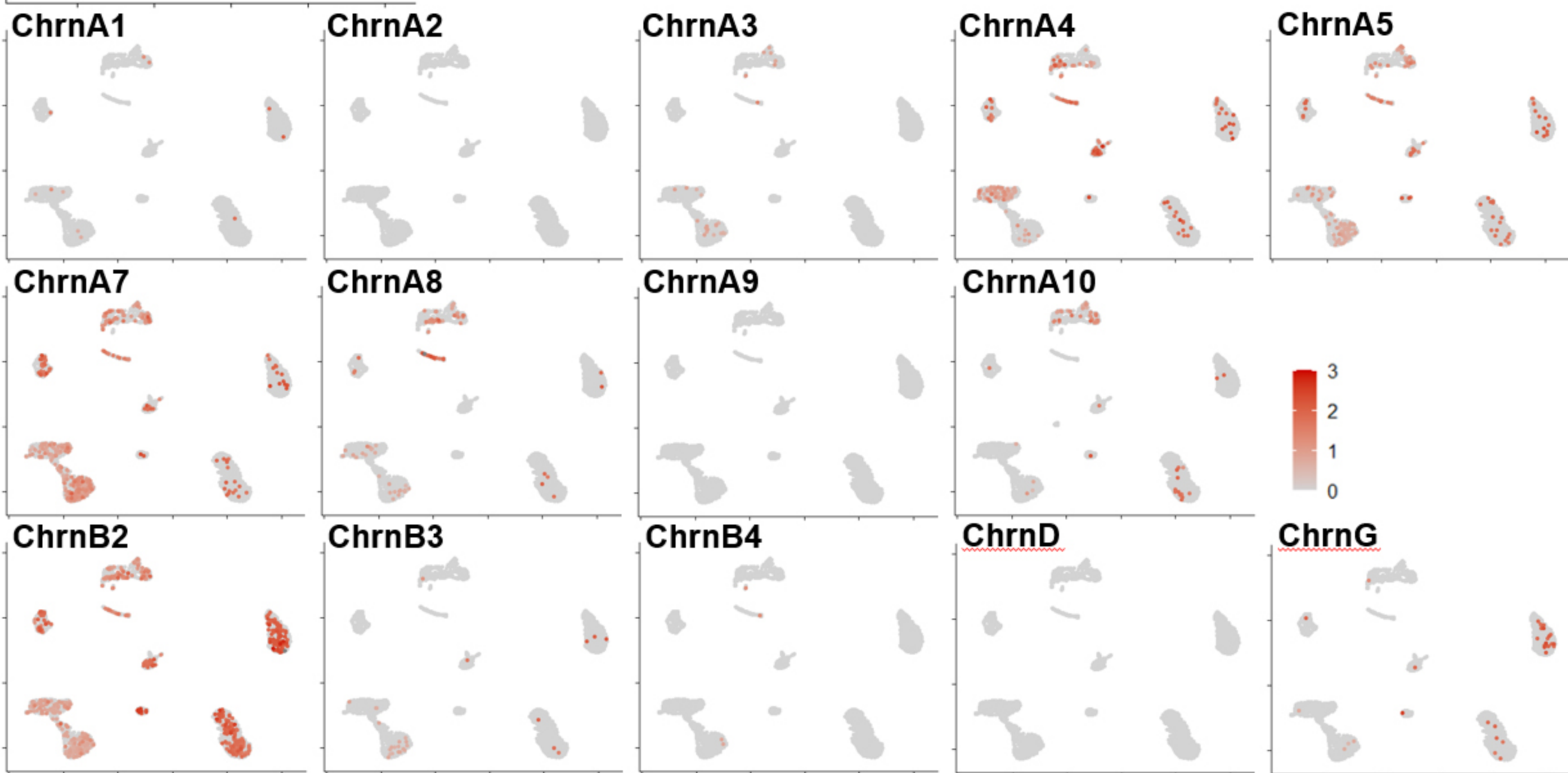
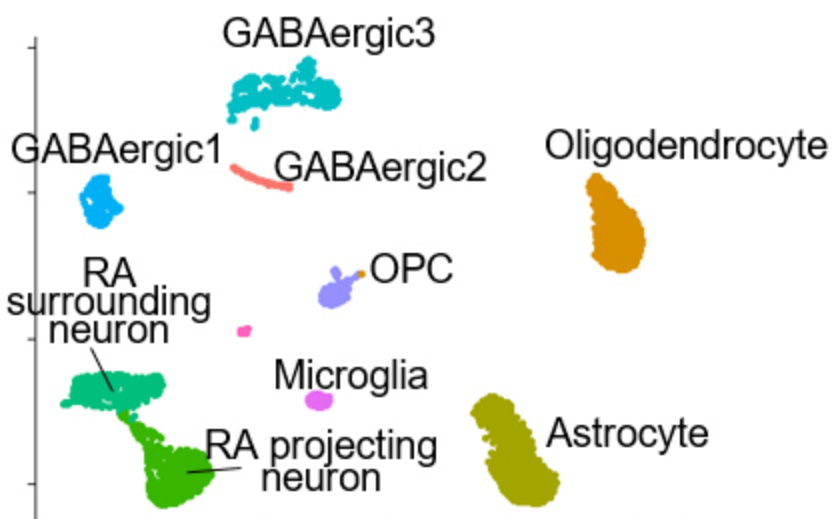


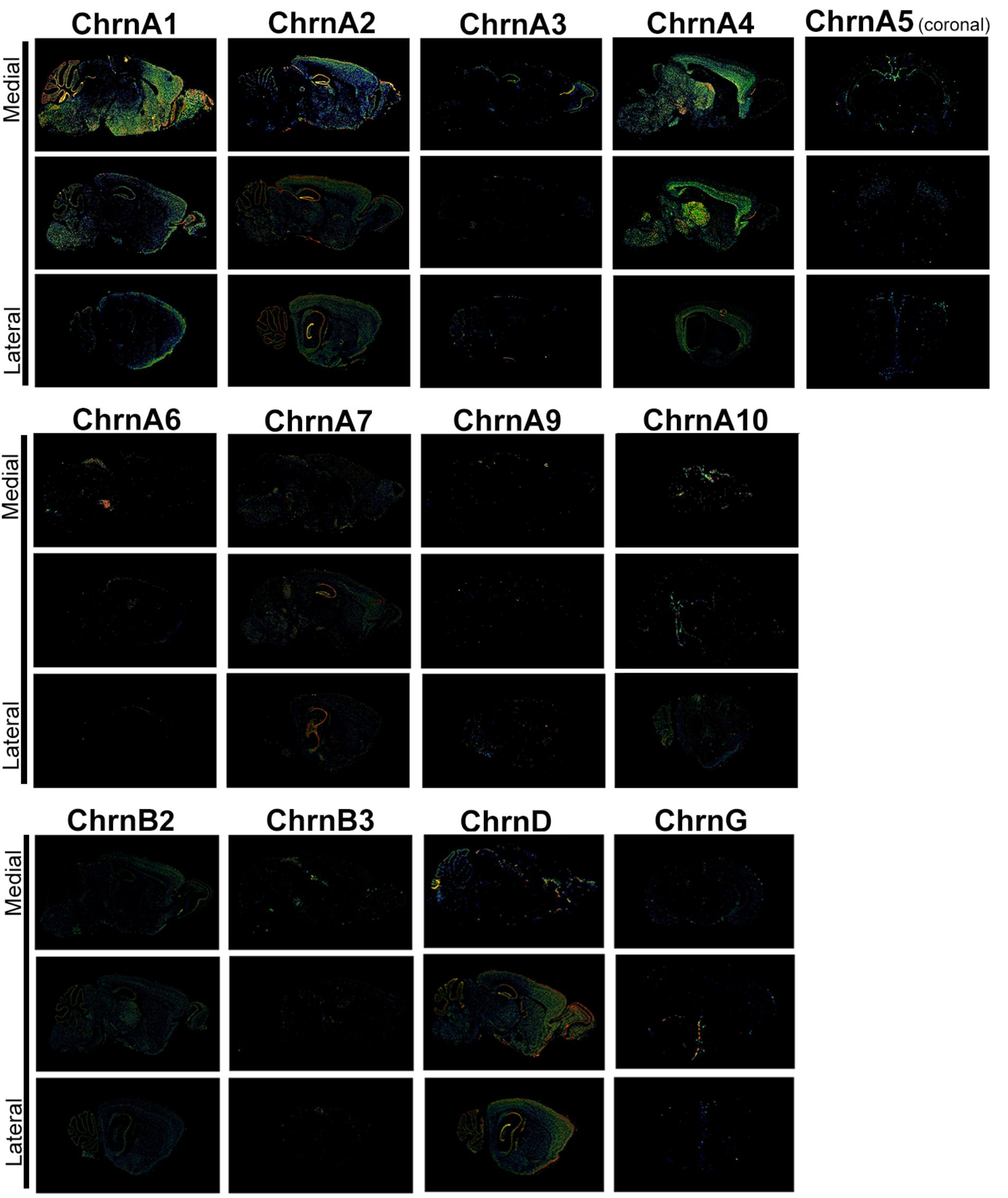




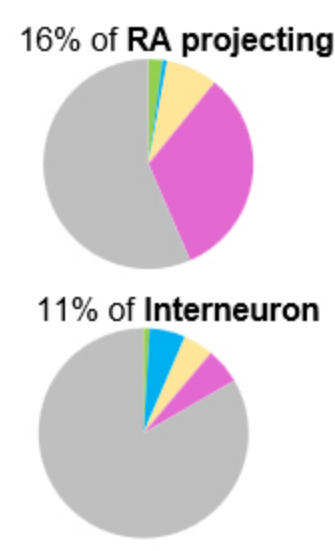
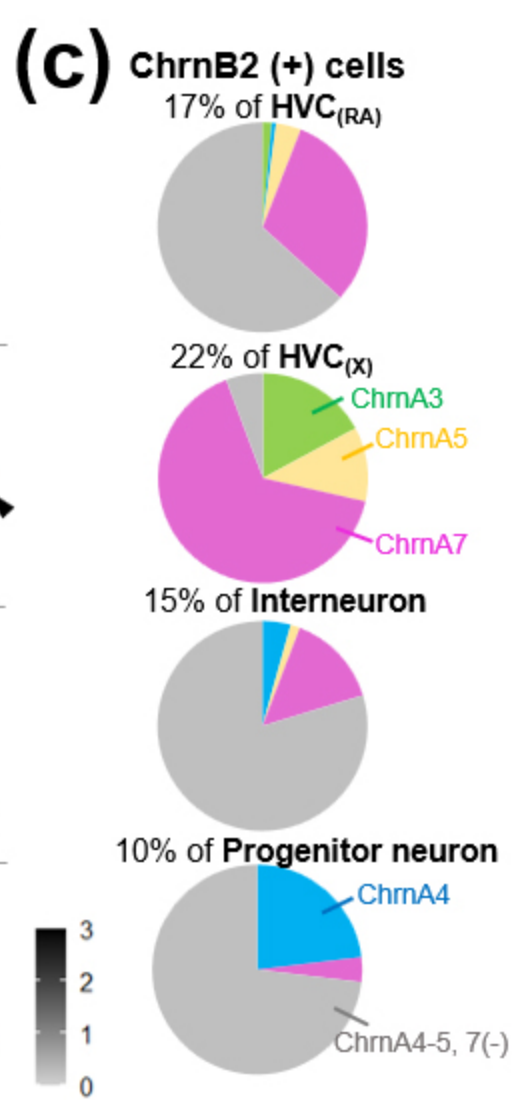
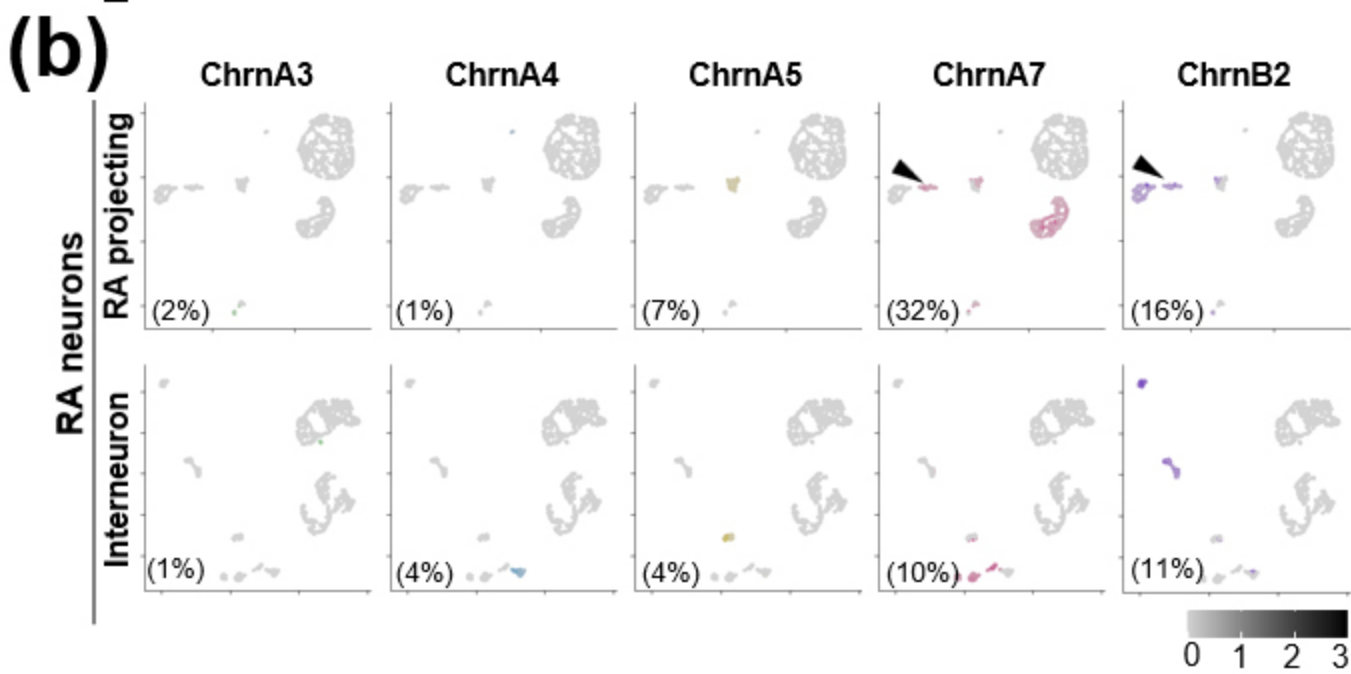
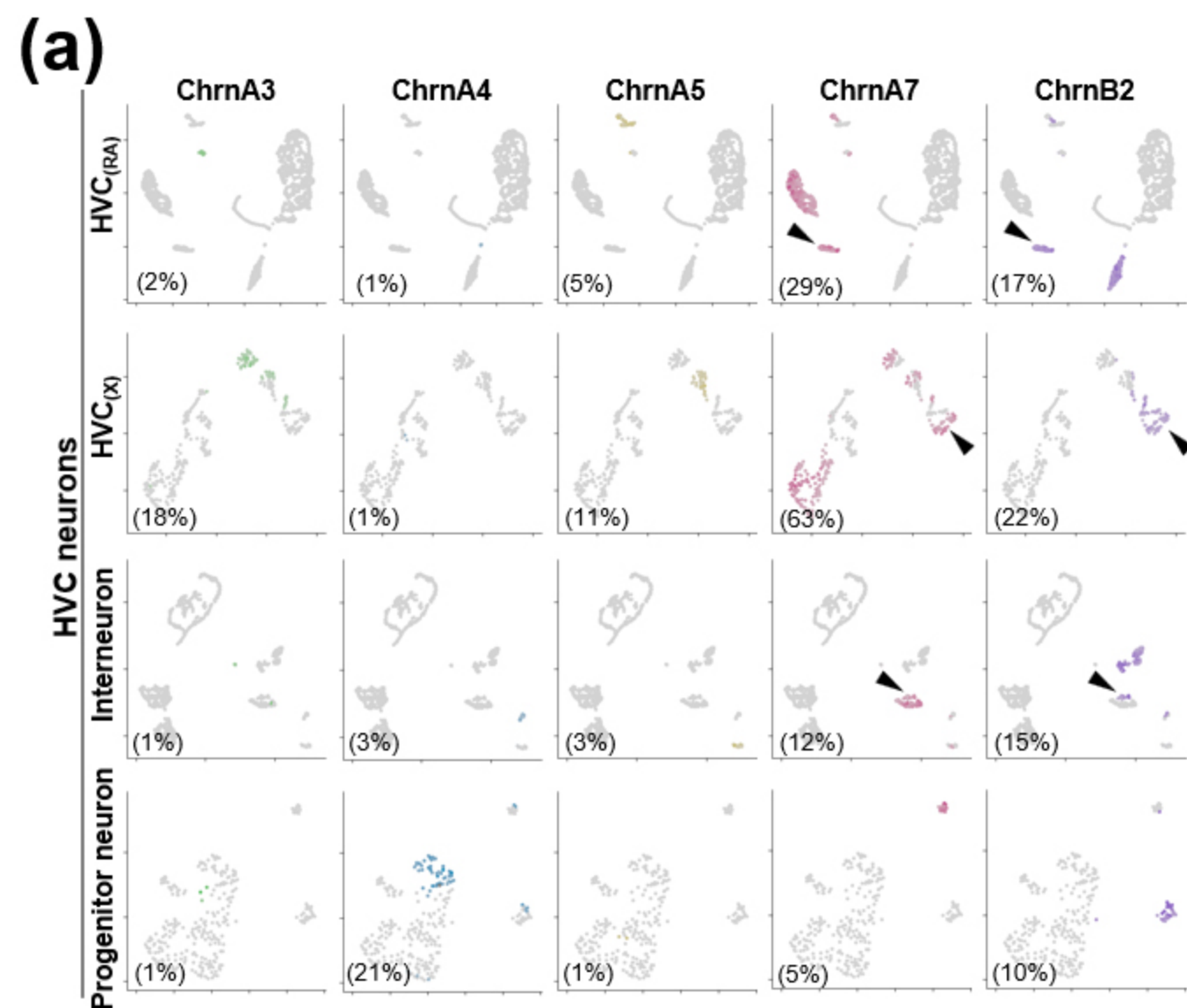


**(a)****(b)**

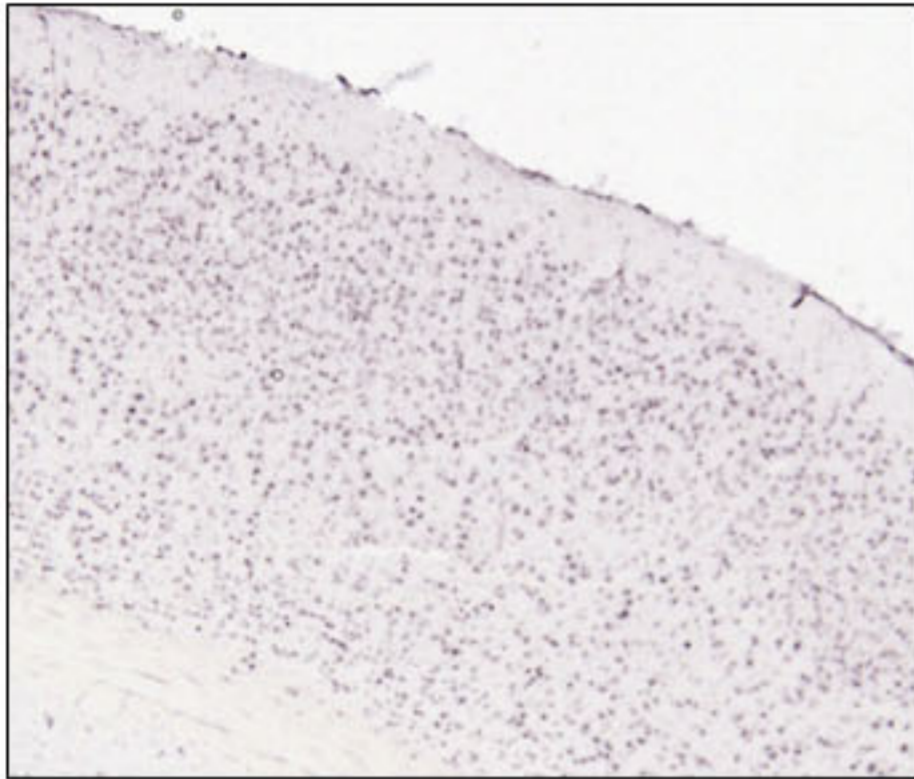
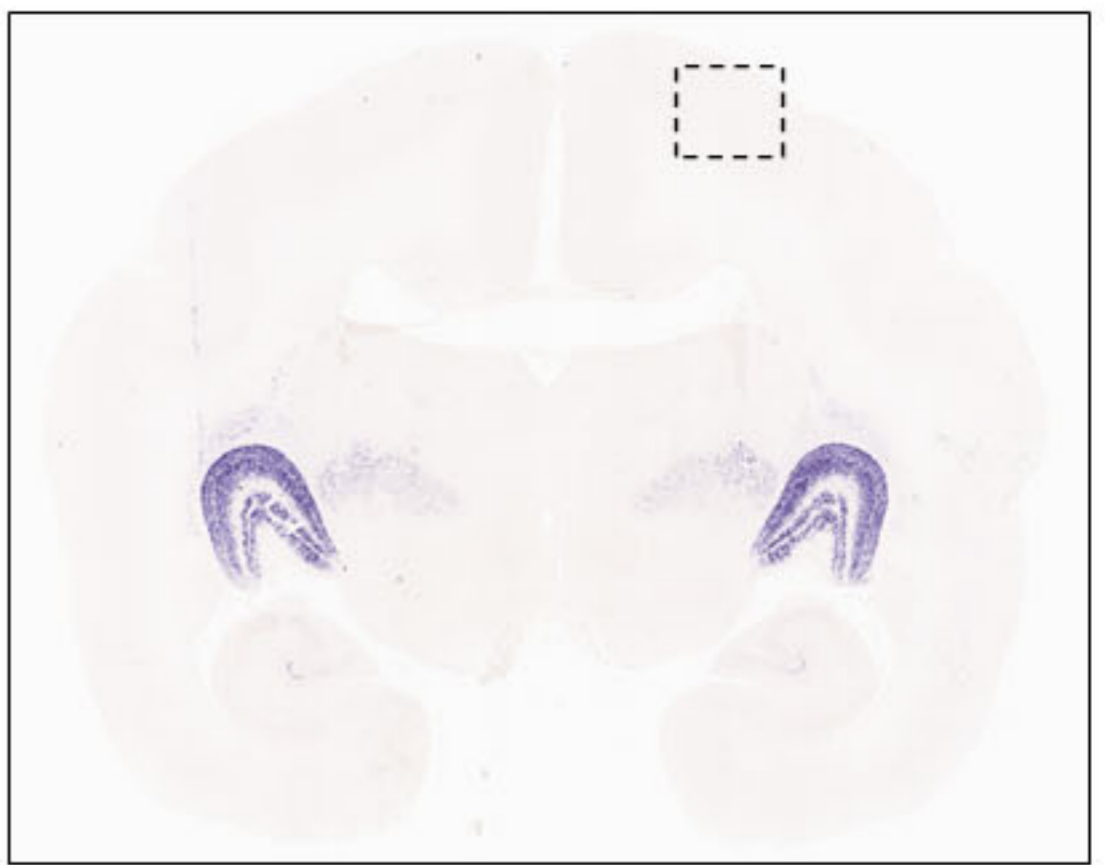
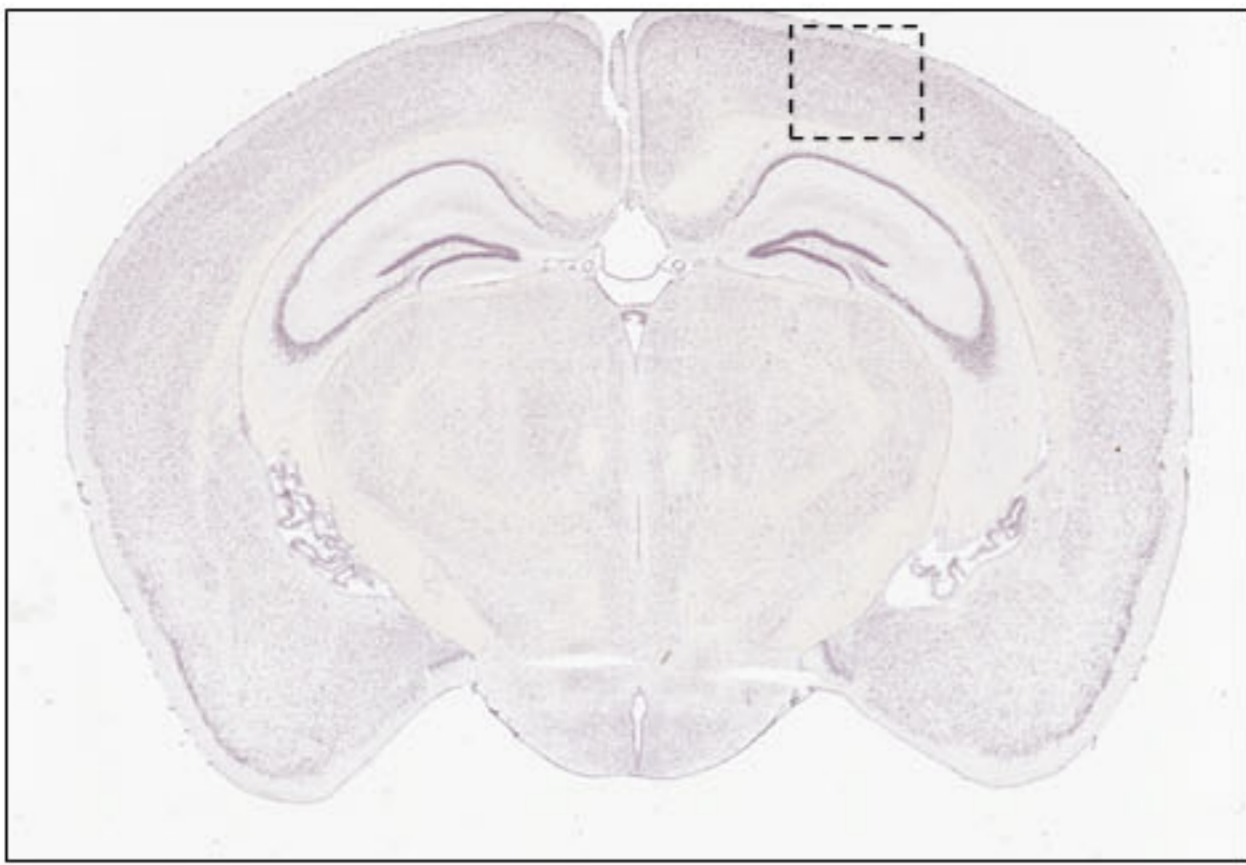




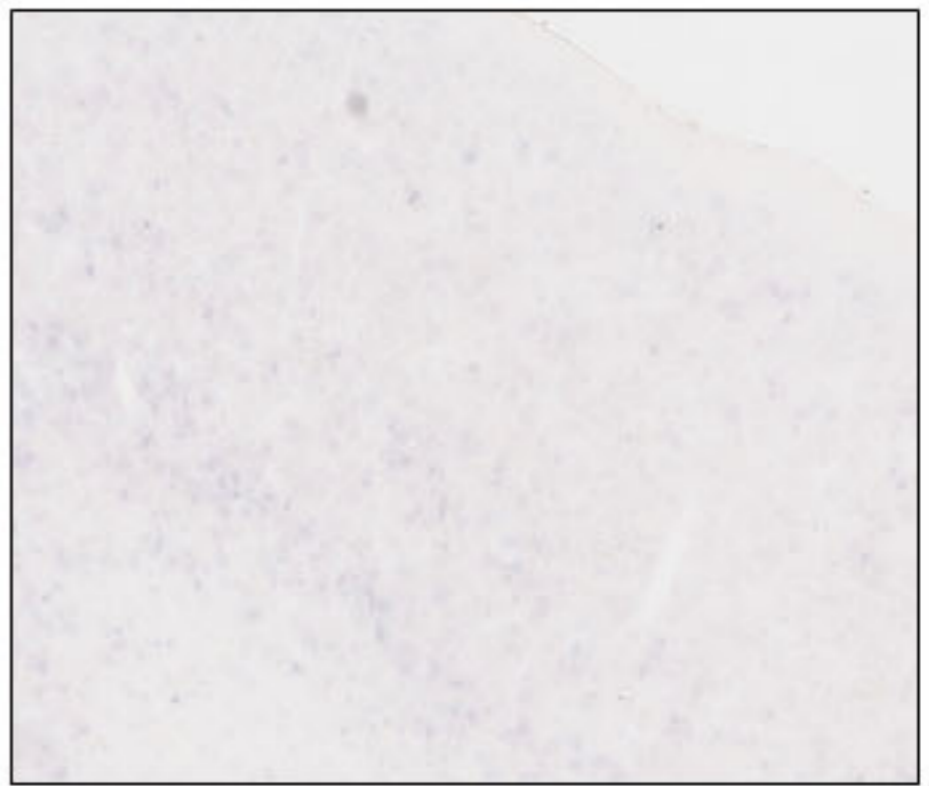
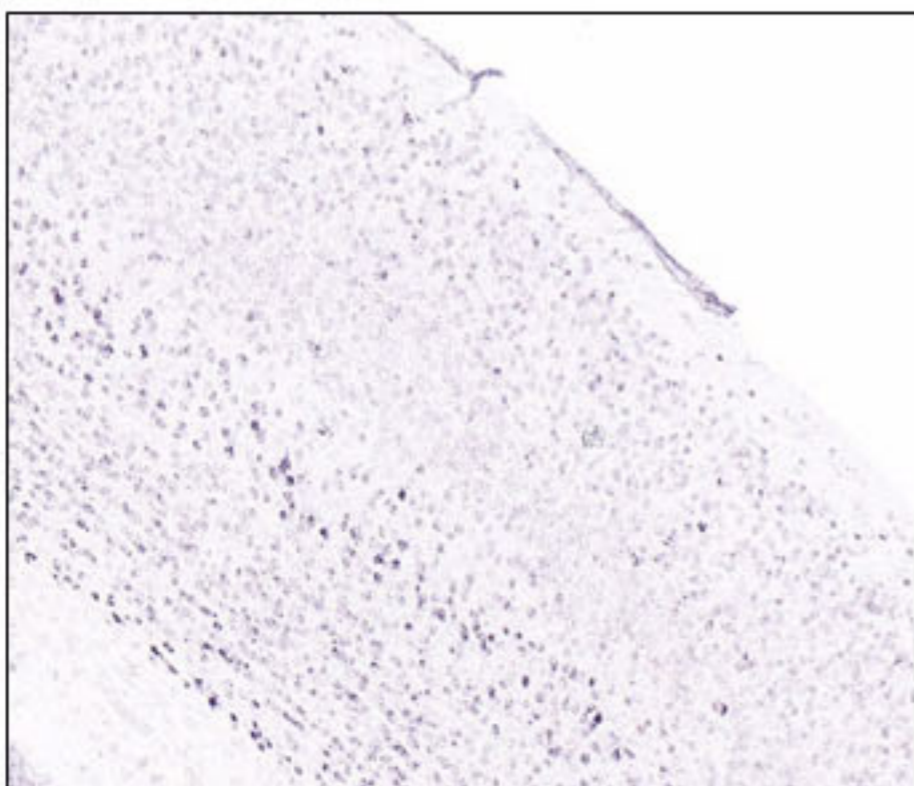
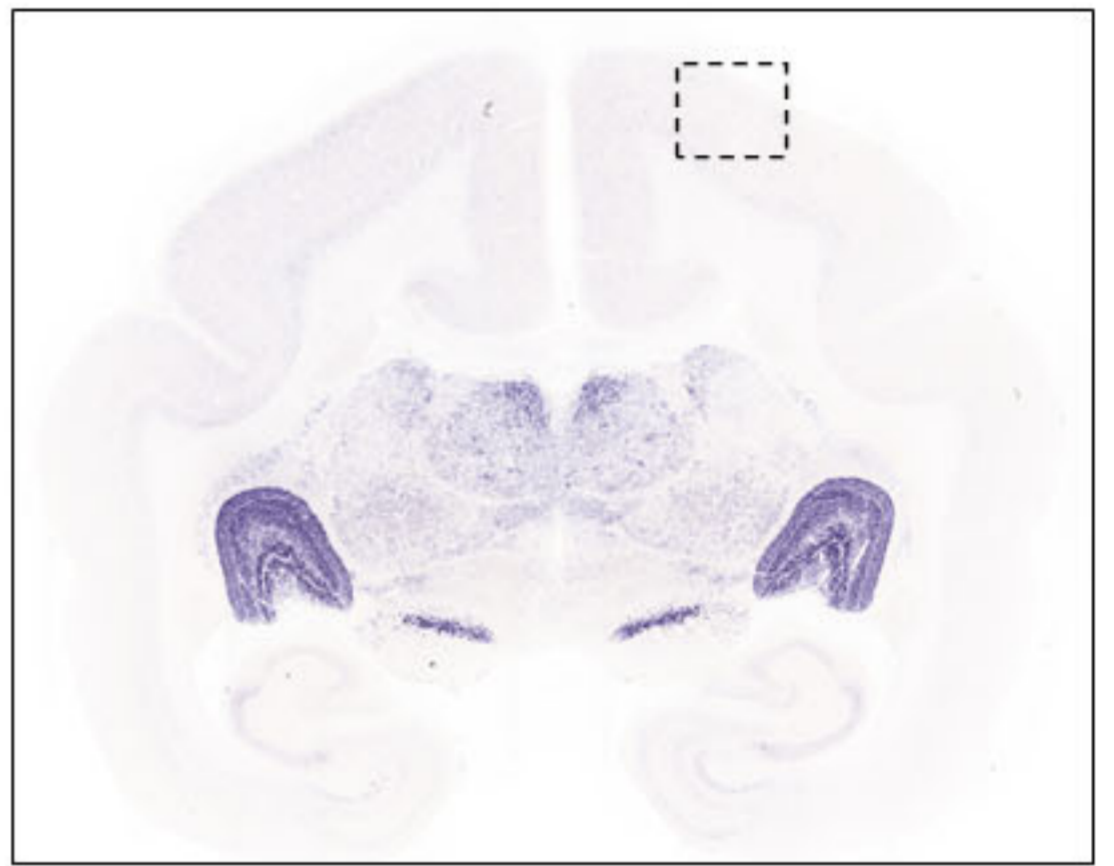
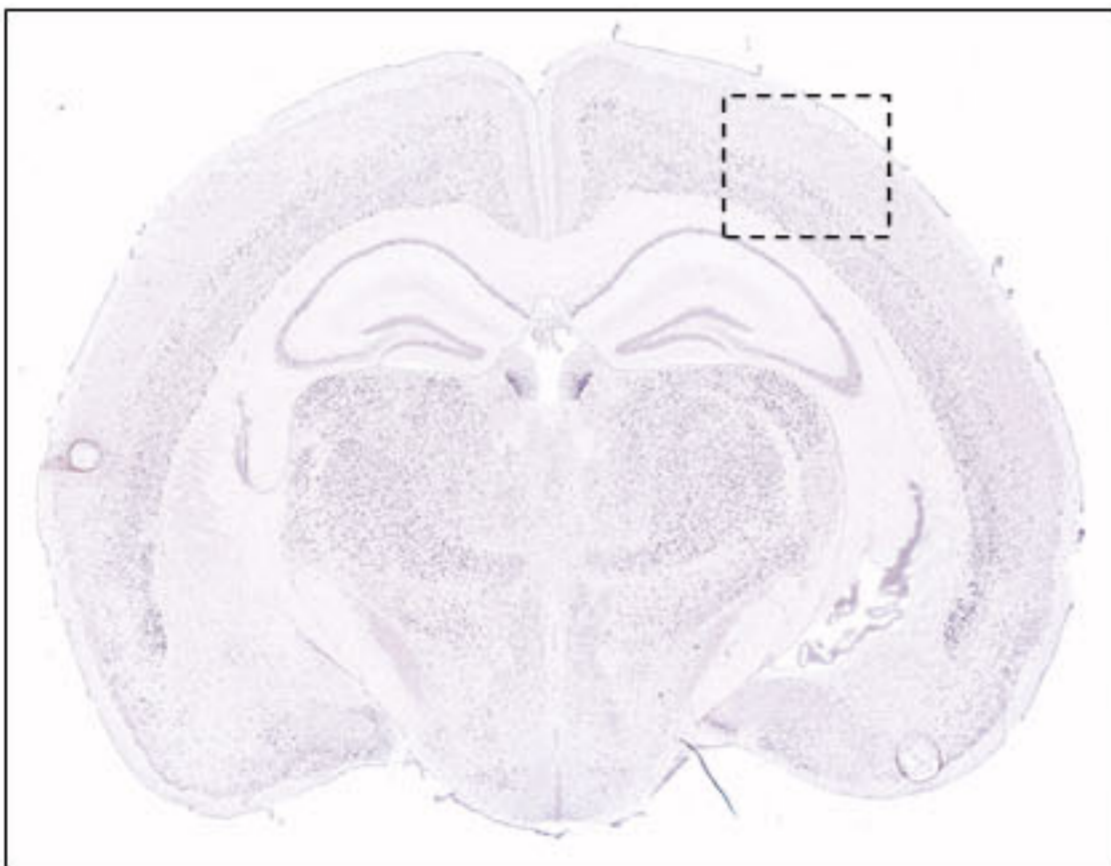




**(a)**



**(b)**



Cloned subunits in this study	Forward primer	Reverse primer	Cloned fragment length (bp)	Accession # of cloned subunits in this study	Accession # of zebra finch predicted nAChR mRNAs	Position at protein coding sequence	Similarity to zebra finch predicted nAChR proteins	Similarity to chicken nAChR proteins	Similarity to human nAChR protein
<b>ChrmA1</b>	5'- AATGGACAGACGTC AACCTC -3'	5'- CTGGAGGTGGAGGGAATCA -3'	592	OL679454	XM_002199046	86-282a.a./457a.a.	99% to XP_002199082	97% to NP_990147	89% to NP_000070
<b>ChrmA2</b>	5'- ACATCACCTTCTACTTCGTC -3'	5'- CGATGATGAAGATCCAGAGG -3'	834	OL679455	XM_041715494	227-503a.a./522a.a.	100% to XP_041571428	73% to NP_990146	67% to NP_000733
<b>ChrmA3</b>	5'- AGTTGGGGATTCCAGGTTG -3'	5'- GTTCTTAGAATACATACCAGG -3'	1,051	OL679456	XM_012569079	126-474a.a./496a.a.	100% to XP_012424533	96% to NP_989747	87% to NP_00073
<b>ChrmA4</b>	5'- TGATGACCACCAATGTGTGG -3'	5'- GCATGGACTCAATGAGCTTC -3'	842	OL679457	XM_012570240	84-363a.a./624a.a.	100% to XP_012425694	98% to NP_001384279	91% to NP_000735
<b>ChrmA5</b>	5'- TGGGTTGTCAGTGAAC -3'	5'- GTGCAGAAATATCTTGCGAAC -3'	854	OL679458	XM_030281197	45-328a.a./445a.a.	100% to XP_030137058	99% to NP_989746	92% to NP_000736
<b>ChrmA6</b>	5'- CAACTGCGATGGGATCCC -3'	5'- CTCGTCTATCACCATAGCTA -3'	1,038	OL679459	XM_002188838	125-460a.a./493a.a.	99% to XP_002188874	93% to NP_990695	80% to NP_004189
<b>ChrmA7</b>	5'- CTGCAAGGAGAGTCCAAAG -3'	5'- GAAGGCCATCAAGCAGAGC -3'	1,326	OL679460	XM_030281037	28-468a.a./502a.a.	100% to XP_030136897	98% to NP_989512	91% to NP_000737
<b>ChrmA8 (7-like)</b>	5'- GCTGCTTGTGGCTGAGATC -3'	5'- CAAACTCCCACTCACTGCAG -3'	563	OL679461	XM_002187662	285-471a.a./511a.a.	99% to XP_002187698	86% to NP_990532	N/A
<b>ChrmA9</b>	5'- TATGTCACATGCTGTTAATG -3'	5'- GAATCTCCCACTCCACATCTT -3'	486	OL679462	XM_030270964	6-166a.a./448a.a.	100% to XP_030126824	98% to NP_990091	91% to NP_060051
<b>ChrmA10</b>	5'- TTCGTGGAGAACGGTGGAGTG -3'	5'- TGATCATGGTCATGGTGGCG -3'	303	OM201170	XM_030284731	203-302a.a./456a.a.	100% to XP_030140591	97% to NP_001094506	83% to NP_065135
<b>ChrmB2</b>	5'- AGCGGGAGCAGATCATGAC -3'	5'- CGCTGGTGACGATGGAGAA -3'	694	OL679463	XM_030291667	72-302a.a./491a.a.	99% to XP_030147527	99% to NP_990144	98% to NP_000739
<b>ChrmB3</b>	5'- TTACCATCCCATGGCACCC -3'	5'- CAAAAGTTGTTCCAGCCACAT -3'	354	OL679464	XM_002189012	331-448a.a./455a.a.	99% to XP_002189048	91% to NP_990143	79% to NP_000740
<b>ChrmB4</b>	5'- GGAAGCATGCCAGCAGATG -3'	5'- CTGGTAACTATTGAGAAGGC -3'	730	OL679465	XM_030281195	26-298a.a.(spliced out 83-120a.a.)/489a.a.	100% to XP_030137055	99% to NP_990150	89% to NP_000741
<b>ChrmD</b>	5'- ATAGTCCTGGAGAACACAATG -3'	5'- GCTTGTCTCCTCCCGGTA -3'	1,169	OL679466	XM_030280650	121-509a.a./518a.a.	99% to XP_030136510	85% to NP_001026488	67% to NP_001298125
<b>ChrmG</b>	5'- ATCTCTGCCATGGCTGTGC -3'	5'- GCCTGTTGAAGTGAGCCA -3'	690	OL679467	XM_030280649	258-487a.a./509a.a.	99% to XP_030136509	91% to NP_001026739	60% to NP_005190

Predicted zebra finch nAChR subunits		Cloned partial cDNAs to make <i>in-situ</i> hybridization probes														
Genbank accession#	nAChR subunits	ChrA1	ChrA2	ChrA3	ChrA4	ChrA5	ChrA6	ChrA7	ChrA8	ChrA9	ChrA10	ChrB2	ChrB3	ChrB4	ChrD	ChrG
XM_002199046	ChrA1	99.7	30.3	16.1	58.0	20.3	23.3	0.0	0.0	0.0	0.0	31.6	12.0	30.2	0.0	0.0
XM_041715494	ChrA2	61.4	100.0	38.4	76.8	45.0	0.0	1.7	0.0	0.0	62.0	68.9	8.8	7.0	26.7	0.0
XM_012569079	ChrA3	30.0	25.3	99.9	66.8	51.6	54.0	0.0	0.0	5.1	0.0	34.2	0.0	11.1	8.9	0.0
XM_012570240	ChrA4	60.0	47.9	42.2	99.1	48.4	42.5	4.7	2.6	27.0	0.0	66.9	9.7	42.3	29.7	0.0
XM_030281197	ChrA5	13.2	19.9	33.1	36.4	100.0	36.7	12.5	0.0	30.3	0.0	14.0	0.0	18.5	3.3	0.0
XM_002188838	ChrA6	37.2	0.0	53.4	56.0	61.6	99.8	0.0	4.0	27.1	0.0	12.0	0.0	33.4	4.8	0.0
XM_030281037	ChrA7	0.0	2.5	0.0	1.9	19.7	0.0	99.7	30.2	0.0	0.0	0.0	4.3	0.0	0.0	0.0
XM_002187662	ChrA8 (7-like)	0.0	0.0	1.0	5.3	22.6	1.0	53.3	99.1	0.0	0.0	4.5	0.0	11.9	0.0	0.0
XM_030270964	ChrA9	9.2	0.0	0.0	15.5	16.9	8.2	0.0	6.9	100.0	67.9	1.9	0.0	12.1	0.0	0.0
XM_030284731	ChrA10	0.0	24.5	0.0	46.5	0.0	0.0	0.0	0.0	64.5	99.0	39.9	0.0	0.0	16.6	0.0
XM_030291667	ChrB2	30.5	44.2	25.8	58.4	19.6	18.3	0.0	0.0	0.0	37.4	99.3	0.0	67.0	21.1	19.7
XM_002189012	ChrB3	34.9	3.7	35.6	57.1	70.9	0.0	1.0	0.0	0.0	0.0	0.0	99.7	0.0	4.5	0.0
XM_030281195	ChrB4	24.8	0.0	10.4	49.7	22.2	29.6	0.0	0.0	0.0	0.0	72.9	0.0	100.0	14.0	0.0
XM_030280650	ChrD	0.0	29.3	9.6	12.9	4.1	5.6	0.0	0.0	0.0	43.9	46.3	0.0	21.9	99.4	22.7
XM_030280649	ChrG	4.1	0.0	2.5	0.0	0.0	0.0	0.0	0.0	0.0	0.0	63.1	0.0	4.2	40.2	98.6